TRIM27 negatively regulates NOD2 by ubiquitination and proteasomal degradation

I n a u g u r a l – D i s s e r t a t i o n

zur

Erlangung des Doktorgrades

der Mathematisch-Naturwissenschaftlichen Fakultät

der Universität zu Köln

vorgelegt von

Birte Helene Zurek

aus Braunschweig

Köln 2011

Berichterstatter: Prof. Dr. Jonathan Howard

Prof. Dr. Mats Paulsson

Tag der mündlichen Prüfung: 18.10.2011

Table of contents

Abbreviations

°C	degree Celsius
µg	microgram
µl	microlitre
A	desoxyadenosine
AAA+	ATPases associated with various cellular activities
AAMP	angio-associated migratory cell protein
AD	acidic activation domain
ADP	adenosine diphosphate
AIM2	absent in melanoma 2
AP-1	activator protein 1
APAF1	apoptotic protease-activating factor 1
APS	ammonium persulfate
ASC	apoptosis-associated speck-like protein containing a CARD
ATG16L1	autophagy-related protein 16-1
ATP	adenosine triphosphate
BIR	baculovirus inhibitory repeat
bp	basepairs
BS	Blau syndrome
BSA	bovine serum albumin
BTN	butyrophilin-related transmembrane glycoproteins
C	desoxycytidine
CARD	caspase activating and recruitment domain
CBB	Coomassie Brilliant Blue
CC	coiled-coil
CD	Crohn's disease
cDNA	complementary DNA
CENTB1	Centaurin β1
CHX	cycloheximide
cIAP	cellular inhibitor of apoptosis proteins
CIITA	class II MHC transactivator
CLR	C-type lectin receptor
C-terminus	carboxyl-terminus
DAI	DNA-dependent activator of IRFs
DAMP	danger-associated molecular pattern
DAP	diaminopimelic acid
DAPI	4',6-diamidino-2-phenylindole
DMEM	Dulbecco's modified Eagle's medium
DMSO	dimethylsulfoxide
DNA	desoxyribonucleic acid
dNTP	desoxynucleotide triphosphate
ds	double stranded
DTT	dithiothreitol
DUOX2	dual oxidase 2

E. coli	*Escherichia coli*
e.g.	*exempli gratia*; for example
EDTA	ethylenediaminetetraacetic acid
ELISA	enzyme-linked immunosorbent assay
EOS	early onset sarcoidosis
ERK	extracellular-signal-regulated kinase
et al.	*et alii*; and others
ETI	effector triggered immunity
FBS	fetal bovine serum
FITC	Fluorescein isothiocyanate
FLS2	flagellin-sensing 2
FMF	familial Mediterranean fever
g	gravitational force
G	desoxyguanosine
GAPDH	glycerinaldehyd-3-phosphat-dehydrogenase
GRIM-19	gene associated with retinoid-interferon-induced mortality 19
GTP	guanosine triphosphate
h	hour
HA	hemagglutinin
HEK	human embryonic kidney
HEPES	2-[4-(2-hydroxyethyl)-1-piperazinyl]-ethanesulfonic acid
HR	hypersensitive response
HRP	horseradish peroxidase
HSP	heat-shock protein
i.e.	*id est*; that is
IBD	inflammatory bowel disease
IF	immunofluorescence
IFI16	interferon-γ-inducible protein 16
IFN	interferon
Ig	immunoglobulin
IKK	IκB kinase
IL	interleukin
IP	immunoprecipitation
IPTG	isopropyl 1-thio-β-D-galactopyranoside
IRF	IFN regulatory factor
ISG15	IFN-stimulated protein of 15 kDa
IκBα	NF-κB inhibitor, alpha
JNK	c-Jun N-terminal kinase
kb	kilobasepairs
kDa	kilodalton
KSHV	Kaposi Sarcoma-associated herpes virus
LB	Lysogeny broth
LC	light chain
LMB	leptomycin B
LPS	lipopolysaccharide

LRR	leucine-rich repeat
M	molar
MAMP	microbe-associated molecular pattern
MAPK	mitogen-activated protein kinase
MAVS	mitochondrial antiviral-signalling protein
MDA5	melanoma differentiation associated gene 5
mDAP	*meso*-diaminopimelic acid
MDP	muramyl dipeptide
MEKK4	mitogen-activated protein kinase kinase kinase 4
mg	milligram
MHC	major histocompatibility complex
MID1	midline 1
min	minute
ml	millilitre
mM	millimolar
mRNA	messenger RNA
MTI	MAMP-triggered immunity
NACHT	domain present in NAIP, CIITA, HET-E and TP1
NAD	NACHT-associated domain
NAD(P)H	nicotinamide adenine dinucleotide (phosphate)
NAIP	neuronal apoptosis inhibitory protein
NALP	NACHT, LRR and PYD-containing protein
NBD	nucleotide-binding domain
NEMO	NF-κB essential modulator
NES	nuclear export sequence
NF-κB	Nuclear factor κ-light-chain-enhancer of activated B cells
ng	nanogram
NIK	NF-κB-inducing kinase
NLR	nucleotide-binding domain and leucine-rich repeat containing protein
NLS	nuclear localization sequence
NOD	Nucleotide-binding oligomerization domain
NP40	Nonidet P-40
nRLU	normalized relative light unit
N-terminus	amino-terminus
o/n	over night
OAS	oligoadenylate synthetase
OD	optical density
OMVs	outer-membrane vesicles
ONPG	*o*-Nitrophenyl-β-D-galactopyranosid
PAGE	polyacrylamid gelelectrophorese
PBS	phosphate buffered saline
PCR	polymerase chain reaction
PFA	paraformaldehyde
PGN	peptidoglycan
PKCα	protein kinase C, alpha

PKR	protein kinase R
PML	promyelocytic leukemia gene
PRR	pattern-recognition receptor
PYD	pyrin domain
PYHIN	pyrin and HIN domain-containing protein
qPCR	quantitative PCR
R protein	resistance protein
RBCC	RING – B-box – coiled-coil
RFP	RET finger protein
RIG-I	retinoic acid-inducible gene I
RING	really interesting new gene
RIP2	receptor-interacting serine/threonine-protein kinase 2
RIPA	radioimmunoprecipitation assay
RLR	RIG-I-like receptor
RNA	ribonucleic acid
RNaseL	ribonuclease L
ROS	reactive oxygen species
rpm	rounds per minute
RT	room temperature
RT-PCR	reverse transcription PCR
SDS	sodium dodecyl sulphate
sec	seconds
SH	superhelical
siRNA	small interfering RNA
SOCS-1	suppressor of cytokine signalling 1
ss	single stranded
STAND	signal transduction ATPases with numerous domains
STING	stimulator of interferon genes
SUMO	small ubiquitin-like modifier
T	desoxythymidine
TAB	TAK1-binding protein
TAK	transforming growth factor (TGF)-beta activated kinase
TBE	TRIS-Borat-EDTA
TBK	TANK-binding kinase
TBS	TRIS buffered saline
TEMED	N,N,N',N'-Tetramethylethylendiamin
Th1	type I helper T cell
TIR	Toll-IL-1 receptor
TLR	Toll-like receptor
TMV	Tobacco mosaic virus
TNFR	TNF receptor
TNF-α	tumour necrosis factor-alpha
TRAF	TNF receptor-associated factor
Tri-DAP	L-Ala-D-γ-Glu-mDAP
TRIM	tripartite motif

TRIS	Tris(hydroxymethyl)-aminomethan
Triton X-100	polyethylene glycol p-(1,1,3,3-tetramethylbutyl)-phenyl ether
Tween 20	polyoxyethylen-(20)-sorbitan monolaureate
U	unit
Ub	ubiquitin
V	volt
WB	Western blot
WH	winged helix
WT	wild type
XIAP	X-linked inhibitor of apoptosis

Symbols for amino acids

Amino acid	Three letter code	One letter code
Alanine	Ala	A
Arginine	Arg	R
Asparagine	Asn	N
Aspartate	Asp	D
Cysteine	Cys	C
Glutamate	Glu	E
Glutamine	Gln	Q
Glycine	Gly	G
Histidine	His	H
Isoleucine	Ile	I
Leucine	Leu	L
Lysine	Lys	K
Methionine	Met	M
Phenylalanine	Phe	F
Proline	Pro	P
Serine	Ser	S
Threonine	Thr	T
Tryptophane	Trp	W
Tyrosine	Tyr	Y
Valine	Val	V

1 Introduction

1.1 Pattern-recognition receptors in innate immunity

Mammals have evolved a variety of innate and adaptive immune responses to eliminate invading pathogens. The innate immune system relies on phagocytic and non-haematopoietic cells and innate immune responses are characterized by recognition of invariant structural signatures of the micro-organisms, so-called microbe-associated molecular patterns (MAMPs), by germline-encoded pattern-recognition receptors (PRRs) (Medzhitov 2007). MAMPs include bacterial cell wall components like lipopolysaccharide (LPS), peptidoglycan (PGN), lipoteichoic acid and cell wall lipoproteins or flagellin, bacterial and viral nucleic acids and fungal constituents. Alternatively, some PRRs are also activated by parasites and danger-associated molecular patterns (DAMPs), which are generally compartmentalized host molecules that delocalize or are produced upon cell damage, like ATP, reactive oxygen species (ROS), DNA, or uric acid, but they also include bacterial toxins and crystals. There are at least four different classes of PRRs: Toll-like receptors (TLRs), retinoic acid-inducible gene (RIG)-I-like receptors (RLRs), C-type lectin receptors (CLRs), and nucleotide-binding domain and leucine-rich repeat containing proteins (NLRs) (see Figure 1.1). They show distinct sub-cellular localization and specifically recognize extracellular, vesicular or cytosolic MAMPs and DAMPs. PRR signalling mainly leads to activation of a common set of transcription factors: NF-κB and AP-1 (activator protein 1) induce transcription of pro-inflammatory cytokines, chemokines and antimicrobial peptides, whereas interferon (IFN) regulatory factors (IRFs) induce type I IFN-dependent antiviral responses.

TLRs are amongst the best studied PRRs (Kawai and Akira 2010). They comprise extracellular leucine-rich repeats mediating ligand binding, transmembrane domains and intracellular Toll-interleukin-1 (IL-1) receptor (TIR) domains, which transmit downstream signalling. So far, 10 TLRs have been identified in man. They reside in the plasma membrane or in endosomal membranes and recognize LPS, lipopeptides or flagellin and other MAMPs in the extracellular space or viral dsRNA, ssRNA and DNA within endosomes. TLRs activate NF-κB, AP-1 and IRFs resulting in the transcription of pro-inflammatory cytokines and type I IFNs.

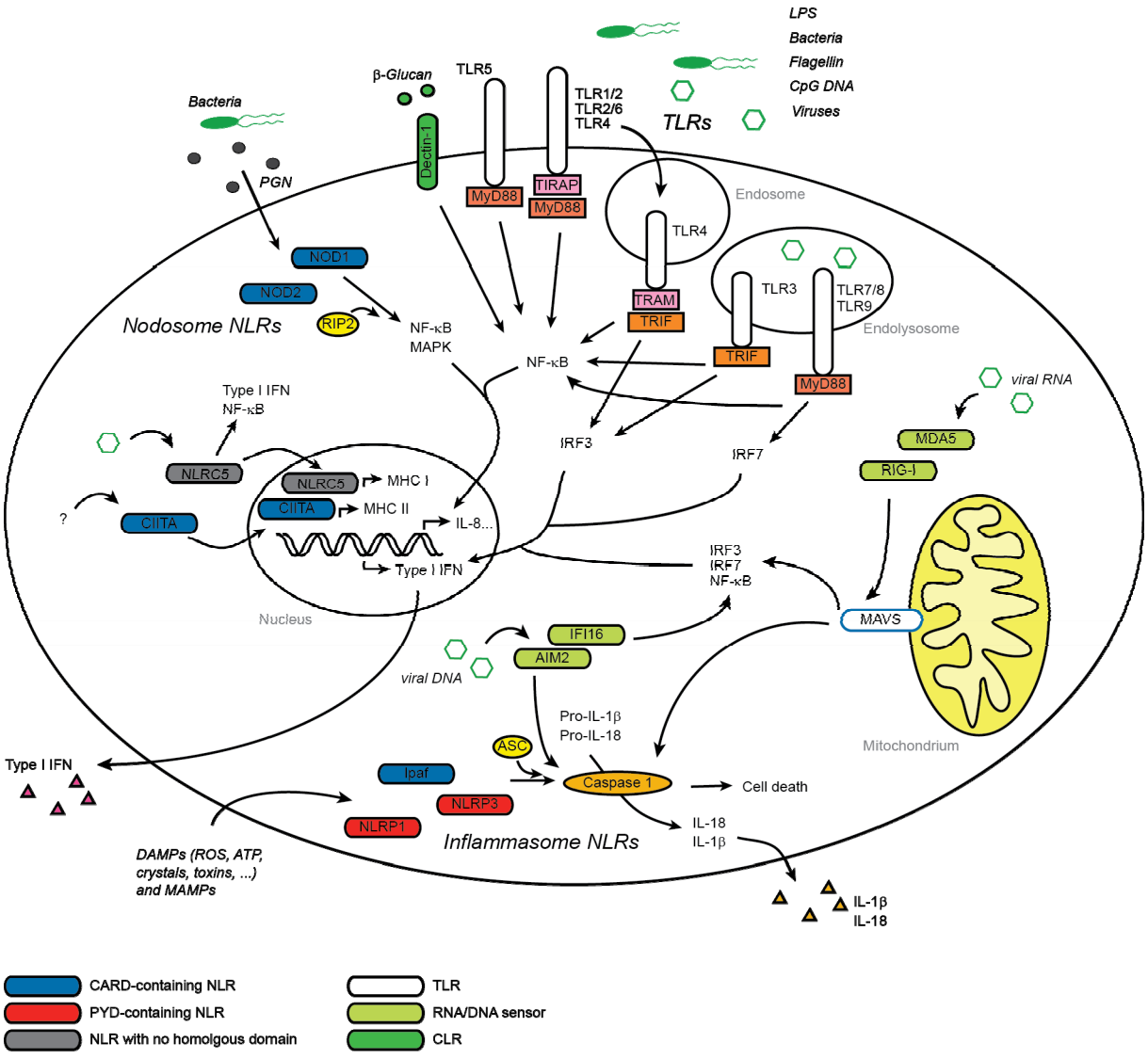

Figure 1.1: Pattern-recognition receptors

Overview of the PRRs and their signalling pathways: Membrane-bound TLRs (white), membrane-bound Dectin-1 as an example for CLRs (green), cytosolic nodosome and inflammasome NLRs (CARD-containing NLRs in blue, PYD-containing NLRs in red), the cytosolic RLRs and the DNA-sensors AIM2 and IFI16 (light green). Important adaptor proteins are shown.

Viruses are not only recognized by TLRs but also by intracellular PRRs. The RLRs RIG-I and melanoma differentiation associated gene 5 (MDA5) both detect viral RNA. They contain two N-terminal CARD domains and interact upon RNA recognition via homotypic CARD-CARD interactions with the adaptor protein mitochondrial antiviral-signalling protein (MAVS; also known as IPS-1, Cardif or VISA). MAVS is bound to the mitochondrial outer-membrane and interaction with RIG-I or MDA5 leads to NF-κB and IRF3/7 activation (O'Neill and Bowie 2010, Takeuchi and Akira 2010). RIG-I has also been shown to interact with ASC (apoptosis-associated speck-like protein

containing a CARD) leading to inflammasome formation (see below), caspase-1 activation and pro-IL-1β processing (Poeck*, et al.* 2010).

The first cytosolic DNA sensor being discovered was DNA-dependent activator of IRFs (DAI, also called ZBP1) (Takaoka*, et al.* 2007). Recently, two other DNA sensors – absent in melanoma 2 (AIM2) and interferon-γ-inducible protein 16 (IFI16) – were detected. Both are pyrin and HIN domain-containing protein (PYHIN) family members and comprise a DNA-binding HIN200 domain and an N-terminal pyrin domain (PYD) mediating association with ASC. Recognition of dsDNA by AIM2 results in inflammasome formation (see below), caspase-1 activation and pro-IL-1β processing as well as induction of pyroptosis (Burckstummer*, et al.* 2009, Fernandes-Alnemri*, et al.* 2009, Hornung*, et al.* 2009, Roberts*, et al.* 2009). IFI16 activates IRF3 and NF-κb via the adaptor protein stimulator of interferon genes (STING) (Unterholzner*, et al.* 2010) and also forms ASC-dependent inflammasomes after recognition of Kaposi Sarcoma-associated herpes virus (KSHV) DNA in the nucleus (Kerur*, et al.* 2011).

Another viral sensor is protein kinase R (PKR; also known as RNA-dependent protein kinase). PKR is activated by binding to dsRNA and subsequently phosphorylates translation initiation factor eIF2α, which inhibits further mRNA translation and viral protein synthesis (Davis and Watson 1996). PKR also activates NF-κB by phosphorylation of NF-κB inhibitor. IFN signalling elicited upon virus recognition by the PRRs described above enhances transcription of PKR and other antiviral proteins like ribonuclease L (RNaseL) and oligoadenylate synthetase (OAS) (summarized in (Boo and Yang 2010)). OAS is activated by binding to dsRNA. Activated OAS converts ATP into 2', 5'-linked oligomers of adenosine, which bind and activate RNaseL. RNaseL subsequently degrades viral ssRNA but also some self mRNA, which can serve as a ligand for RIG-I and MDA5.

CLRs are transmembrane receptors and recognize extracellular carbohydrates of bacteria, viruses or fungi. CLR activation results in the production of pro-inflammatory cytokines.

1.2 NOD-like receptors

In the last decade another class of intracellular PRRs, the nucleotide-binding domain and leucine-rich repeat containing protein family (NLR) has been discovered (Franchi*, et al.* 2009, Magalhaes*, et al.* 2011). NLRs are characterized by a tripartite domain architecture similar to human apoptotic protease-activating factor 1 (APAF1). The N-terminal effector domain mediates downstream signal transduction of activated NLRs via homotypic protein-protein interactions and adopts a death domain fold, which is either a caspase activating and recruitment domain (CARD), a pyrin (PYD), or a baculovirus inhibitory repeat (BIR) domain. Some NLR proteins (like NLRC5 and NLRX1), however, show no obvious homology to any of these specific domains. Based on their N-terminal domain NLRs are classified into different sub-groups (Ting*, et al.* 2008a) (see Figure 1.2). The effector domain is followed by a central nucleotide-binding domain (NBD), which includes an ATPase domain (see chapter 1.2.3) and is necessary for oligomerization upon ligand recognition. The NBD consists of the NACHT (domain present in NAIP, CIITA, HET-E and TP1), winged helix (WH) and superhelical (SH) domain. The WH and SH domains together are sometimes called the NACHT-associated domain (NAD). The C-terminal leucine-rich repeats (LRRs) are thought to function in auto-regulation and MAMP recognition, although direct MAMP-LRR interaction for NLR proteins remains elusive.

Several PYD-containing NLRs are reported to form large multiprotein complexes called inflammamsomes and function similar to apoptosomes (Schroder and Tschopp 2010). Whereas the latter activate pro-apoptotic caspases to trigger apoptosis, inflammasomes activate pro-inflammatory caspases (human caspase-1, -4, and -5) (Martinon and Tschopp 2007). The best characterized inflammasome-forming NLR is NLRP3. Various MAMPs, DAMPs, whole pathogens and environmental irritants are known to activate NLRP3 (reviewed in (Schroder and Tschopp 2010)), making direct ligand binding unlikely. NLRP3 activation leads to oligomerization via the NBD domain, recruitment of the adaptor protein ASC followed by recruitment of pro-caspase-1. Auto-activation of pro-caspase-1 leads to processing and secretion of IL-1β and IL-18.

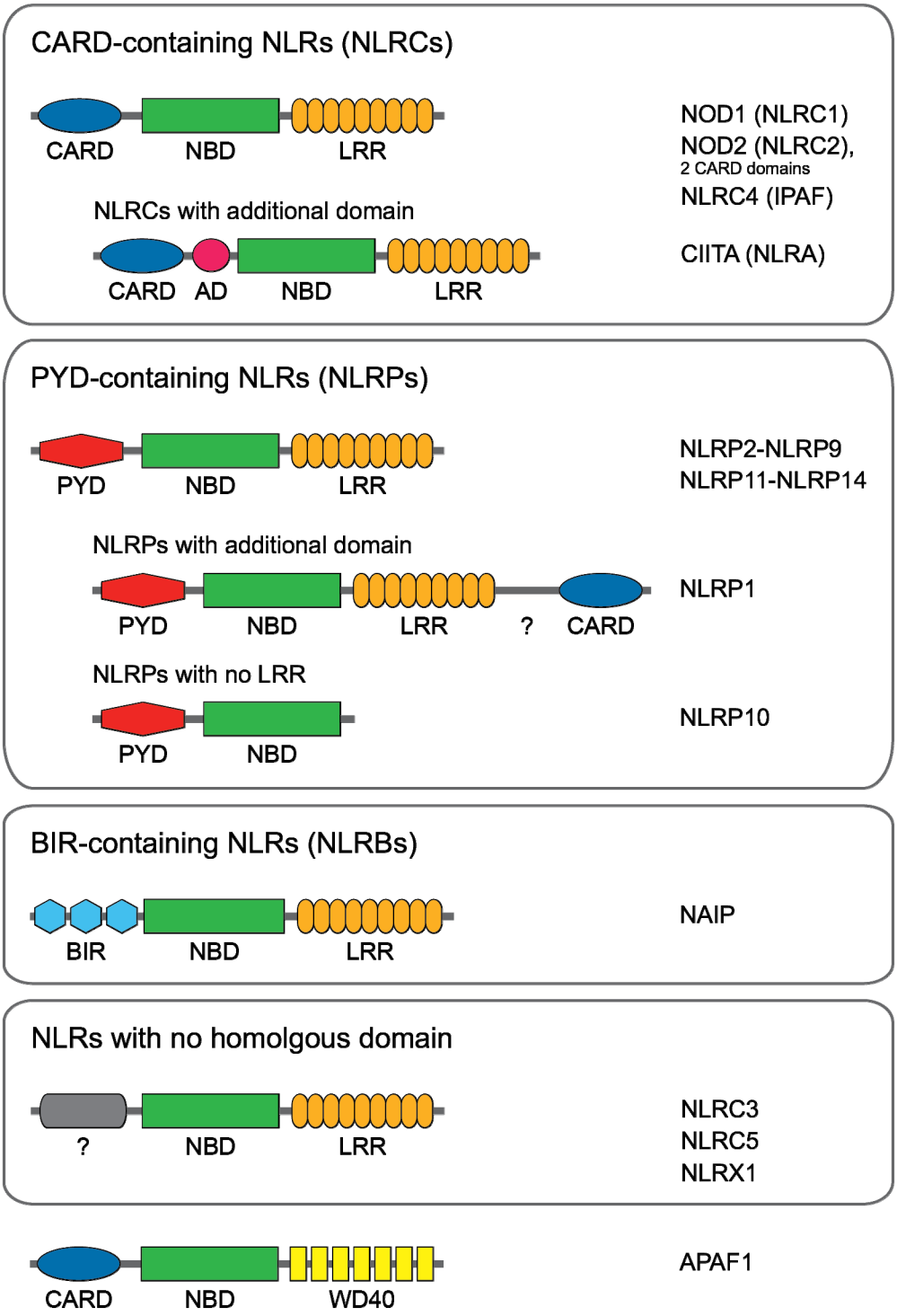

Figure 1.2: The human NLR family

Domain architecture of the 22 human NLR proteins and the NLR-relative APAF1 is shown. The number of LRRs or WD40 repeats differs from each other, NLR proteins also differ in length. Protein names are according to the standard nomenclature (Ting*, et al.* 2008a), aliases are in brackets.

AD, acidic activation domain; BIR, baculovirus inhibitory repeat; CARD, caspase activating and recruitment domain; LRR, leucine-rich repeat; NBD, nucleotide-binding domain; PYD, pyrin domain.

Figure adapted from (Kufer and Sansonetti 2011).

An additional C-terminal CARD domain makes NLRP1 inflammasome formation independent of ASC, although the presence of ASC enhanced caspase-1 activation (Faustin*, et al.* 2007). NLRC4 (IPAF) inflammasomes are also independent of ASC, as NLRC4 belongs to the CARD-containing NLRs (Poyet*, et al.* 2001). However, some pathogens triggering NLRC4 inflammasome formation require ASC for full caspase-1 activation, although the role of ASC remains unclear (Mariathasan*, et al.* 2004, Franchi*, et al.* 2007, Suzuki*, et al.* 2007). Apart from IL-1β processing some inflammasomes can also induce a form of caspase-1-dependent programmed cell death called pyroptosis (Bergsbaken*, et al.* 2009), characterized by loss of plasma membrane integrity (Ting*, et al.* 2008b).

Although most NLRs act in pathogen recognition, such a function has not yet been identified for class II major histocompatibility complex (MHC) transactivator (CIITA), one of the founding members of the NLR family. CIITA has long been recognized to regulate MHC class II gene expression by acting as a scaffold for assembly of DNA-binding transcription factors and histone modifiers in the nucleus (Steimle*, et al.* 1993, Zika and Ting 2005). Expression of MHC class II genes is likely mainly controlled by CIITA levels that are induced upon IFN-γ treatment (Harton and Ting 2000). CIITA nuclear localization and transcriptional activity are dependent on GTP-binding and a functional Walker A box (Harton*, et al.* 1999).

Relatives of NLR proteins are also found in plants (Jones and Dangl 2006, Lukasik and Takken 2009). The majority of plant resistance (R) proteins belong to the NB-LRR family containing a central NBD domain and C-terminal LRRs. Either a TIR domain (as in TLRs) or a coiled-coil (CC) region is present at the N-terminus. The first layer of plant innate defence is the MAMP-triggered immunity (MTI) characterized by detection of extracellular pathogens by membrane-bound PRRs. Pathogens have evolved mechanisms to avoid recognition by delivering pathogen effectors (also called avirulence genes) that suppress the immune response. These effectors are detected by R proteins representing the second layer of plant defence responses, the so called effector triggered immunity (ETI). Induction of MTI and ETI result in rapid ion fluxes, oxidative burst and transcriptional reprogramming, whereas ETI also induces programmed cell death at the site of infection, the hypersensitive response (HR), to restrict pathogen colonization.

1.2.1 NOD1 and NOD2 signalling

NOD1 and NOD2 belong to the first NLR proteins identified (Inohara*, et al.* 1999, Ogura*, et al.* 2001b). Both are members of the NLRC sub-group harbouring one or two CARD domains at their N-terminus, respectively. Their localization is mainly cytoplasmic, but both are also recruited to the plasma membrane (McDonald*, et al.* 2005, Lecine*, et al.* 2007, Kufer*, et al.* 2008). Of note, signalling competence seems to be crucial for NOD2 membrane localization (Barnich*, et al.* 2005a). NOD1 and NOD2 recognize breakdown products of bacterial PGN: Whereas NOD2 senses muramyl dipeptide (MDP) (Girardin*, et al.* 2003b, Inohara*, et al.* 2003), present in nearly all Gram-positive and Gram-negative bacteria, NOD1 specifically recognizes *meso*-diaminopimelic acid (mDAP)-containing PGN fragments (Chamaillard*, et al.* 2003, Girardin*, et al.* 2003a), which are found in most Gram-negative and only in certain Gram-positive bacteria like *Listeria* and *Bacillus* species. NOD1 and NOD2 are thought to reside in an inactive auto-repressed state in the cytosol and ligand sensing results in conformational changes allowing homo-oligomerization via the NACHT domain to form the signalling-active complex called nodosome.

NOD1 and NOD2 oligomerization is followed by recruitment of receptor-interacting protein 2 (RIP2; also called RICK) via CARD-CARD interactions (Inohara*, et al.* 1999, Ogura*, et al.* 2001b) and auto-activation of RIP2 by induced proximity (Inohara*, et al.* 2000) (overview of the signalling pathway depicted in Figure 1.3). RIP2 kinase activity is dispensable for downstream signalling, but is important for RIP2 stability (Windheim*, et al.* 2007, Hasegawa*, et al.* 2008, Nembrini*, et al.* 2009). K63-linked ubiquitination of RIP2 at K209 is necessary for recruitment of the ubiquitin-binding proteins TAK1-binding protein 1 (TAB1), TAB2 and/or TAB3 in a complex with TAK1 (transforming growth factor-β activated kinase 1) (Abbott*, et al.* 2007, Hasegawa*, et al.* 2008). E3 ligases mediating RIP2 ubiquitination with K63- but also K48-linked ubiquitin chains are cellular inhibitor of apoptosis proteins 1 and 2 (cIAP1/2), ITCH and putatively X-linked inhibitor of apoptosis (XIAP) (Bertrand*, et al.* 2009, Krieg*, et al.* 2009, Tao*, et al.* 2009). NF-κB essential modulator (NEMO; also known as IKKγ) is recruited to the intermediate region of RIP2 (Hasegawa*, et al.* 2008) and is subsequently ubiquitinated at K285 (Abbott*, et al.* 2004) involving TRAF6 (Abbott*, et al.* 2007). Subsequently, IκB kinase α (IKKα) and IKKβ bind to NEMO (Inohara*, et al.* 2000, Girardin*, et al.* 2001) and are phosphorylated by the auto-activated serine

threonine kinase TAK1 (Shim, *et al.* 2005). The activated IKK complex phosphorylates the NF-κB inhibitor IκBα, targeting it for poly-ubiquitination (Liu and Chen 2011). Ubiquitinated IκBα is degraded by the 26S proteasome allowing NF-κB to localize to the nucleus and initiate target gene transcription.

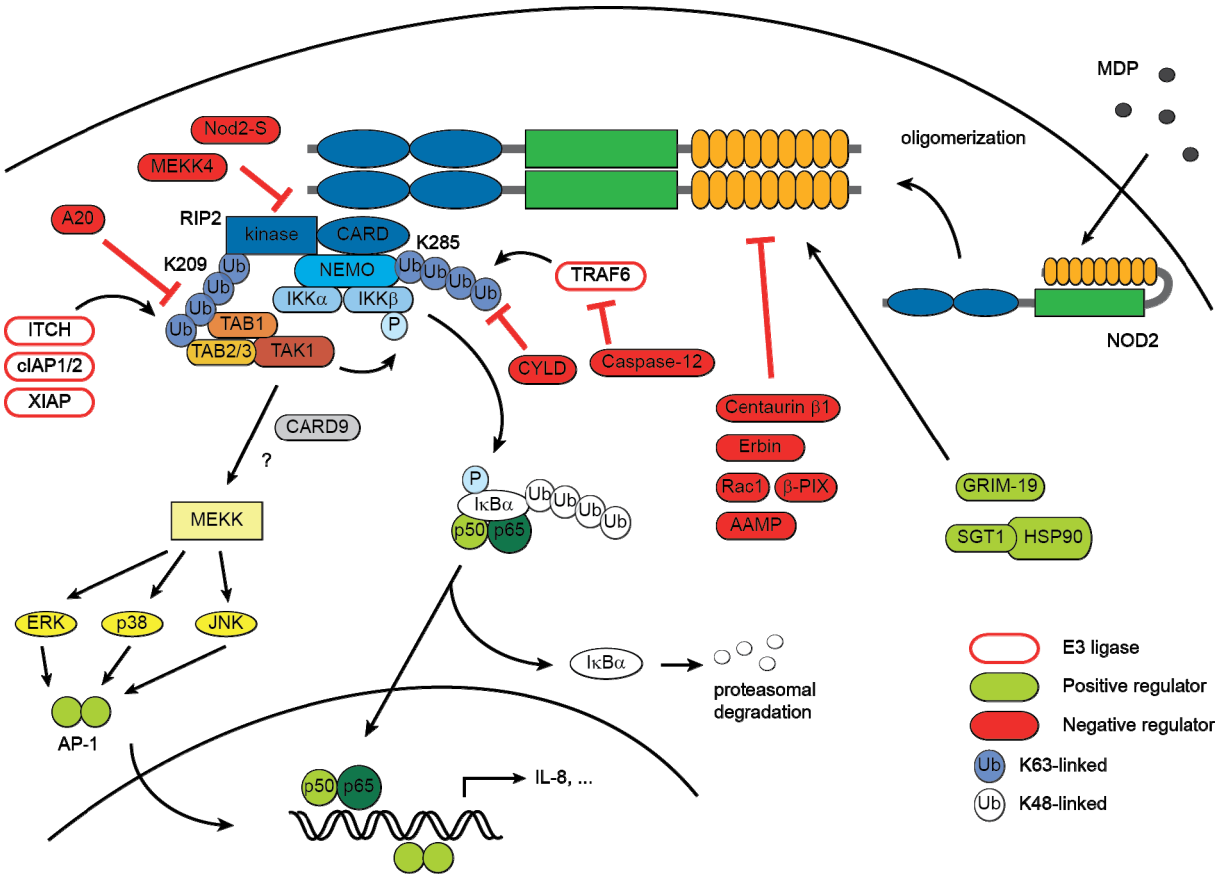

Figure 1.3: NOD2 signalling pathway

NOD2 signalling pathway including positive (green) and negative (red) regulators is shown. RIP2 and NEMO ubiquitination sites are indicated. Apart from certain regulators, the NOD2 signalling pathway depicted here is in principal the same as for NOD1. Refer to text for more details.

Dependent on RIP2 and TAK1, NOD1 and NOD2 also activate the mitogen-activated protein (MAP) kinases p38, c-Jun N-terminal kinase (JNK) and extracellular signal-regulated kinase (ERK), although the signalling pathways are not well resolved (Kobayashi, *et al.* 2005, da Silva Correia, *et al.* 2007a, Park, *et al.* 2007a). At least for NOD2-mediated p38 activation involvement of CARD9 has been shown (Hsu, *et al.* 2007). MAPK signalling results in the activation of AP-1 transcription factors. The activation of NF-κB and AP-1 mediated by NOD1 and NOD2 signalling leads to

secretion of pro-inflammatory cytokines and chemokines and to the production of antimicrobial peptides (Franchi*, et al.* 2009).

Several mediators of the signalling pathway have been identified, although many more factors affecting NOD2 signalling are known. A20 broadly suppresses pro-inflammatory signalling and also inhibits NOD1- and NOD2-induced NF-κB activation by de-ubiquitination of RIP2 (Hasegawa*, et al.* 2008, Hitotsumatsu*, et al.* 2008), whereas CYLD has been shown to de-ubiquitinate NEMO (Abbott*, et al.* 2004). Heat-shock protein (HSP) 90 and SGT1 are linked with R protein function in plant defence. Both NOD1 and NOD2 interact with the SGT1/HSP90 complex. Inhibition of HSP90 decreased NOD2-mediated signalling (Mayor*, et al.* 2007) and reduced NOD1 and NOD2 protein levels (da Silva Correia*, et al.* 2007b). However, SGT1 is only essential for NOD1 signalling but dispensable for NOD2 activation (da Silva Correia*, et al.* 2007b).

The GTPase-activating protein Centaurin β1 (CENTB1), a member of the ADP-ribosylation factor family binds NOD1 and NOD2 and down-regulates NOD-specific NF-κB activation (Yamamoto-Furusho*, et al.* 2006). Erbin specifically binds NOD2 at the plasma membrane and inhibits NOD2-mediated NF-κB activation and cytokine secretion (McDonald*, et al.* 2005, Kufer*, et al.* 2006b). Both, Erbin and CENTB1 are up-regulated in response to NOD2 activation supporting a negative regulatory role. Rac1, which is involved in cytoskeletal reorganisation, and its guanine nucleotide exchange factor β-PIX both interact with NOD2 in a MDP-dependent manner. They recruit NOD2 to the plasma membrane leading to negative regulation of NOD2 signalling by enabling interaction with Erbin (Eitel*, et al.* 2008). Inhibition of the NOD2-Rac1 interaction and disruption of the actin cytoskeleton both enhance NOD2 signalling (Legrand-Poels*, et al.* 2007) indicating that membrane recruitment is important for negative regulation. The angio-associated migratory cell protein (AAMP) binds NOD2 and negatively regulates NF-κB activation (Bielig*, et al.* 2009), whereas GRIM-19 (gene associated with retinoid-interferon-induced mortality 19) is required for NOD2-mediated NF-κB activation and bacterial clearance (Barnich*, et al.* 2005b). MEKK4 and Caspase-12 interfere with NOD2-RIP2 and RIP2-TRAF6 interaction, respectively, and thereby negatively influence NF-κB activation (Clark*, et al.* 2008, LeBlanc*, et al.* 2008). Two NOD2 isoforms are reported to impair NOD2 signalling. NOD2-C2, containing the two CARD domains reduces MDP-induced

NOD2 WT-mediated NF-κB activation (Kramer*, et al.* 2010). NOD2-S possessing a complete CARD1 and a truncated CARD2 competes with NOD2-RIP2 binding thereby inhibiting NF-κB activation (Rosenstiel*, et al.* 2006).

NOD2 has also been shown to activate the non-canonical NF-κB pathway via the NF-κB-inducing kinase (NIK) in macrophages (Pan*, et al.* 2006) and to interact with the NAD(P)H oxidase family member DUOX2 at the plasma membrane of intestinal epithelial cells to induce ROS production, required for direct bactericidal activity (Lipinski*, et al.* 2009). Furthermore, NOD2 has also been reported to be involved in antiviral signalling. It interacts with 2'-5'-oligoadenylate synthetase type 2 (OAS2) (see above) and can enhanced RNaseL activity in response to poly I:C (Dugan*, et al.* 2009). Additionally, NOD2 has been suggested to detect viral ssRNA, leading to IRF3-mediated type-I IFN responses. This involves the mitochondrial protein MAVS, which is also critical for IFN signalling by the RLRs RIG-I and MDA5 (Sabbah*, et al.* 2009).

NOD1 and NOD2 are both involved in inducing autophagy in response to bacterial infection by recruiting the key autophagy regulator ATG16L1 to the entry foci of invading bacteria (Cooney*, et al.* 2009, Travassos*, et al.* 2009). This response is independent of NF-κB activation, while the involvement of RIP2 is under debate.

1.2.2 NOD1 and NOD2 in bacterial infection and disease

Although several studies show that NOD1 and NOD2 are involved in sensing pathogenic and non-pathogenic bacteria *in vitro*, much less is known about their *in vivo* function in host defence. NOD1 deficient mice intragastrically infected with the non-invasive pathogen *Helicobacter pylori* have higher bacterial loads compared to wild type mice (Viala*, et al.* 2004). *H. pylori* recognition by NOD1 relies on a cag pathogenicity island encoding a type IV secretion system to deliver PGN into the host cell (Viala*, et al.* 2004). NOD2 has been shown to be crucial for detection of invasive *Listeria monocytogenes* in the intestine. NOD2 deficient mice orally infected with *L. monocytogenes* are more susceptible to infection, have a higher bacterial load and impaired α-defensin production compared to wild type mice (Kobayashi*, et al.* 2005). The mechanisms how NOD1 and NOD2 ligands enter the cytosol are poorly

understood. Apart from the bacterial secretion systems described above, there is also evidence that PGN fragments are delivered into the cytosol by pore-forming bacterial toxins (Ratner*, et al.* 2007), via endocytosis (Marina-Garcia*, et al.* 2009), selective plasma membrane transporters (Ismair*, et al.* 2006, Swaan*, et al.* 2008) and bacterial outer-membrane vesicles (OMVs) (Kaparakis*, et al.* 2009, Bielig*, et al.* 2011).

NOD1 and NOD2 function together with TLRs in bacterial sensing. Several publications show synergistic production of pro-inflammatory cytokines upon stimulation with TLR and NOD1 or NOD2 agonists (Chamaillard*, et al.* 2003, Fritz*, et al.* 2005, Tada*, et al.* 2005, Park*, et al.* 2007b). As a form of protection against overwhelming cytokine production TLR ligands induce a transient state of tolerance against subsequent TLR stimulation and also continued MDP stimulation induces refractoriness to NOD1 and NOD2 agonists (Kim*, et al.* 2008a). Recent publications have revealed that macrophages and mice rendered tolerant to TLR stimulation remained responsive to NOD1 and NOD2 stimulation (Kim*, et al.* 2008b). This indicates the importance of NOD1 and NOD2 function when TLR signalling is silenced *i.e.* in the gastrointestinal tract. NOD1 and NOD2 are also implicated in the induction of adaptive immunity. Both have been shown to have adjuvant activity, mediate T cell differentiation (Kobayashi*, et al.* 2005, Fritz*, et al.* 2007) and are important for neutrophil recruitment upon bacterial infections (Frutuoso*, et al.* 2010, Hasegawa*, et al.* 2011).

Mutations in *nod2* (CARD15) have the strongest predisposition for the development of Crohn's disease (CD) in the western population (Hugot*, et al.* 2001, Ogura*, et al.* 2001a). About 30 % of the patients suffering from CD harbour mutations in *nod2 (Hruz and Eckmann 2010)*. CD is a chronic inflammatory bowel disease (IBD) of the gastrointestinal mucosa characterized by aphthous lesions, ulceration and transmural granulomatous inflammation (Hruz and Eckmann 2010). About 80 % of the known *nod2* mutations are associated with CD (Lecat*, et al.* 2010), with NOD2 1007fs (also called NOD2 3020insC or NOD2fs) being the most frequent (8.2 %) (Ogura*, et al.* 2001a). Other mutations are linked with early onset sarcoidosis (EOS) and Blau syndrome (BS), two auto-inflammatory disorders (Lecat*, et al.* 2010). EOS- and BS-associated mutations mostly affect the NBD domain and show increased basal NF-κB activation. In contrast, CD-associated mutations are usually located near or within

the LRRs and lead to a loss-of-function phenotype. Several publications demonstrate decreased cytokine production by different cell types harbouring the NOD2fs mutation in response to MDP (Inohara*, et al.* 2003, Netea*, et al.* 2004, Netea*, et al.* 2005, Kramer*, et al.* 2006), impaired α-defensin production in the inflamed gastrointestinal tract of CD patients with the NOD2fs mutation (Wehkamp*, et al.* 2004) as well as accumulation of bacterial endotoxin in the intestinal tissue (Kosovac*, et al.* 2010). NOD2fs also fail to recruit ATG16L1 to the plasma membrane leading to impaired clearance of invasive bacteria by autophagy (Travassos*, et al.* 2009). However, CD is characterized by high levels of NF-κB activation and TNFα production, and both anti-TNFα therapy as well as NF-κB inhibitors are efficient in treating CD (Hruz and Eckmann 2010). This would rather suggest that CD-associated NOD2 mutations are gain-of-function mutations and promote inflammatory responses. Accordingly, a study using NOD2fs knock-in mice reported increased NF-κB activation in response to MDP (Maeda*, et al.* 2005). These different findings illustrate the still unresolved role of NOD2 in CD and indicate the complexity underlying CD development.

In contrast, polymorphisms in *nod1* (CARD4) are mainly found in the non-coding region and are associated with increased development of atopic eczema and asthma, along with increased serum IgE levels (Hysi*, et al.* 2005, Weidinger*, et al.* 2005). However, the mechanism by which NOD1 variants increase susceptibility to develop allergic diseases is unknown.

1.2.3 AAA+ ATPases

The apoptotic protease-activating factor 1 (APAF1) activates pro-caspase-9 downstream of mitochondria to induce apoptosis. Crystal structures revealed that APAF1 resides in an auto-inhibited, monomeric, ADP-bound state (Li*, et al.* 1997, Riedl*, et al.* 2005, Reubold*, et al.* 2011). Upon intrinsic cell death stimuli, cytrochrome c is released from mitochondria and binds to the C-terminal WD40 repeats of APAF1. This induces conformational changes, leading to the formation of an oligomeric signalling complex called apoptosome via the NBD domains (Riedl*, et al.* 2005, Reubold*, et al.* 2011). APAF1 has been shown to hydrolyse ATP (Riedl*, et al.* 2005), but the exact role of ATP hydrolysis in the activation process remains unclear. Since

no high resolution structural data on NLRs are available to date, the current model of NLR activation is deducted from APAF1 and from *in vitro* studies on purified NLRP1, NLRP3, NLRP12, and NLRC4 (Lu*, et al.* 2005, Duncan*, et al.* 2007, Faustin*, et al.* 2007, Ye*, et al.* 2008). Based on these data Danot *et al.* proposed a model for STAND ATPases (see below) comprising the following steps: (I) elicitor recognition, (II) conformational changes leading to a semi-opened state, (III) nucleotide exchange (ATP for ADP) to drive oligomerization, and (IV) deactivation of the signalling platform by ATP hydrolysis (Danot*, et al.* 2009).

APAF1 as well as all NLR proteins are members of the STAND (signal transduction ATPases with numerous domains) clade within the AAA+ (ATPases associated with various cellular activities) ATPase superfamily. Nucleotide binding and hydrolysis by STAND ATPases is mediated by conserved residues within the ATPase domain, most prominently the Walker A (P-loop) and B box (Hanson and Whiteheart 2005, Proell*, et al.* 2008). The Walker A box lysine (GxxxxG**K**[S/T]; x, any amino acid) interacts with a phosphate moiety of ATP (see also Table 1, page 59). The canonical Walker B box (hhhhD[D/E]; h, hydrophobic amino acid) consists of two acidic residues, where the first co-ordinates a Mg^{2+} ion required for ATP hydrolysis and the second primes a H_2O molecule for the hydrolysis reaction (Iyer*, et al.* 2004). NLR proteins with the exception of NAIP and NLRP11, however, contain a modified Walker B box lacking the second acidic residue. Instead, in most NLR proteins, including NOD1 and NOD2, the canonical Walker B box is followed by a conserved patch of acidic residues, the extended Walker B box (D[GAS]h**DE**) (Proell*, et al.* 2008). Other ATPase motifs are the Sensor 1, which co-ordinates an ATP γ-phosphate, whereas the conserved proline in the GxP motif is thought to interact with the adenine moiety. The AAA+ ATPase motif Sensor 2 is lacking in STAND clade ATPases. It is replaced by the WH domain in APAF1 and especially the conserved histidine is involved in co-ordinating the ADP β-phosphate group (Riedl*, et al.* 2005). Structural alignments revealed that this is also the case for NLRs (Proell*, et al.* 2008).

1.3 TRIM proteins

Tripartite motif-containing (TRIM) proteins are present in all metazoans, although the number varies between species (Sardiello*, et al.* 2008). They are involved in a broad

range of biological processes like cell proliferation, differentiation, development, morphogenesis and apoptosis and many TRIM proteins are expressed in response to IFNs (Rajsbaum*, et al.* 2008, Carthagena*, et al.* 2009). Members of the TRIM protein superfamily possess a RBCC motif at the N-terminus, which consists of a RING (really interesting new gene) and one or two B-box domains followed by a coiled-coil (CC) region.

RING domains are zinc-binding domains and represent the major type of E3 ligases in eukaryotes. E3 ligases mediate the conjugation of proteins with ubiquitin, small ubiquitin-like modifier (SUMO) or the ubiquitin-like molecule IFN-stimulated protein of 15 kDa (ISG15) (Bailly*, et al.* 1997, Deshaies and Joazeiro 2009). Ubiquitin is a small 8.5 kDa protein that can be attached by an isopeptide bond between the ubiquitin C-terminal carboxyl group and the N-terminal or lysine (K) ε-amino group of target proteins. This results in either mono-ubiquitination or poly-ubiquitination, where the ubiquitin molecules are linked by internal lysines to form chains. Protein ubiquitination plays an important role in the regulation of a range of cellular processes, depending on the linkage type. Assembly of at least four ubiquitin molecules linked via K48 typically targets proteins for proteasomal degradation by the 26S proteasome (Hershko and Ciechanover 1998), whereas mono-ubiquitination and K63-linked chains are associated with the modification of signal transduction processes (reviewed in (Chen and Sun 2009)). The ubiquitination pathway involves activation of ubiquitin by an E1 ubiquitin-activating enzyme and ubiquitin transfer from E1 to an E2 ubiquitin-conjugating enzyme. The E3 ubiquitin ligase interacts with ubiquitin-bound E2 and the target protein, bringing them into close proximity to induce ubiquitin transfer from E2 to the target (Deshaies and Joazeiro 2009). The E3 ubiquitin ligase activity is crucial for many TRIMs to mediate their effect on signalling pathways as demonstrated *in vitro* for several TRIM proteins in conjunction with specific E2s (Napolitano*, et al.* 2011).

The B-box domains are also zinc-binding motifs, but B-box 1 and 2 differ in their consensus sequences. They are unique for TRIMs and structurally related to the RING domain. TRIM proteins either contain one or both B-boxes, although B-box 1 is never present without B-box 2. No overall function has been ascribed to this domain, but they seem to be involved in viral recognition by some TRIM proteins and mutations within the B-boxes of TRIM18 (also called midline 1, MID1) are associated

with X-linked Opitz syndrome (Ozato*, et al.* 2008). The CC region mediates TRIM homo-oligomerization to large complexes, which occupy discrete cytoplasmic or nuclear sub-compartments (Reymond*, et al.* 2001).

TRIM proteins differ from each other by their C-terminal domain, although most TRIM family members are characterized by a PRY, a SPRY, or combined PRY-SPRY domain (Ozato*, et al.* 2008, McNab*, et al.* 2010). The ~61 aa PRY and the ~140 aa SPRY domains together are also called B30.2 domain and are thought to mediate target binding. The SPRY domain is evolutionarily more ancient as it is found in animals, plants and fungi, whereas the B30.2 domain is only found in vertebrates with an adaptive immune system (Rhodes*, et al.* 2005). In humans, B30.2/PRY-SPRY domains are only present at the C-terminus in TRIM proteins and in butyrophilin-related transmembrane glycoproteins (BTNs), which are receptors of the immunoglobulin superfamily (Henry*, et al.* 1997). Based on their C-terminal domain TRIM proteins are grouped into 11 classes, with different sub-cellular localization, cell-specific expression and function (Ozato*, et al.* 2008).

1.3.1 TRIM proteins regulating immune responses

Recently, members of the TRIM family have been implicated in regulating antiviral and antimicrobial immune responses. The importance of TRIM proteins in regulating immune homeostasis is also highlighted by inherited disorders that are associated with mutations in some of these genes. TRIM20/pyrin is mutated in the inflammatory disease familial Mediterranean fever (FMF) (French_FMF_Consortium 1997, International_FMF_Consortium 1997). The most prominent example for the immune function of a TRIM protein involves TRIM5α which is required for restricting retroviral infection in higher primates (reviewed in (Nakayama and Shioda 2010)).

Important functions in the induction of innate immune responses have also been described for TRIM8, TRIM23, TRIM25, and TRIM56. TRIM8 decreases suppressor of cytokine signalling 1 (SOCS-1) protein levels leading to an inhibition of IFNγ signalling repression (Toniato*, et al.* 2002). TRIM23 induces K27-linked ubiquitination of NEMO necessary for NF-κB and IRF3 activation downstream of TLR3 and RIG-I (Arimoto*, et al.* 2010). TRIM25 mediates K63-linked ubiquitination of the RIG-I CARD

in response to viral RNA leading to interaction with MAVS and antiviral signalling (Gack*, et al.* 2007), whereas TRIM56 is involved in dsDNA-mediated type I IFN activation (Tsuchida*, et al.* 2010).

In contrast, TRIM proteins can also negatively regulate inflammatory responses: Mouse TRIM30α induces ubiquitination and degradation of TAB2 and TAB3 thereby inhibiting TLR-induced NF-κB activation and has also been shown to negatively regulate NLRP3 inflammasome activation (Shi*, et al.* 2008, Hu*, et al.* 2010). Additionally, some TRIM proteins such as TRIM21/Ro52 are reported to have both positive as well as negative regulatory functions, depending on the experimental context (Kong*, et al.* 2007, Higgs*, et al.* 2008, Yang*, et al.* 2009, Higgs*, et al.* 2010).

1.3.2 TRIM27

TRIM27 is a member of the TRIM superfamily and exhibits the classical PRY-SPRY domain C-terminal of the RBCC motif (see Figure 1.4). It is a 58 kDa protein and is expressed as two isoforms with isoform TRIM27β being truncated within the PRY-SPRY domain (aa position 358). TRIM27 was reported to be highly expressed in mouse spleen and thymus (Tezel*, et al.* 1999) and in cells of the hematopoietic compartment (Rajsbaum*, et al.* 2008). In contrast to many other TRIM proteins, TRIM27 expression is not altered by type I and II IFNs (Rajsbaum*, et al.* 2008, Carthagena*, et al.* 2009).

TRIM27 exhibits either nuclear or cytosolic localization depending on the cell type, suggesting different functions in different tissues (Cao*, et al.* 1997, Tezel*, et al.* 1999). A nuclear export sequence (NES) within the CC region is involved in different sub-cellular localization by differential masking of this theme (Harbers*, et al.* 2001). Furthermore, it has been shown that TRIM27 cytoplasmic localization is enhanced by protein kinase C α (PKCα) activation, although the signalling pathway remained unclear as TRIM27 is not a substrate of PKCα (Harbers*, et al.* 2001). Originally, TRIM27 (alternatively named RET finger protein, RFP) was identified as a part of the *rfp/ret* transforming gene generated by DNA rearrangements, in which the RING finger is essential for the oncogenic potential (Hasegawa*, et al.* 1996).

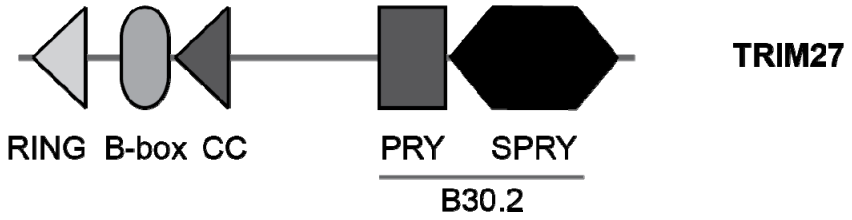

Figure 1.4: TRIM27 domain architecture

The classical RBCC motif at the TRIM27 N-terminus comprises a RING domain, a B-box 2 and a CC region. The C-terminal B30.2 domain is composed of a PRY and a SPRY domain. See also (Ozato*, et al.* 2008).

Like other TRIM proteins, TRIM27 can form homo-oligomers involving the B-box and CC domain (Cao*, et al.* 1997). Hetero-oligomerization has been observed between TRIM27 and TRIM19/PML (promyelocytic leukemia gene) in PML nuclear bodies (Cao*, et al.* 1998). In addition, TRIM27 interaction with int-6/eIF3e has been described in PML nuclear bodies (Morris-Desbois*, et al.* 1999). Int-6/eIF3e is a subunit of the translation initiation factor eIF3, has also been shown to interact with the 26S proteasome in fission yeast (Yen*, et al.* 2003) and to regulate protein stability (Buchsbaum*, et al.* 2007, Chen*, et al.* 2007). Furthermore, TRIM27 interaction with members of the PIAS family results in targeting of TRIM27 to nuclear bodies by TRIM27 SUMOylation (Matsuura*, et al.* 2005). TRIM27 has also been shown to be a DNA-binding protein (Isomura*, et al.* 1992).

Although the molecular function for TRIM27 remains largely elusive, TRIM27 has been shown to confer E3 ubiquitin ligase activity *in vitro* with the enzymes UBE2D1 and D3 (Napolitano*, et al.* 2011) and also to possess SUMO E3 ligase activity (Chu and Yang 2011). Functionally TRIM27 is thought to play a role as a transcriptional repressor (Shimono*, et al.* 2000, Bloor*, et al.* 2005), as a negative regulator of NF-κB and IFN-signalling pathways (Zha*, et al.* 2006), in apoptosis (Dho and Kwon 2003) and in cell cycle regulation (Patel and Ghiselli 2005).

1.4 Aim of this study

The NLR family member NOD2 is critically involved in mediating antimicrobial innate immune responses. However, NOD2 regulation is still poorly understood. As TRIM proteins are emerging as important regulators of innate immune responses (Ozato*, et al.* 2008, McNab*, et al.* 2010), a yeast two-hybrid screen was conducted to identify TRIM proteins physically interacting with NOD2. The aim of the first project of this study was to verify the hits found in the screen and to further characterize their function on NOD2 and NOD2-mediated signalling pathways.

The NOD2 ATPase domain seems to play an important role in regulating NOD2 activity because mutations mapping to this domain are associated with elevated basal NOD2 activity in auto-inflammatory disorders, whereas mutation of the Walker A box inhibit NOD2 signalling. Therefore, the second project of this study aimed to analyse conserved amino acids within the ATPase domain of NOD1 and NOD2 in a comparative systematic mutational approach.

2 Materials and Methods

2.1 Materials

2.1.1 Reagents, chemicals and substances

All chemicals were purchased from Roth, Merck or Sigma-Aldrich, unless otherwise noted.

Reagent	Manufacturer
3 MM CHR Chromatography Paper	Whatman
Anti-FLAG M2 Affinity Gel	Sigma-Aldrich
ATP	Sigma-Aldrich
c-myc AC, clone 9E10	Santa Cruz Biotechnology
Complete protease inhibitor cocktail tablets, EDTA-free	Roche
DAPI	Invitrogen, Molecular Probes
D-Luciferin	Sigma-Aldrich
dNTP Mix	Fermentas
Dulbecco's modified Eagle's medium	Biochrom AG
FBS	Biowest
FuGENE 6 Transfection Reagent	Roche
GeneRuler DNA Ladder, Low Range	Fermentas
Glutathione Sepharose	Amersham Biosciences
HiPerFect Transfection Reagent	Qiagen
illustra PuReTaq Ready-to-go PCR Beads	GE Healthcare
L-[35S]-methionine	Perkin Elmer
Lambda Hind III/phiX Hae III Marker	Roth
Leptomycin B	Sigma-Aldrich
Lipofectamin 2000 Reagent	Invitrogen
MDP	InvivoGen
PageRuler Prestained Protein Ladder	Fermentas
PBS (1x), for cell culture	Biochrom AG
Pefablock SC (AEBSF)	Fluka Analytical
Penicillin/Streptomycin	Biochrom AG

Phalloidin-FITC	Sigma-Aldrich
ProLong Gold Antifade Reagent	Invitrogen, Molecular Probes
Protein G Sepharose	GE Healthcare
Protran Nitrocellulose Transfer Membrane, 0.2 µm	Whatman
Restore Plus Western Blot Stripping Buffer	Thermo Scientific
Rotiphorese Gel 30 (37.5:1)	Roth
RPMI 1640 medium	Biochrom AG
SuperSignal West Femto Maximum Sensitivity Substrate	Thermo Scientific
SuperSignal West Pico Luminol/Enhancer Solution	Thermo Scientific
TNF-α	InvivoGen
Tri-DAP	InvivoGen
Trypsin/EDTA (10x)	Biochrom AG
X-tremeGENE 9 DNA Transfection Reagent	Roche

2.1.2 Kits

Kit	**Manufacturer**
BD OptEIA Human IL-8 ELISA Set	BD
Bio-Rad D_C Protein Assay	Bio-Rad
DuoSet ELISA (human IL-8 and IL-6)	R&D Systems
NucleoBond PC500 (Plasmid DNA preparation, Maxi)	Macherey-Nagel
NucleoSpin Extract II (PCR clean-up and gel extraction)	Macherey-Nagel
NucleoSpin Plasmid (Plasmid DNA preparation, Mini)	Macherey-Nagel
Qproteome Cell Compartment Kit	Qiagen
Rapid DNA Ligation Kit	Fermentas
RevertAid First Strand cDNA Synthesis Kit	Fermentas
RNeasy Mini	Qiagen
TnT coupled reticulocyte lysate system	Promega

2.1.3 Buffers and media

Buffers and media were autoclaved for 20 min at 121 °C or sterile filtered. All buffers and media were prepared with deionised millipore water and stored at RT, unless

otherwise noted. 1x buffers were prepared by 1:10 dilution of 10x buffers in deionised millipore water.

Buffer	**Compound**
Blocking solution	5 % milk powder in 1x PBS or 1x TBS
Buffer A	150 mM NaCl, 50 mM TRIS pH 7.5; before use add 2 mM DTT
Buffer B	500 mM NaCl, 50 mM TRIS pH 7.5 ; before use add 2 mM DTT
CBB	0.25 % CBB, 10 % acetic acid, 45 % ethanol
Destain buffer	7 % acetic acid, 25 % ethanol
D-Luciferin	0.27 mg/ml D-Luciferin in 50 mM Tris pH 8.0; -20 °C
DNA loading dye (10x)	50 % Saccharose, 100 mM EDTA, 0.25 % Bromphenolblue
LB Agar plates	1 L LB Medium + 1.5 % Bacto-Agar, supplemented with appropriate antibiotics (50 µg/ml Kanamycin, 100 µg/ml Ampicillin); 4 °C
LB Medium	10 g Bacto-Tryptone, 5 g Bacto-Yeast extract, 10 g NaCl, 1 L H_2O
Lower TRIS	1.5 M TRIS, 0.4 % SDS, pH 8.8
Lysis buffer	25 mM TRIS pH 8.0, 8 mM $MgCl_2$, 15 % glycerol, 1 % Triton X-100; before use add 1 mM DTT; 4 °C
NP40 lysis buffer	150 mM NaCl, 50 mM TRIS pH 7.4, 1 % NP40; 4 °C, freshly add protease- and phosphatase inhibitors
ONPG development buffer	1:4 dilution of ONPG stock solution in ONPG dilution buffer
ONPG dilution buffer	60 mM $Na_2HPO_4x2\ H_2O$, 40 mM NaH_2PO_4, 10 mM KCl, 1 mM $MgSO_4x7\ H_2O$, pH 7.0
ONPG stock solution	4 mg/ml ONPG in ONPG dilution buffer; 4 °C
PBS (10x)	1.37 M NaCl, 26.82 mM KCl, 80.9 mM $Na_2HPO_4x2\ H_2O$, 17.63 mM KH_2PO_4, pH 7.4
PBST	1x PBS + 0.05 % Triton X-100
Ponceau S	0.2 % Ponceau S, 3 % acetic acid

Reading buffer	Lysis buffer supplemented with 1 mM DTT, 0.54 µg/ml D-Luciferin, 1.33 mM ATP
RIPA lysis buffer	150 mM NaCl, 50 mM TRIS pH 7.4, 1 % Triton X-100, 0.1 % SDS, 0.5 % deoxycholic acid sodium salt ; 4 °C, freshly add protease- and phosphatase inhibitors
SDS running buffer (10x)	250 mM TRIS, 1.92 M glycine, 34.67 mM SDS
SDS sample buffer (6x)	7 ml 0.5 M TRIS pH 6.8 containing 0.4 % SDS, 3 ml glycerol, 1 g SDS, 1.2 mg bromphenol blue; -20 °C, freshly add 60 µl β-mercaptoethanol /1 ml sample buffer
TBE (10x)	0.89 M TRIS, 0.89 M boric acid, 20 mM Na_2EDTA pH 8.0
TBS (10x)	50 mM TRIS, 150 mM NaCl, pH 7.5
TBST	1x TBS + 0.05 % Triton X-100
Transfer buffer (10x)	250 mM TRIS, 1.92 mM glycine
Transfer buffer (1x)	1:10 dilution of 10x Transfer buffer + 20 % methanol
Transformation buffer	15 mM $CaCl_2$, 250 mM KCl, 10 mM PIPES, 55 mM $MnCl_2x4\ H_2O$, pH 6,7; sterile filtered
Triton buffer	100 mM NaCl, 10 mM HEPES pH 5.6, 1 % Triton-X-100
Triton lysis buffer	150 mM NaCl, 50 mM TRIS pH 7.4, 1 % Triton X-100 ; 4 °C, freshly add protease- and phosphatase inhibitors
Upper TRIS	0.5 M TRIS, 0.4 % SDS, pH 6.8

2.1.4 Enzymes

All restriction enzymes were purchased from Fermentas.

Enzyme	**Manufacturer**
Pfu DNA Polymerase	Fermentas
PfuTurbo DNA Polymerase AD	Statagene
Phusion	Finnzymes, BioLabs
T4 DNA Polymerase	Fermentas
T7 RNA Polymerase	Promega

2.1.5 Antibodies

Primary Antibodies

Antigen	Type	Clone	Dilution	Source
Actin	Rabbit polyclonal	A2066	WB 1:500	Sigma-Aldrich
Flag	Mouse monoclonal		WB 1:2000 IF 1:20,000	Stratagene
GAPDH	Rabbit polyclonal	FL-335	WB 1:1000	Santa Cruz Biotechnology
HA	Rabbit polyclonal	Y-11	WB 1:500	Santa Cruz Biotechnology
HA	Mouse monoclonal	12CA5	WB 1:1000	Roche
Lamin A/C	Rabbit polyclonal		WB 1:500	Cell Signaling Technology
Myc	Rabbit polyclonal	A-14	WB 1:1000	Santa Cruz Biotechnology
Myc	Mouse monoclonal	9E10	WB 1:1000 IF 1:1000	Sigma-Aldrich
NOD1	Rat monoclonal	7B10	WB 1:100	(Kufer, *et al.* 2008)
NOD2	Rat monoclonal	4A11	WB 1:100	(Kufer, *et al.* 2006b)
RIP2	Rabbit polyclonal		WB 1:500	Cayman Chemicals
TRIM27	Rabbit polyclonal	Y-11	WB 1:400 IF 1:500	IBL
Ub	Mouse monoclonal	P4D1	WB 1:1000	Santa Cruz Biotechnology
Ub K48-specific	Mouse monoclonal	Apu2	WB 1:1000	Millipore
Ub K63-specific	Mouse monoclonal	Apu3	WB 1:1000	Millipore

Secondary Antibodies

Antigen	Type	Label	Dilution	Source
Mouse IgG	Goat	HRP	WB 1:4000	Bio-Rad Laboratories
Mouse IgG, LC-specific	Goat	HRP	WB 1:4000	Jackson ImmunoResearch
Rabbit IgG	Goat	HRP	WB 1:4000	Bio-Rad Laboratories
Rabbit IgG, LC-specific	Mouse monoclonal	HRP	WB 1:4000	Jackson ImmunoResearch
Rat IgG	Goat	HRP	WB 1:4000	Jackson ImmunoResearch
Mouse IgG	Goat	AlexaFluor 488	IF 1:250	Invitrogen, Molecular Probes
Mouse IgG	Goat	AlexaFluor 546	IF 1:250	Invitrogen, Molecular Probes
Rabbit IgG	Goat	AlexaFluor 546	IF 1:250	Invitrogen, Molecular Probes
Rabbit IgG	Goat	AlexaFluor 405	IF 1:250	Invitrogen, Molecular Probes

2.1.6 Bacteria

Strain	Genotype	Reference
E. coli DH5α	F$^-$ Φ80*lac*ZΔM15 Δ(*lac*ZYA-*arg*F)U169 *deo*R *rec*A1 *end*A1 *hsd*R17 (r_k^-, m_k^+) *pho*A *sup*E44 *thi*-1 *gyr*A96 *rel*A1 λ^-	Invitrogen
E. coli XL1Blue	*recA1 endA1 gyrA96 thi-1 hsdR17 supE44 relA1 lac* [F' *proAB lacI^{q}ZΔM15* Tn*10* (Tet^r)]	Stratagene
E. coli BL21(DE3)-pLysS	F-, *ompT*, *hsdS$_B$* (r_B-, m_B-), *dcm*, *gal*, λ(DE3), pLysS, Cm^r	Stratagene

2.1.7 Cell lines

Cell line	Characteristics	Reference (No)
HEK293T	Human embryonic kidney cells transformed with adenovirus type 5 and expressing simian virus 40 large T antigen	ATCC (CRL 11268)
HeLa	Human epithelial cervix adenocarcinoma cells	ATCC (CCL 2)
THP1	Human peripheral blood monocytic cell line from acute monocytic leukaemia	ATCC (TIB 202)

2.1.8 Plasmids

Vector	Insert	Tag	Reference
NF-κB reporter Igκ-luciferase	-	-	(Munoz, *et al.* 1994)
pcDNA3	-	-	Invitrogen
pcDNA3.1/3xmyc-A, -B and -C	-	Myc	H. Sillje (MPI Biochemistry, Martinsried)
pcDNA3.1/3xmyc-B	TRIM27 B30.2	Myc	This study
pcDNA3.1/3xmyc-B	TRIM27 WT	Myc	This study
pcDNA3.1/3xmyc-B	TRIM27 ΔB30.2	Myc	This study
pcDNA3.1/3xmyc-B	TRIM27 ΔRING	Myc	This study
pcDNA3.1/3xmyc-B	TRIM27 ΔRING+BBox	Myc	This study
pcDNA3.1/3xmyc-C	NOD1 WT	Myc	A. Neerincx (Universität zu Köln)
pcDNA3.1/3xmyc-C	NOD2 WT	Myc	A. Neerincx, (Universität zu Köln)
pcDNA3.1/3xmyc-C	NOD2 K305R	Myc	A. Neerincx, (Universität zu Köln)
pcDNA3.1/3xmyc-C	TRIM27 WT	Myc	This study
pcDNA3.1/3xmyc-C	TRIM27 CC16/31AA	Myc	This study
pcDNA-β-Gal	-	-	(Kufer, *et al.* 2006b)

pCMV-SPORT 6	Human TRIM27	-	imaGenes
pCMV-Tag2A, B and C	-	Flag	Stratagene
pCMV-Tag2B	NOD1 WT	Flag	(Kufer, *et al.* 2008)
pCMV-Tag2B	NOD1 K208R	Flag	(Kufer, *et al.* 2008)
pCMV-Tag2B	NOD1 K208A	Flag	(Zurek, *et al.* 2011b)
pCMV-Tag2B	NOD1 D284A	Flag	(Zurek, *et al.* 2011b)
pCMV-Tag2B	NOD1 D287A	Flag	(Zurek, *et al.* 2011b)
pCMV-Tag2B	NOD1 E288A	Flag	(Zurek, *et al.* 2011b)
pCMV-Tag2B	NOD1 R333A	Flag	(Zurek, *et al.* 2011b)
pCMV-Tag2B	NOD1 P391A	Flag	(Zurek, *et al.* 2011b)
pCMV-Tag2B	NOD1 H517A	Flag	(Zurek, *et al.* 2011b)
pCMV-Tag2B	NOD2 WT	Flag	(Kufer, *et al.* 2006b)
pCMV-Tag2B	NOD2 K305R	Flag	(Kufer, *et al.* 2006b)
pCMV-Tag2B	NOD2 D379A	Flag	(Zurek, *et al.* 2011b)
pCMV-Tag2B	NOD2 D382A	Flag	(Zurek, *et al.* 2011b)
pCMV-Tag2B	NOD2 D382E	Flag	(Zurek, *et al.* 2011b)
pCMV-Tag2B	NOD2 E383A	Flag	(Zurek, *et al.* 2011b)
pCMV-Tag2B	NOD2 E383K	Flag	(Zurek, *et al.* 2011b)
pCMV-Tag2B	NOD2 R426A	Flag	(Zurek, *et al.* 2011b)
pCMV-Tag2B	NOD2 P486A	Flag	(Zurek, *et al.* 2011b)
pCMV-Tag2B	NOD2 H603A	Flag	(Zurek, *et al.* 2011b)
pCMV-Tag2B	NOD2 CARD	Flag	(Kufer, *et al.* 2006b)
pCMV-Tag2B	NOD2 ΔCARD	Flag	(Kufer, *et al.* 2006b)
pCMV-Tag2B	NOD2 NBD	Flag	(Kufer, *et al.* 2006b)
pCMV-Tag2B	NOD2 ΔLRR	Flag	(Kufer, *et al.* 2006b)
pCMV-Tag2B	NOD2 LRR	Flag	(Kufer, *et al.* 2006b)
pCR3.V72-Met-VSV	RIP2	VSV	M. Thome (University of Lausanne)
pGEX-II	-	GST	I. Roux (Institut Pasteur, Paris)
pGEX-II	TRIM27 WT	GST	This study
pGEX-II	TRIM27 ΔRING	GST	This study

pGEX-II	TRIM27 ΔRING+B-box	GST	This study
pRK5-HA	Ubiquitin WT	HA	Addgene
pUNO	Human IKKβ	HA	InvivoGen

2.1.9 Oligonucleotides

Primers were synthesized by MWG-Biotech AG. RT-PCR primers for TRIM27 were purchased from Qiagen (QT00051954).

Primer	Application	Sequence (5'-3')
GAPDH_fwd	RT-PCR	GGTATCGTGGAAGGACTCATGAC
GAPDH_rev	RT-PCR	ATGCCAGTGAGCTTCCCGTTCAG
Myco_fwd	Mycoplasma detection	CACCATCTGTCACTCTGTTAACC
Myco_rev	Mycoplasma detection	GGAGCAAACAGGATTAGATACCC
Seq_NOD2_fwd1	NOD2 sequencing	TGGAGAACATGCTGGACCTG
Seq_NOD2_fwd2	NOD2 sequencing	AGTGCATGGCCAAACCACTC
Seq_NOD2_fwd3	NOD2 sequencing	AGGAACTGTTGCTGCAGGAG
TRIM27_aa1_fwd	Cloning of TRIM27 deletion constructs	GCGCGGATCCGATGGCCTCCGGGAGTGTGG
TRIM27_aa133_fwd	Cloning of TRIM27 deletion constructs	GCGCGGATCCGGAGGAGGCGGTGGAGGGC
TRIM27_aa295_rev	Cloning of TRIM27 deletion constructs	GCGCGAATTCTGTGAACTGCTTTAGACTCTCCG
TRIM27_aa296_fwd	Cloning of TRIM27 deletion constructs	GCGCGGATCCGGAAAAAATGCAGTCAGATATGGA
TRIM27_aa513_rev	Cloning of TRIM27 deletion constructs	GCGCGAATTCTCAAGGGGAGGTCTCCATGG
TRIM27_aa63_fwd	Cloning of TRIM27 deletion constructs	GCGCGGATCCGAGGCACATGCGGCCCAACC
TRIM27_Bam_fwd	Cloning of TRIM27 into pCMV-Tag2B, BamHI	GCGCGGATCCATGGCCTCCGGGAGTGTG
TRIM27_C16A_fwd	Site-directed mutagenesis: TRIM27 E3	CAGCAGGAGACCACCGCCCCCGTGTGCCTGCA

TRIM27_C31A_fwd	Site-directed mutagenesis: TRIM27 E3	CCCATGATGCTCGACGCCGGCC ATAACATCTG
TRIM27_Eco_rev	Cloning of TRIM27 into pCMV-Tag2B, EcoRI	GCGCGAATTCTCAAGGGGAGGT CTCCATGG

2.1.10 siRNA

siRNA	Target sequence (5'-3')	Company (Name; Number)
CTR		Qiagen (AllStars Negative CTR, 1027281)
NOD2	CTGCCACATGCAAGAAGTATA	Qiagen (CARD15_3; SI00133049)
TRIM27-1	AAGACTCAGTGTGCAGAAAAG	Qiagen (Zha*, et al.* 2006)
TRIM27-3	CAGAACCAGCTCGACCATTTA	Qiagen (Hs_RFP_6, SI03062794)

2.1.11 Technical equipment and software

Technical equipment	Supplier
Biofuge Pico	Heraeus Instruments GmbH
Centrifuge 5415R	Eppendorf
FV-1000 laser scanning microscope (objective: PlanApo, x60/1.40 oil, ∞/0.17)	Olympus
Gel electrophoresis	Bio-Rad Laboratories
Luminescent Image Analyzer, LAS-4000	Fujifilm
Luminometer Centro XS3 LB960	Berthold Technologies
Megafuge 1.0	Heraeus Instruments GmbH
Microtiter plate reader Photometer	Anthos Micosysteme GmbH
Multifuge 4KR	Heraeus Instruments GmbH
Nano Photometer™	Implen GmbH
OD600 DiluPhotometer™	Implen GmbH
PhosphorImager	Bio-Rad Laboratories

Thermocycler	MWG-Biotech
Trans Blot SD, Semi-dry Transfer cell	Bio-Rad Laboratories

Software	**Supplier**
Adobe Acrobat Pro	Adobe Systems GmbH
Adobe Illustrator CS5	Adobe Systems GmbH
Adobe Photoshop CS5	Adobe Systems GmbH
EndNote X	Thomson Reuters
FV10-ASW 1.6	Olympus
Microsoft Office 2003	Microsoft
WCIF ImageJ	(Rasband 2007)

2.2 Methods

2.2.1 Cell biological methods

Cell culture

HEK293T and HeLa cells were cultivated at 37 °C in a 5 % CO_2 atmosphere in Dulbecco's modified Eagle's medium (DMEM) supplemented with 10 % heat-inactivated fetal bovine serum (FBS), penicillin and streptomycin (100 IU/ml and 100 mg/ml, respectively). THP1 cells were cultivated in RPMI 1640 supplemented as described above (supplemented media are subsequently referred to as medium). Cells were continuously tested for absence of mycoplasma infection by PCR.

To freeze cells, they were centrifuged for 5 min at 1000 rpm and RT and the pellet was resuspended in medium supplemented with 10 % DMSO. 1 ml aliquots were frozen o/n at -80 °C in an isopropanol-containing box.

To thaw cells, they were incubated at 37 °C until thawed and subsequently 10 ml medium was added. After centrifugation for 5 min at 1000 rpm and RT the pellet was resuspended in fresh medium and the cells were transferred into a cell culture dish and cultured as described above.

Transient DNA transfection

For transient DNA transfection cells were seeded in DMEM without antibiotics into the adequate cell culture dish 24 h prior to transfection in order to reach a cell density of about 60-70 %. For transfection Lipofectamin 2000 (2.5 µl/1 µg DNA) or FuGENE6 (3 µl/1 µg DNA) were used according to the manufacturer's instructions.

siRNA transfection

For siRNA transfection in THP1 cells $2x10^5$ cells/well were seeded in 500 µl medium in 24-well plates and differentiated with 0.1 µM PMA. 24 h later medium was removed and replaced by 100 µl fresh medium. Transfection mixes were prepared using 100 nM siRNA, 6 µl HiPerFect and 100 µl medium without supplementaries per well. After 5-10 min at RT transfection mixes were added to the cells. 6 h later 400 µl medium were added to the cells. The medium was changed one day after transfection. 72 h after siRNA transfection cells were stimulated o/n with 10 µM MDP or left unstimulated. Supernatants were collected and IL-8 secretion was determined by ELISA. Cell lysates were subjected to Western blot analysis for knock-down control.

Luciferase reporter gene assay

$3x10^4$ HEK293T cells per well were seeded in 96-well plates and transfected with 8.6 ng β-galactosidase, 13 ng luciferase NF-κB-reporter, different amounts of Flag-NOD1 or Flag-NOD2 (0.1, 0.5, 1 ng) or 0.1 ng NOD2 or 10 ng IKKβ expression plasmids either with or without myc-TRIM27 as indicated, added up with pcDNA to 51 ng total DNA using FuGene6 (Roche) (see also (Zurek*, et al.* 2011a)). Cells were directly stimulated with 500 nM Tri-DAP, 50 nM MDP or 10 ng/ml TNF or left unstimulated, as indicated. After 16 h, cells were lysed in luciferase lysis buffer and luciferase activity was measured using a standard plate luminometer. Standard deviation (SD) was calculated from triplets and luciferase activity was normalized as a ratio to β-galactosidase activity.

Significance was assessed with a two-sided Student's t-test (*, $P<0.05$; **, $P<0.01$; ***, $P<0.005$).

Indirect immunofluorescence

For indirect immunofluorescence microscopy, HeLa cells were seeded in 24-well plates on glass cover slips and transiently transfected with 0.8 µg of expression plasmids, as indicated using Lipofectamin 2000 transfection reagent according to the manufacturer's instructions. After 24 h, cells were fixed with 3 % paraformaldehyde (PFA) in PBS for 10 min and permeabilized with 0.5 % Triton X-100 in cold PBS for 5 min. Cells were blocked in 3 % bovine serum albumin (BSA) in PBS for 20 min and incubated successively in primary and secondary antibodies. Primary antibody: mouse anti-Flag (1:20,000), rabbit anti-TRIM27 (1:500) and mouse anti-myc (1:1000). Secondary antibody: goat anti-rabbit AlexaFluor 546 (1:250) and goat anti-mouse AlexaFluor 488 (1:250). DNA was stained with DAPI (5 µg/ml) and F-actin with Phalloidin-FITC (2.5 µg/ml). Cells were mounted in ProLong Gold antifade reagent. Image acquisition of z-stacks was performed on an Olympus FV-1000 laser scanning microscope (objective: Olympus PlanApo, 60x/1.40 oil, ∞/0.17) and processed using ImageJ software (Rasband 2007).

2.2.2 Molecular biological methods

Mycoplasma PCR

Cell culture supernatants were cooked for 5 min at 100 °C, briefly centrifuged and transferred on ice. 1 µl cell culture supernatant, 0.8 µl each Myco forward and reverse primer and 22.4 µl H_2O were mixed with illustra PuReTaq Ready-to-go PCR beads and the PCR was run with the following protocol. PCR products were subsequently analysed by 2% agarose gel electrophoresis.

Time	Temperature	No of cycles
2 min	94 °C	
2 min	57 °C	
2 min	72 °C	
30 sec	92 °C	34x
1 min	57 °C	
1 min	72 °C	
4 min	72 °C	
∞	4 °C	

Production of chemical competent bacteria

500 ml LB medium were inoculated with 1.5 ml of an *E. coli* DH5α preparatory culture. Bacteria were grown until OD_{600}=0.3-0.6 at 20 °C and 100 rpm. Bacteria were cooled for 10 min on ice and centrifuged for 15 min at 4000 rpm and 2 °C. The pellet was subsequently washed with 150 ml ice cold transformation buffer and centrifuged. The pellet was then resuspended in 40 ml transformation buffer and 3 ml DMSO. 500 µl aliquots were snap-frozen in liquid nitrogen and stored at -80 °C.

Bacterial transformation

50 µl chemical competent *E. coli* DH5α were transformed with ~100 ng plasmid DNA. Bacteria and DNA were incubated 30 min on ice and subsequently for 1 min at 42 °C. After cool down on ice, bacteria were directly plated on LB-agar plates containing 100 µg/ml ampicillin when transformed with a plasmid carrying an ampicillin resistance marker. When the transformed plasmid contains a kanamycin resistance marker bacteria were diluted in 250 µl LB medium and incubated for 45 min at 37 °C before plated on LB-agar plates containing 50 µg/ml kanamycin. Bacteria were grown o/n at 37 °C.

Isolation of plasmid DNA from *E. coli*

Bacteria were cultured o/n at 37 °C in 5 ml (Miniprep) or 100 ml (Maxiprep) LB medium supplemented with the appropriate antibiotic. Isolation of plasmid DNA was performed using the NucleoBond PC20 or PC500 plasmid preparation kit according to the manufacturer's instructions. The Maxiprep DNA was solved in ~200 µl 10 mM TRIS pH 8. Concentration and purity were determined using a nanodrop photometer measuring absorbance at 260 and 280 nm.

Isolation of RNA from human cell lines

RNA was isolated from human cell lines using the RNeasy Mini kit according to manufacturer's instructions. RNA was eluted with RNase-free water. Concentration and purity were determined using a nanodrop photometer measuring absorbance at 260 and 280 nm.

Reverse transcription of RNA

Reverse transcription of 1 µg isolated RNA into cDNA was performed using the RevertAid First Strand cDNA Synthesis kit and oligo-dT primer according to manufacturer's instructions.

End-point RT-PCR

PCRs of cDNA templates were performed according to the following protocol. The number of cycles depends on the gene and is indicated for each experiment. Reaction mixes were prepared on ice. PCR products were subsequently analysed by agarose gel electrophoresis.

Substance	Volume
Taq buffer (+KCl, -$MgCl_2$) [10x]	5 µl
$MgCl_2$ [25 mM]	4 µl
dNTPs [10 mM]	1 µl
Taq DNA polymerase [5 U/µl]	0.5 µl
Primer fwd	1 µl [10 pmol/µl] (GAPDH) 5 µl [10x] (TRIM27)
Primer rev	1 µl [10 pmol/µl] (GAPDH) 5 µl [10x] (TRIM27)
cDNA	1 µl (GAPDH) / 2 µl (TRIM27)
H_2O	Up to 50 µl

PCR was run according to the following program.

Time	Temperature	No of cycles
15 min	95 °C	
15 sec	94 °C	25-30x
30 sec	55 °C	
30 sec	72 °C	
5 min	72 °C	
∞	4 °C	

Restriction digestion of plasmid DNA

The required amount of plasmid DNA was digested by 5 U/µg DNA of the appropriate restriction enzyme for 2 h. Buffer and temperature conditions were adjusted according to the enzymes used.

Agarose gel electrophoresis

PCR products and digested plasmid DNA were separated and analysed by agarose gel electrophoresis. Agarose (1-2 %) was dissolved and boiled in 1x TBE. After cooling down the gel was poured into a gel tray and ~0.5 µg/ml ethidiumbromide was added. Samples were diluted with 10x DNA loading dye and loaded onto the gel. 5 µl GeneRuler Low Range DNA Ladder or Lambda Hind III/phiX Hae III Marker were used as standards. Samples were run for 30-60 min at 80 V and detected and/or cut out under UV light.

Ligation of DNA fragments

The digested DNA fragment was ligated into the linearised vector with an insert:vector ratio of 3:1 using the Rapid DNA Ligation kit according to the manufacturer's instructions. For a negative control H_2O instead of insert was used.

Site-directed mutagenesis

Point mutations were introduced by PCR using the QuikChange site-directed mutagenesis procedure (Stratagene). Primers used are listed above. Reaction mixes were prepared on ice according to the following protocol.

Substance	Volume
Phusion	25 µl
Plasmid DNA [100 ng/µl]	0.5 µl
Primer fwd [10 pmol/µl]	1.2 µl
Primer rev [10 pmol/µl]	1.2 µl
H_2O	Up to 50 µl

PCR was run according to the following program.

Time	Temperature	No of cycles
30 sec	95 °C	
10 sec	98 °C	20x
30 sec	65 °C	
3:45 min	72 °C	
∞	4 °C	

To digest the parental plasmid DNA, 1.5 µl Dpn I were added to the PCR reaction mix and incubated for 2 h at 37 °C. Subsequently 50 µl chemical competent bacteria were transformed with 2 µl digested PCR reaction mix.

2.2.3 Biochemical methods

Yeast two-hybrid screen

Binary two-hybrid screening was performed as described by Gyuris *et al.* (Gyuris*, et al.* 1993). Briefly, the bait plasmids (pEG202) express the cDNA fused directionally to the first 202 residues of LexA under the control of the constitutive ADH promoter. Prey plasmids (pJG4-5) express the cDNA fused to the B42 activation domain, the SV40T nuclear localization signal and an HA-tag under the control of the inducible GAL1 promoter. EGY42/EGY48 diploid strain was generated by mating for every pairwise combination. Six LexA-operators lacZ in the pSH18-34 vector and a genome integrated 4 LexA-operators LEU2 are used as reporters. The expression of two reporters was used to establish the interaction, blue-turning colonies and growth in the absence of Leu.

Expression and purification of recombinant protein from *E. coli*

TRIM27 and its deletion constructs were expressed as amino-terminal glutathione S-transferase (GST)-fusion proteins in Rosetta2 (DE3) pLys cells following overnight isopropyl 1-thio-β-D-galactopyranoside (IPTG, 100 µM) induction at 20 °C. Bacteria were lysed by a freeze-and-thaw cycle followed by addition of 1.5 % sarkosyl and pulsed sonication. GST-fusion proteins were purified from bacterial extracts with glutathione-Sepharose beads, followed by extensive washing with buffer A, buffer B and again buffer A. TRIM27 protein bound to glutathione-Sepharose beads was stored in buffer A at -80 °C.

In vitro transcription and translation

In vitro transcription/translation (IVT) of NOD2 was performed in the presence of L-[35S]-methionine (10 mCi/ml) using the TnT coupled reticulocyte lysate system and

T7 RNA polymerase according to the manufacturer's instructions. IVT preparation was diluted three times in PBS and incubated with recombinant TRIM27 protein bound to glutathione-Sepharose beads for 2 h at 4 °C. Beads were precipitated and washed five times with RIPA buffer before SDS loading buffer containing β-mercaptoethanol was added. Proteins were analysed by Laemmli sodium dodecylsulfate-polyacrylamide gel electrophoresis (SDS-PAGE) and followed by Coomassie staining. Autoradiographs were recorded using a PhosphorImager.

Protein concentration measurement

Protein concentrations were determined using the Bio-Rad D_C Protein Assay according to the manufacturer's instructions.

IL-8 ELISA

Secretion of IL-8 from human cells was determined by ELISA according to the manufacturer's instructions.

Co-immunoprecipitation

For immunoprecipitation, HEK293T cells were seeded in 6 cm dishes and transiently transfected with 1 µg of each plasmid as indicated using Lipofectamin 2000 or FuGENE6. After 24 h incubation cells were lysed in NP40 lysis buffer or RIPA lysis buffer containing phosphatase inhibitors (20 µM β-glycerophosphate, 5 mM NaF, 100 µM Na_3VO_4), protease inhibitors (Complete) and 2 mM EDTA. Lysates were cleared for 20 min at 14,000 *g* and 4 °C. Flag-tagged NOD2 was immunoprecipitated with anti-Flag beads (M2 agarose), myc-tagged TRIM27 with anti-myc beads (c-myc AC, clone 9E10) for 3 h at 4 °C. Beads were precipitated and washed five times with lysis buffer before SDS loading buffer containing β-mercaptoethanol was added. For ubiquitination analysis, 1 M NaCl was added to the washing buffer. Typically, 10 times more precipitate than input was loaded onto the gel. Proteins were separated by SDS-PAGE and subsequently transferred on nitrocellulose membrane by semi-dry Western blotting.

Subcellular fractionation

Isolation of membrane and cytosolic fractions was conducted as described (Barnich, *et al.* 2005a). Briefly, HEK293T cells were seeded in 6 cm cell-culture dishes and transiently transfected with 1 µg plasmid as indicated using Lipofectamine 2000. The cells were lysed in 300 µl Triton buffer supplemented with 2 mM EDTA, 4 mM Na_3VO_4, 40 mM NaF and protease inhibitor cocktail (Complete). The cytosolic fraction was obtained by centrifugation for 30 min at 10,000 *g* and 4 °C. Subsequently, the pellet was resuspended in 200 µl of Triton buffer containing 1 % SDS and was sonicated for 120 sec. After 5 min of centrifugation at 10,000 *g* and 4 °C, the resulting supernatant was collected. Equal amounts of proteins were subjected to SDS-PAGE and Western blot.

Isolation of cytosolic and nuclear fractions was performed using the Qproteome Cell Compartment kit according to the manufacturer's instructions.

The purity of the extracts was verified by immunoblotting using antibodies detecting cytosolic GAPDH or nuclear lamin A/C.

SDS-PAGE

Proteins were separated by SDS-PAGE (Laemmli 1970). Resolving and stacking gel were produced according to the following protocol. Samples were diluted in 6x Laemmli sample buffer containing β-mercaptoethanol, boiled for 5 min at 95 °C and loaded onto the gel. 2 µl PageRuler Prestained Protein Ladder was used as standard. Samples were run at 120 V until they reach the resolving gel and subsequently at 195 V until the dye front completely drained off the gel.

	Resolving gel		**Stacking gel**
	7.5 %	*10 %*	*5 ml*
H_2O [ml]	2.8	2.1	4.5
Lower TRIS [ml]	5		-
Upper TRIS [ml]	-		0.625
Acrylamide [ml]	1.9	2.5	0.325
TEMED [µl]	25		12.5
10 % APS [µl]	50		25

Western blot

Proteins separated by SDS-PAGE were subsequently transferred for 30-40 min at 15 V onto nitrocellulose membrane by semi-dry Western blotting. Blotting efficiency was controlled by Ponceau-S staining. Membranes were blocked for a minimum of 30 min at RT with blocking solution. Membranes were incubated successively with primary and secondary antibody. All antibodies were diluted in blocking solution. After incubation with antibody, membranes were washed three times with PBST or TBST. Proteins were detected by final incubation with SuperSignal West Pico Chemiluminescent Substrate or Femto Maximum Sensitivity Substrate. Signals were recorded on an electronic imaging system (LAS4000, Fujifilm).

Coomassie staining

Proteins were separated by SDS-PAGE and the gel was subsequently incubated in Coomassie brilliant blue (CBB) for 30 min at RT followed by incubation in destain buffer for 30 min at RT. The gel was further destained in H_2O. The gel was dried between cellophane for ~1 h at 80 °C in a drying plant.

3 Results

3.1 Characterization of TRIM27 as a new interaction partner of NOD2

3.1.1 TRIM27 is a new interaction partner of NOD2

Members of the TRIM protein family are emerging as important regulators of innate immune responses. We were interested in whether TRIM proteins could contribute to the NOD2 signalling pathway and regulate NOD2 activity. To search for TRIM proteins that physically interact with human NOD2, a binary yeast two-hybrid screen was conducted with most human TRIM proteins as bait and NOD2 as prey. This identified interactions of NOD2 with TRIM8, TRIM27, and TRIM50 (Figure 1.2). Of note, homo-interactions for all TRIM proteins were observed indicating the correct folding as previously reported (Reymond*, et al.* 2001).

prey / bait	NOD2 fl	TRIM1	TRIM5	TRIM8	TRIM11	TRIM13	TRIM18	TRIM20	TRIM21	TRIM27	TRIM50
TRIM1		XX									
TRIM5			XX								
TRIM8	x			XX						XX	
TRIM11					XX						
TRIM13						XX					
TRIM18							XX			XX	
TRIM20								XX			
TRIM21									XX		
TRIM27	x									XX	
TRIM50	x										x

Figure 3.1: Yeast two-hybrid screen
Results of a yeast two-hybrid screen using NOD2 full length (NOD2 fl) and several TRIM proteins as bait and prey, as indicated. x, weak interaction; XX, strong interaction. Screen performed by L. Napolitano and G. Meroni.

Next, these interactions were verified in co-immunoprecipitation experiments in human cells. To this end, co-immunoprecipitations experiments in HEK293T cells expressing Flag-NOD2 and Myc-tagged TRIM proteins were performed using anti-Flag beads. A strong interaction of NOD2 with TRIM27 was observed (Figure 3.2A), but no robust interaction was identified with the other TRIM proteins tested (data not shown). To assess the specificity of this interaction TRIM27 was tested for NOD1 binding. NOD1 is another member of the NLR family that is closely related to NOD2. As shown in Figure 3.2A, NOD1 had only low affinity for TRIM27. Reciprocal co-immunoprecipitations confirmed a strong interaction of TRIM27 with NOD2, but not with NOD1 (Figure 3.2B).

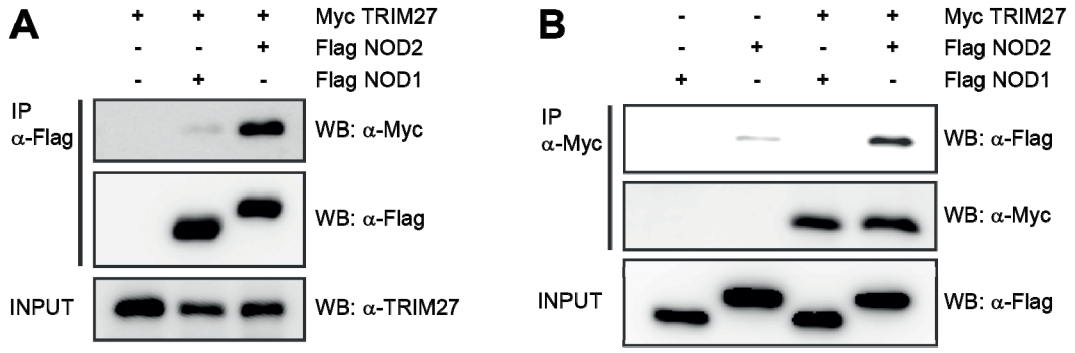

Figure 3.2: Co-immunoprecipitation of NOD2 and TRIM27
To verify NOD2-TRIM27 interaction, HEK293T cells were transfected with Myc-TRIM27 and Flag-NOD1 or –NOD2. 24 h later, lysates were subjected to immunoprecipitation using anti-Flag (A) or anti-Myc beads (B). Western blots of immunoprecipitates (IP) and total lysates (Input) were performed using the indicated antibodies.

To establish this interaction for endogenous TRIM27, several cell lines were tested for the amount of endogenous TRIM27 using endpoint RT-PCR to find an appropriate cell system. Because HEK293T cells strongly express TRIM27 (Figure 3.3A), these cells were transfected with Flag-NOD2. Subsequently NOD2 was immunoprecipitated using anti-Flag beads. Endogenous TRIM27 co-precipitated with NOD2 (Figure 3.3B), validating the NOD2-TRIM27 interaction for endogenous TRIM27.

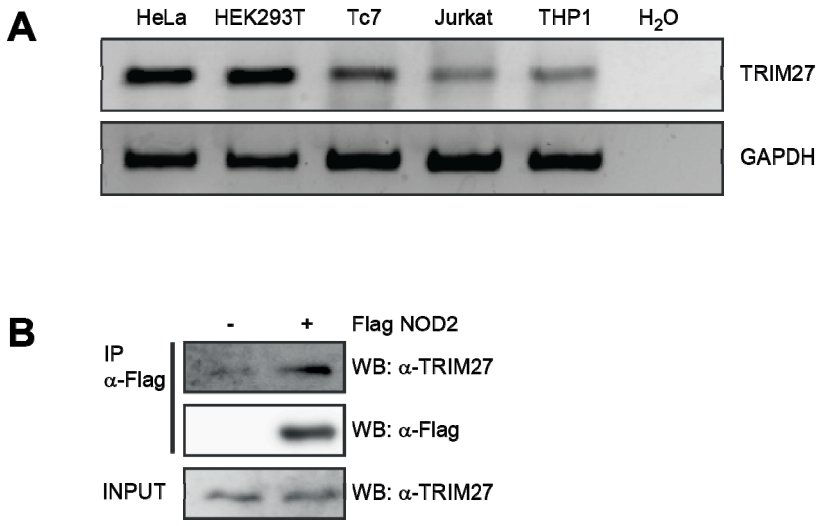

Figure 3.3: TRIM27 mRNA expression in different cell lines
(A) To define TRIM27 expression in different cell lines, end-point RT-PCR analysis of TRIM27 mRNA was performed. Amplification of GAPDH served as control. (B) To determine NOD2 interaction with endogenous TRIM27, HEK293T cells were transfected with Flag-NOD2. 24 h later, lysates were subjected to immunoprecipitation using anti-Flag beads and subsequently detected with the indicated antibodies.

To elucidate which of the protein domains mediated the NOD2-TRIM27 interaction, a series of co-immunoprecipitation experiments was performed with NOD2 deletion mutants lacking the two CARD domains (ΔCARDs) or the LRRs (ΔLRR) or comprising only the CARD (CARDs) or NBD (NBD) domains (depicted in Figure 3.4A, upper panels). NOD2 binding to TRIM27 was found to be independent of the CARD domains and the LRRs. Instead, the NOD2 NBD domain was sufficient to mediate interaction (Figure 3.4A, lower panels). Of note, binding of TRIM27 to NOD2 ΔLRR appeared to be stronger than to wild type NOD2. Next, TRIM27 domains needed for NOD2 binding were determined. TRIM27 constructs lacking the RING domain (ΔR), lacking both RING and B-box domains (ΔR+BB), TRIM27 missing the C-terminal PRY-SPRY domain (ΔP-S) or comprising only this domain (P-S) were used (depicted in Figure 3.4B, upper panels). Deletion of the RING or both RING and B-box domains did not abolish the interaction with NOD2. In contrast, no NOD2 binding to TRIM27 ΔPRY-SPRY was observed (Figure 3.4B, lower panels). The expression of TRIM27 ΔPRY-SPRY was weak, hence NOD2 binding at low affinity cannot formally be excluded (see Input panel in Figure 3.4B). However, a strong interaction of NOD2 with the TRIM27 PRY-SPRY domain alone was observed, showing that this domain is at least sufficient for NOD2 binding.

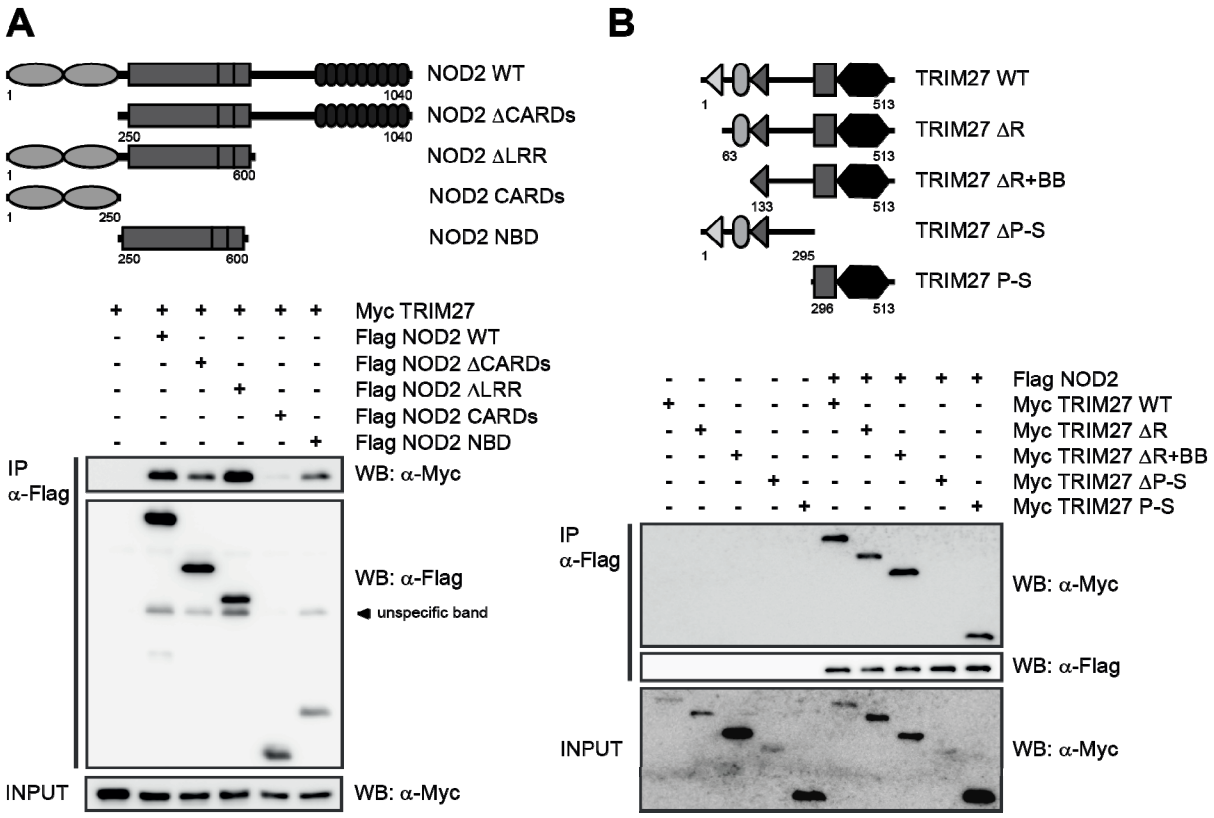

Figure 3.4: NOD2 NBD and TRIM27 PRY-SPRY domain are necessary for interaction
(A) The depicted NOD2 deletion constructs (top panels) were used to map the domains required for TRIM27 binding. Each of the NOD2 mutants shown was transfected with Myc-TRIM27 in HEK293T cells. Lysates were subjected to immunoprecipitation using anti-Flag beads and probed with the indicated antibodies. (B) The depicted TRIM27 deletion constructs (top panels) were used to map the domains required for NOD2 binding. Each of the TRIM27 mutants shown was transfected with or without Flag-NOD2 in HEK293T cells. Lysates were subjected to immunoprecipitation using anti-Flag beads and probed with the indicated antibodies.

To investigate if the NOD2-TRIM27 interaction was direct or dependent on adaptor molecules, direct protein-protein interaction assays were performed. To this end, *in vitro* transcribed and translated NOD2 was incubated with recombinant expressed GST-tagged TRIM27 protein bound to glutathione-Sepharose. NOD2 strongly bound to TRIM27 WT and TRIM27 ΔRING and also to a somewhat weaker extent to TRIM27 ΔRING+B-box. No non-specific binding was observed to GST alone, which was used as a control (Figure 3.5).

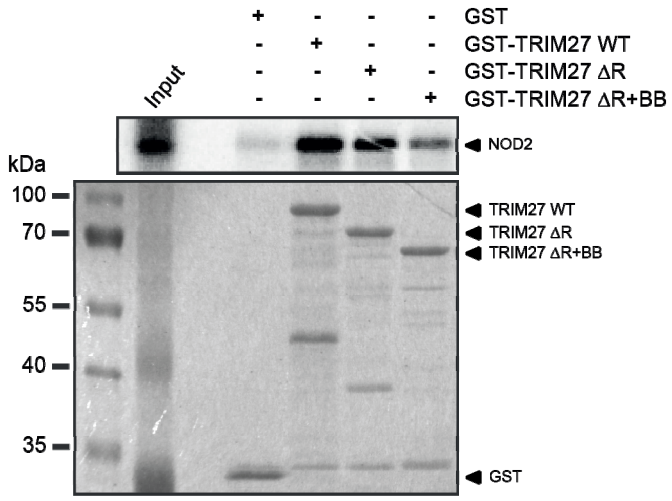

Figure 3.5: NOD2-TRIM27 binding is direct
To test whether NOD2-TRIM27 binding is direct, *in vitro* transcribed and translated L-[35S]-methionine-labelled NOD2 was incubated with recombinant GST-tagged TRIM27 protein (WT, ΔRING, ΔRING+B-box) or GST alone bound to glutathione-Sepharose beads. Both, the Coomassie stained gel (bottom) and the autoradiograph (top) are shown.

NOD2 is activated by MDP, a bacterial peptidoglycan fragment. To explore whether activation of NOD2 by MDP has an influence on NOD2-TRIM27 complex formation, co-immunoprecipitations were performed in HEK293T cells expressing Flag-NOD2 and Myc-TRIM27 stimulated with 10 µM MDP for 1, 2 or 3 h. Binding of TRIM27 to NOD2 was enhanced about 2-fold 3 h after MDP stimulation compared to untreated controls (Figure 3.6).

Collectively, these findings demonstrated that TRIM27 is a new direct interaction partner of NOD2 and that this interaction is modulated by NOD2 activation.

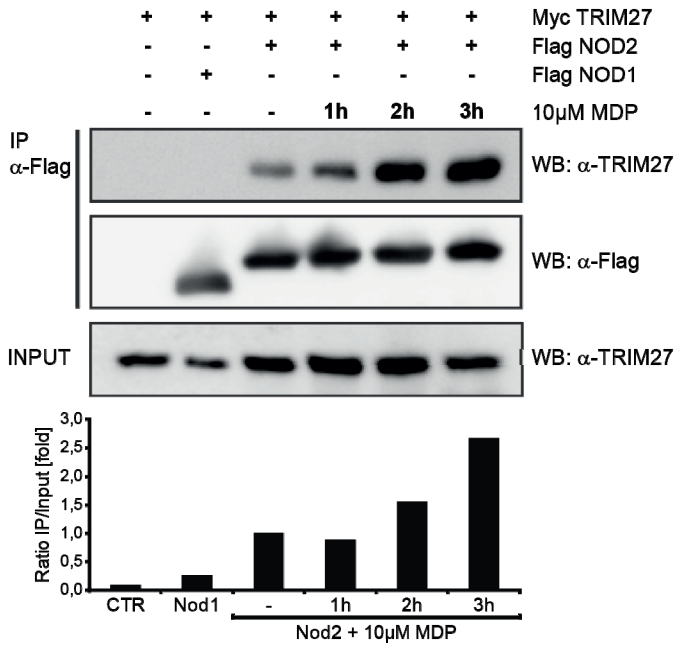

Figure 3.6: MDP enhanced NOD2-TRIM27 binding
To test whether NOD2-TRIM27 binding is influenced by NOD2 activation, HEK293T cells were transfected with Myc-TRIM27 and Flag-NOD1 or -NOD2. 24 h post-transfection, cells were stimulated with 10 µM MDP for 1, 2, or 3 h, as indicated. Lysates were subjected to immunoprecipitation using anti-Flag beads and probed using the indicated antibodies. For densitometric analysis, TRIM27 IP-signals were normalized to input signals. The ratio of IP to input signals is shown in fold.

3.1.2 TRIM27 promotes K48-linked ubiquitination and proteasomal degradation of NOD2

Recently, TRIM27 has been shown to interact with a subset of E2 enzymes and to possess E3 ubiquitin ligase activity *in vitro* (Napolitano*, et al.* 2011). To investigate if TRIM27 can ubiquitinate NOD2, we first asked if NOD2 is subjected to ubiquitination in human cells. HEK293T cells were transfected with Flag-NOD2 or Flag-NOD1 as a control, followed by immunoprecipitation of the Flag-tagged proteins under stringent washing conditions. At steady-state conditions poly-ubiquitination was detected for NOD2 but not for NOD1 or in control IPs with the matrix alone (Figure 3.7A, left panel). Of note, we observed a single mono-ubiquitination band for both, NOD1 and NOD2.

To decipher the type of ubiquitin linkage on NOD2, K48- or K63-linkage specific anti-ubiquitin antibodies were used. The results show that the NOD2 ubiquitin chains were predominantly K48-linked (Figure 3.7A, middle and right panel). Given that TRIM27 was found to physically interact with NOD2, the next step was to determine

whether TRIM27 has an influence on NOD2 ubiquitination. To this end, HEK293T cells were transfected with Flag-NOD2, Myc-TRIM27 WT and HA-ubiquitin. The ubiquitin signal in NOD2 precipitates, detected either by anti-HA or the K48-linkage specific antibody, was increased upon over-expression of TRIM27 (Figure 3.7B). In contrast, over-expression of a TRIM27 E3 ligase-deficient mutant (named 'TRIM27 E3') in which the two conserved catalytic cysteine residues within the TRIM27 RING domain (C16 and C31) were mutated to alanine, significantly reduced NOD2 ubiquitination compared to TRIM27 WT (Figure 3.7B). Of note, TRIM27 E3 still bound NOD2 to the same extent as TRIM27 WT, indicating that the mutation did not affect binding affinity.

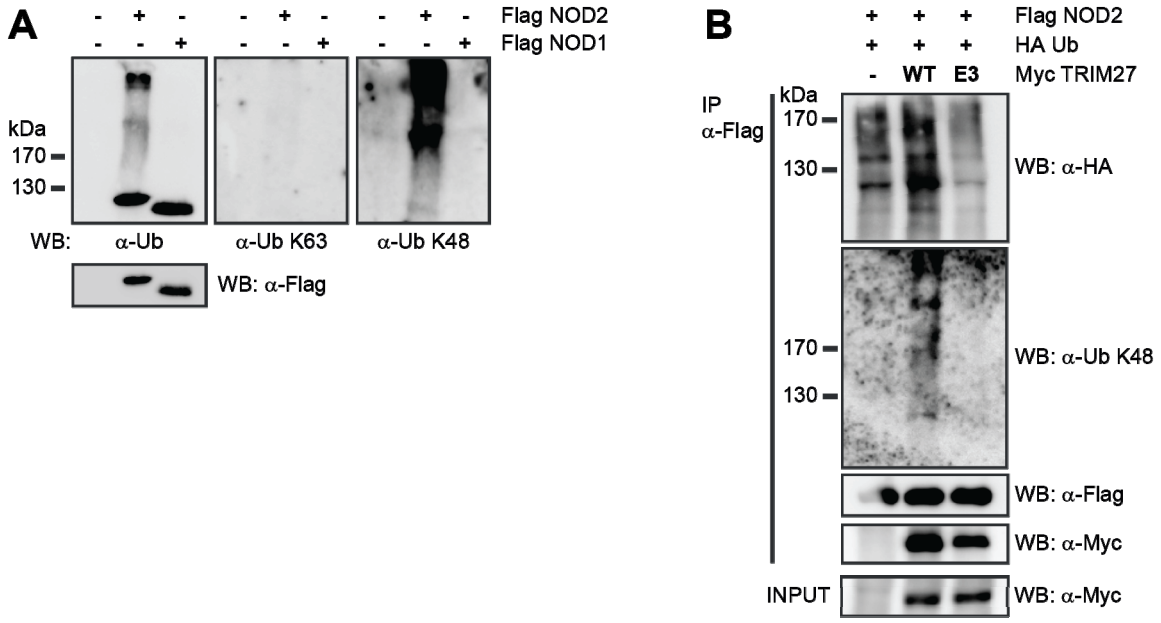

Figure 3.7: NOD2 is ubiquitinated with K48-linked ubiquitin chains
(A) To determine NOD2 ubiquitination, HEK293T cells were transfected with Flag-NOD1 or –NOD2. Lysates were subjected to immunoprecipitation using anti-Flag beads and Western blots of immunoprecipitates were performed using the indicated antibodies. Experiment was done by I. Schoultz. (B) To test if TRIM27 influences NOD2 ubiquitination, HEK293T cells were transfected with Flag-NOD2 and HA-ubiquitin together with or without Myc-TRIM27 WT or E3 mutant. Lysates were subjected to immunoprecipitation using anti-Flag beads and Western blots of immunoprecipitates (IP) and total lysates (Input) were performed using the indicated antibodies. Ubiquitin signals were detected using a HA- or a K48-specific ubiquitin antibody.

K48-linked ubiquitination of proteins usually targets them for degradation by the 26S proteasome (Hershko and Ciechanover 1998). To investigate if NOD2 is subjected to proteasomal degradation, HEK293T cells transfected with small amounts of Flag-

NOD2 were treated with cycloheximide (CHX) to block protein neosynthesis and changes in NOD2 protein levels were monitored by Western blot analysis. This showed that NOD2 was readily degraded in a time-dependent manner (Figure 3.8A, top). Of note, NOD1 was not subjected to rapid protein turn-over (data not shown). TRIM27 WT over-expression did not significantly influence the kinetics of NOD2 degradation (Figure 3.8A, top).

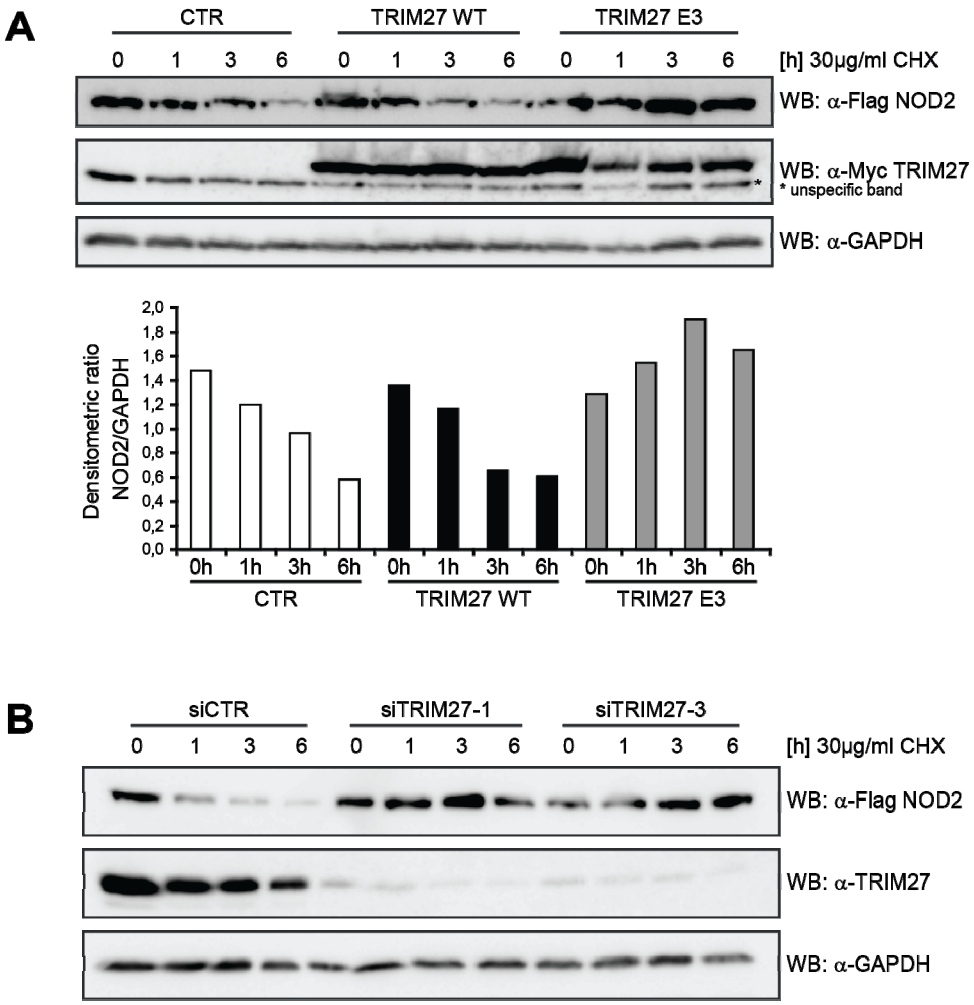

Figure 3.8: TRIM27 contributes to degradation of NOD2
(A) To examine, if NOD2 stability is influenced by TRIM27 over-expression, HEK293T cells seeded in 6-well plates were transfected with 0.25 µg Flag-NOD2 and 0.25 µg Myc-TRIM27 WT, E3 mutant or empty vector (CTR). 24 h post-transfection, cells were treated with 30 µg/ml cycloheximide (CHX) for 0, 1, 3 or 6 h, as indicated. Western blot analysis (top) of total cell lysates was performed using the indicated antibodies. GAPDH served as loading control. Densitometric analysis (bottom) of the NOD2 signals normalized to GAPDH signals. (B) To test if NOD2 degradation is inhibited by TRIM27 knock-down, HEK293T cells were transfected with siCTR, siTRIM27-1 or siTRIM27-3 for 48 h, subsequently seeded in 6-well plates and transfected with 0.5 µg Flag-NOD2. 24 h later, cells were treated as described in (A). Western blot analysis of total cell lysates was performed using the indicated antibodies. GAPDH served as loading control.

In contrast, over-expression of the TRIM27 E3 ligase-deficient mutant strongly inhibited NOD2 degradation. This was further evaluated by densitometric analysis of the Flag-NOD2 signal normalized to the GAPDH loading control (Figure 3.8A, bottom). To elucidate the contribution of endogenous TRIM27 on NOD2 degradation, HEK293T cells were transfected with two different TRIM27-specific siRNA duplexes and NOD2 protein levels were monitored after blocking protein neosynthesis as described above. In cells transfected with scrambled control siRNA NOD2 was degraded (Figure 3.8B) as previously observed. In contrast, in cells treated with either of the two TRIM27-specific siRNA duplexes NOD2 degradation upon cycloheximide treatment was effectively inhibited (Figure 3.8B). Both siRNA duplexes reduced TRIM27 levels nearly to the detection limit as shown by Western blot analysis (Figure 3.8B).

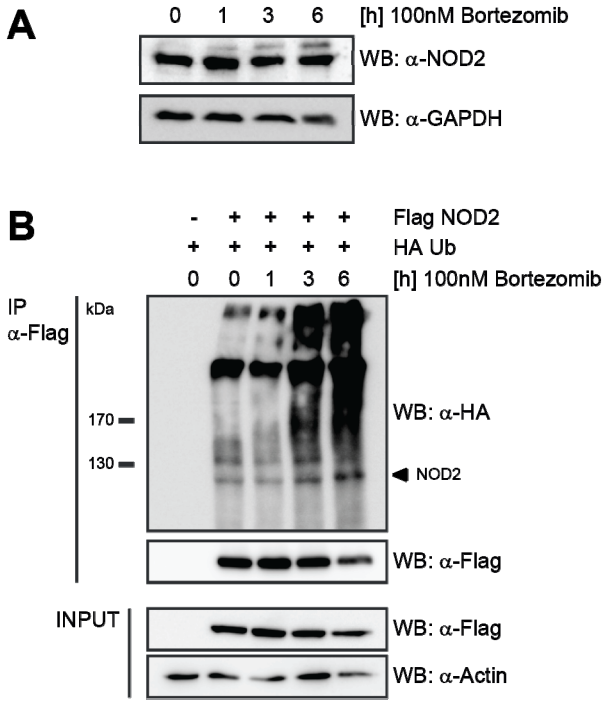

Figure 3.9: NOD2 is degraded by the proteasome
(A) To test whether NOD2 is degraded by the proteasome, HEK293T cells were transfected with 0.25 µg Flag-NOD2. 24 h post-transfection, cells were treated with 100 nM Bortezomib for 0, 1, 3 or 6 h, as indicated. Western blot analysis of total cell lysates was performed using the indicated antibodies. GAPDH served as loading control. (B) To determine whether ubiquitinated NOD2 accumulated after proteasome inhibition, HEK293T cells were seeded in 6-well plates and transfected with 0.5 µg HA-ubiquitin with or without 0.5 µg Flag-NOD2. 24 h post-transfection, cells were treated as described in A and lysates were subjected to immunoprecipitation using anti-Flag beads. Western blots of immunoprecipitates (IP) and total lysates (Input) were performed using the indicated antibodies. Actin served as loading control.

To determine whether NOD2 degradation occurred via the 26S proteasome, the proteasome inhibitor bortezomib (also called Velcade, MG-341 or PS-341) was used. NOD2 degradation was effectively inhibited in HEK293T cells transfected with Flag-NOD2 and treated with 100 nM bortezomib (Figure 3.9A). Moreover, ubiquitinated NOD2 accumulated upon bortezomib treatment (Figure 3.9B).

Taken together, these data revealed that K48-linked ubiquitination targets NOD2 for 26S proteasomal degradation and that this process is dependent on functional TRIM27.

3.1.3 TRIM27 is co-localized with NOD2 in the nucleus

In HeLa cells TRIM27 predominantly exhibited nuclear localization (Cao*, et al.* 1997), whereas in HEK293T cells TRIM27 was also found at distinct sub-cellular structures (Figure 3.10). NOD2 is a cytoplasmic protein but can also localize to the plasma membrane (Barnich*, et al.* 2005a, Kufer*, et al.* 2006a, Legrand-Poels*, et al.* 2007), whereas other NLR proteins such as NLRC5 and CIITA also show nuclear localization (Cressman*, et al.* 1999, Harton*, et al.* 1999, Benko*, et al.* 2010, Meissner*, et al.* 2010).

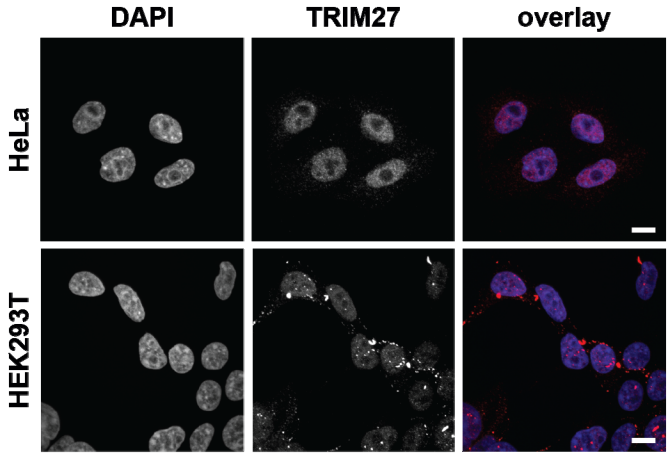

Figure 3.10: Localization of endogenous TRIM27 in HeLa and HEK293T cells
Indirect immunofluorescence images of HeLa and HEK293T cells grown on cover slips. Fixed cells were permeabilized and stained with DAPI and anti-TRIM27 antibody, detected by AlexaFluor 546 labelled secondary antibody. Images with signals for DAPI, TRIM27 and an overlay (blue: DAPI, red: TRIM27) are shown. Bars, 10 µm.

Previous experiments indicated that transiently over-expressed NOD2 is sometimes found in the nucleus (Kufer*, et al.* 2006a). To investigate this in more detail, immunofluorescence analyses were performed in HeLa cells transfected with Myc-NOD2 WT. Nuclear shuttling of NOD2 could indicate low steady-state levels of NOD2 protein in the nucleus. To prevent shuttling, nuclear export was blocked using the specific nuclear export inhibitor leptomycin B (LMB). In untreated samples, NOD2 WT localized mainly to the cytosol as well as partially to the nucleus (Figure 3.11A, upper panels). After LMB treatment NOD2 WT localized predominantly to the nucleus. In contrast, NOD1 and a NOD2 Walker A mutant (K305R) that is unable to induce NF-κB activation (Ogura*, et al.* 2001b, Zurek*, et al.* 2011b), did not localize to the nucleus, even after LMB treatment (Figure 3.11A, lower panels and B).

To substantiate the results obtained by immunofluorescence analysis, cytosolic and nuclear fractionations were prepared from HEK293T cells expressing either Flag-NOD1, -NOD2 or -NOD2 K305R. Immunoprecipitation of the Flag-tagged proteins from the cytosolic and nuclear fractions showed that a small portion of NOD2 already localized to the nucleus without LMB treatment (Figure 3.12, top). NOD2 nuclear localization increased about two-fold upon LMB treatment, as measured by normalized densitometric analysis (Figure 3.12, bottom). In contrast, all NOD1 and NOD2 K305R were found in the cytoplasm.

The data clearly show that NOD2 is able to enter the nucleus in a Walker A-dependent manner, which was also observed for NLRC5 (Neerincx, unpublished data) and CIITA (Harton*, et al.* 1999).

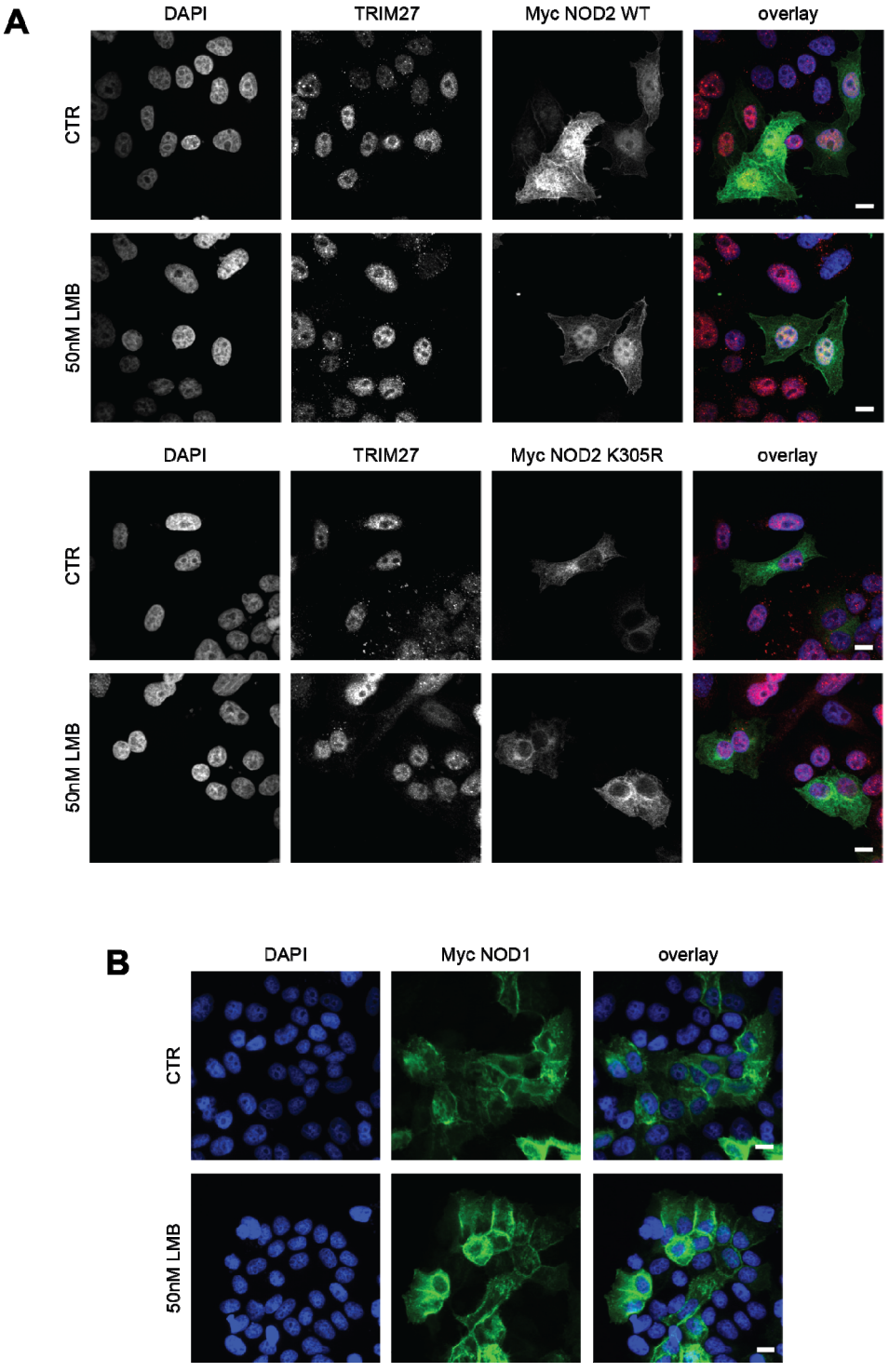

Figure 3.11: NOD2 WT localizes to the nucleus whereas NOD2 K305R or NOD1 do not
(A) To analyse NOD2-TRIM27 co-localization in human cells, indirect immunofluorescence microscopy was performed. HeLa cells grown on cover slips were transfected with Myc-NOD2 WT (top panels) or Myc-NOD2 K305R (bottom panels). 24 h post-transfection, cells were treated with 50 nM Leptomycin B (LMB) for 4 h or left untreated. Fixed cells were permeabilized and stained with DAPI, anti-Myc and anti-TRIM27 antibody, detected by AlexaFluor 488 and AlexaFluor 546 labelled secondary antibody, respectively. Images with signals for the two antibodies, DAPI and an overlay (blue: DAPI, red: TRIM27, green: NOD2) are shown. Bars, 10 µm. (B) To test if NOD1 also localizes to the nucleus, indirect immunofluorescence microscopy was performed as described above. NOD1 images were generated by A. Neerincx.

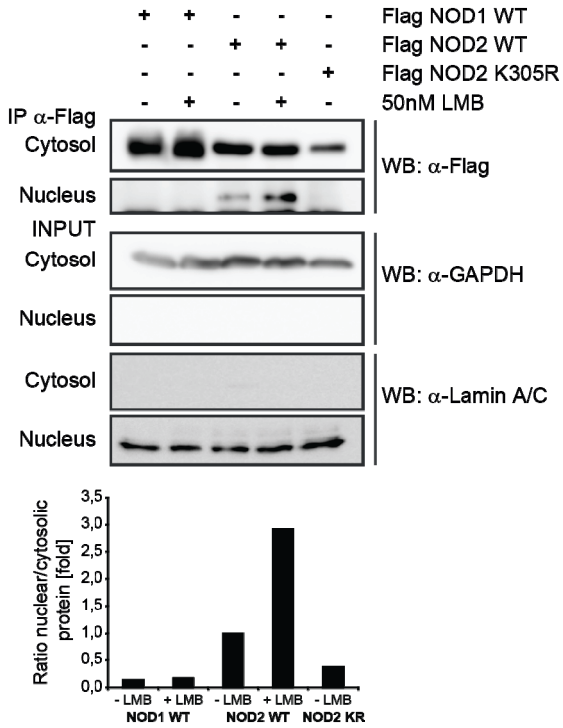

Figure 3.12: NOD2 nuclear localization confirmed by biochemical fractionation
To confirm NOD2 nuclear localization biochemically, HEK293T cells were transfected with Flag-NOD1, Flag-NOD2 WT or K305R. 24 h post-transfection cells were treated with 50 nM LMB for 4 h or left unstimulated. Cellular fractions were prepared and subsequently used for immunoprecipitation with anti-Flag beads. Western blot analysis of precipitated protein was performed using the indicated antibodies. For densitometric analysis, cytosolic and nuclear signals were normalized to GAPDH and Lamin A/C, respectively. The ratio of nuclear to cytosolic protein is shown as fold expression.

3.1.4 TRIM27 negatively regulates NOD2 signalling

Finally, the influence of TRIM27 on NOD2-mediated signalling was investigated. To this end NF-κB luciferase assays were used in HEK293T cells co-transfected with different amounts of TRIM27. Over-expression of TRIM27 clearly reduced MDP-induced NOD2-mediated NF-κB activation in a dose-dependent manner (Figure 3.13A). This effect of TRIM27 on NOD2-mediated signalling can not be explained by inhibition of RIP2-NOD2 complex formation as NOD2 was still able to bind RIP2 in the presence of TRIM27 (Figure 3.14).

Importantly, TRIM27 over-expression had no influence on TNF-induced NF-κB activation (Figure 3.13B). TNF is a potent activator of NF-κB via signalling through the TNF receptor (TNFR)-pathway. The NOD2- and TNFR-signalling pathways converge at the level of the TAK1 complex that subsequently activates the IKK

complex (Chen and Goeddel 2002, Kufer 2008). Over-expression of IKKβ induces NF-κB activation and this was used to conduct an epistatic analysis of TRIM27 function. In line with the results obtained with NOD2- and TNF-mediated NF-κB activation, TRIM27 over-expression had no effect on IKKβ-mediated NF-κB signalling (Figure 3.13C), suggesting that TRIM27 acts at the level of NOD2.

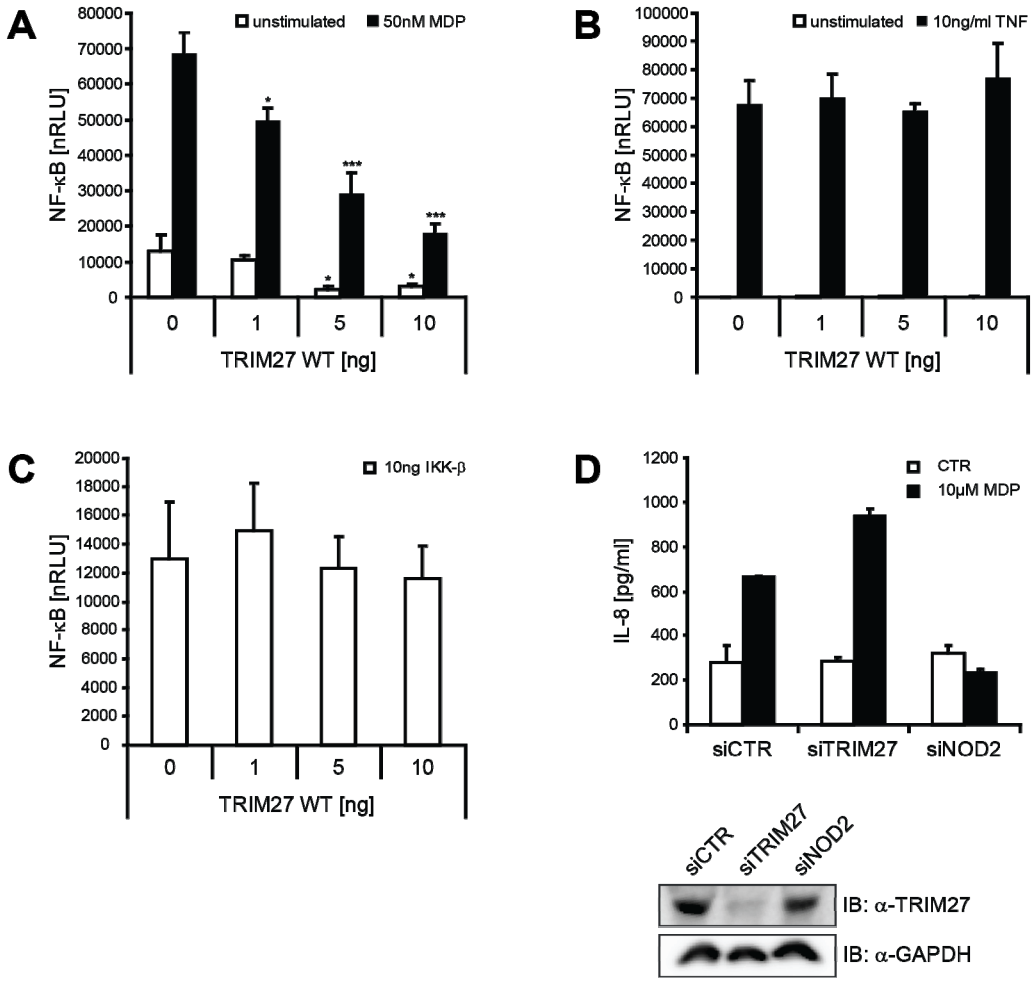

Figure 3.13: TRIM27 negatively regulates NOD2 signalling
(A, B) To determine the influence of TRIM27 over-expression on MDP-induced NOD2-mediated (A) and on TNF-induced (B) NF-κB activation, HEK293T cells were transfected with (A) or without (B) 0.1 ng NOD2 and 0, 1, 5 or 10 ng TRIM27, as indicated, together with a NF-κB luciferase reporter system. Cells were left unstimulated or stimulated for 16 h with 50 nM MDP (A) or 10 ng/ml TNF (B). Normalized luciferase activity (nRLU) of unstimulated (white bars) and stimulated (black bars) samples is shown. Values are means + SD. (C) The influence of TRIM27 on NF-κB activation induced by over-expression of components downstream of the NOD2 signalling cascade was tested. HEK293T cells were transfected with 10 ng IKKβ together with 0, 1, 5 or 10 ng TRIM27, as indicated, and a NF-κB luciferase reporter system. Normalized luciferase activity (nRLU) is shown. Values are means + SD. (D) To determine the effect of TRIM27 knock-down, THP1 cells were differentiated and transfected with siCTR, siTRIM27-1 or siNOD2 for 72 h. Cells were then stimulated with 10 µM MDP o/n or left unstimulated. Supernatants were collected and secreted IL-8 was determined by ELISA. TRIM27 knock-down efficiency is shown by Western blot analysis. *, P<0.05; ***, P<0.005.

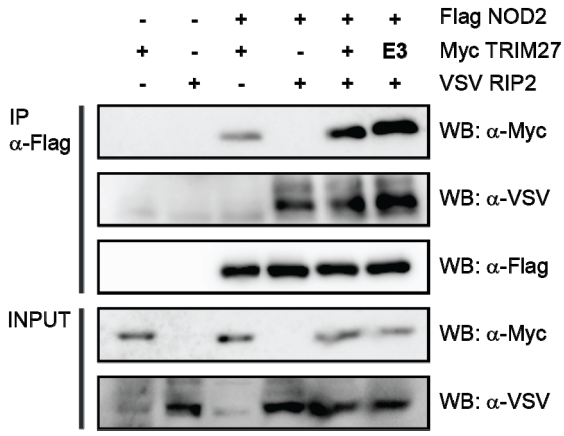

Figure 3.14: NOD2 still binds RIP2 in the presence of TRIM27
To determine whether NOD2 still binds RIP2 in the presence of TRIM27, HEK293T cells were transfected with Myc-TRIM27 WT or E3 and/or VSV-RIP2 together with or without Flag-NOD2. Lysates were subjected to immunoprecipitation using anti-Flag beads. Western blots of immunoprecipitates (IP) and total lysates (Input) were performed using the indicated antibodies.

To determine the effect of endogenous TRIM27 on NOD2-mediated signalling, THP1 cells, which possess a functional NOD2 signalling pathway were used (Uehara*, et al.* 2005). THP1 is a monocytic cell line and can be differentiated to a macrophage-like state. They also express TRIM27 mRNA (Figure 3.3A). Differentiated THP1 cells were transfected with TRIM27- or NOD2-specific siRNA or control siRNA for 72 h and subsequently stimulated with 10 µM MDP. A hallmark of NOD2-mediated NF-κB activation is the production of the pro-inflammatory cytokine IL-8. The amount of IL-8 in the THP1 supernatants was determined by ELISA. TRIM27 knock-down increased MDP-induced IL-8 secretion, whereas NOD2 knock-down completely abolished IL-8 secretion (Figure 3.13D). Western blot analysis confirmed the efficiency of TRIM27 knock-down.

About 30 % of the patients suffering from Crohn's disease (CD) harbour mutations in *nod2 (Hruz and Eckmann 2010)*. However, it is still under debate how *nod2* mutations contribute to disease development. CD patients suffer from a chronic inflammatory response of the gastrointestinal tract associated with excessive NF-κB activation, suggesting that negative regulators – like TRIM27 – should be induced. To test this, RNA was isolated from colon biopsy samples of CD patients and healthy individuals as controls. qPCR analysis revealed significantly increased TRIM27 mRNA expression in CD patients compared to healthy controls (Figure 3.15).

Collectively, these data support a role for TRIM27 as a specific negative regulator of NOD2-mediated signalling and suggest a role of TRIM27 in CD.

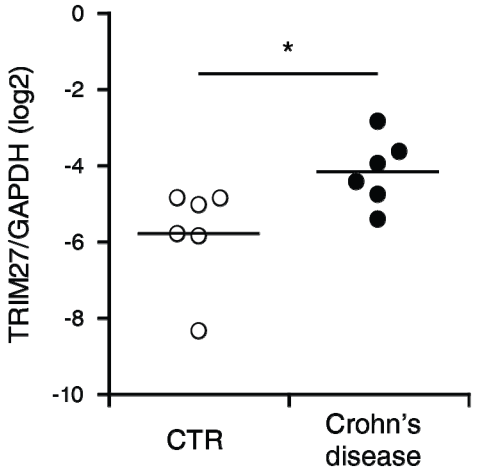

Figure 3.15: TRIM27 expression in Crohn's disease patients
qPCR of TRIM27 mRNA expression in colonic biopsies derived from patients with Crohn's disease and healthy controls (CTR) with no evidence of mucosal inflammation. Each symbol represents one patient. TRIM27 mRNA expression normalized to GAPDH is shown. *, $P<0.05$ (n=6). Experiment done by E. Bennek and G. Sellge.

3.2 *Analysis of the NOD1 and NOD2 ATPase domain*

3.2.1 Characterization of active site residues critical for NOD1 and NOD2 signalling

Sequence alignments of human NLR proteins and APAF1, previously revealed highly conserved amino acid residues in the NBD domain, which presumably affect ATPase activity (Proell, *et al.* 2008). To decipher the molecular details involved in NOD1 and NOD2 activation, single point mutants of these conserved residues were generated (amino acid exchanged to alanine) and analysed for their effect on elicitor- and auto-activation-induced NF-κB activity in luciferase reporter gene assays in HEK293T cells (summarized in Table 1, page 59). The localization of the mutated residues is depicted in Figure 3.16.

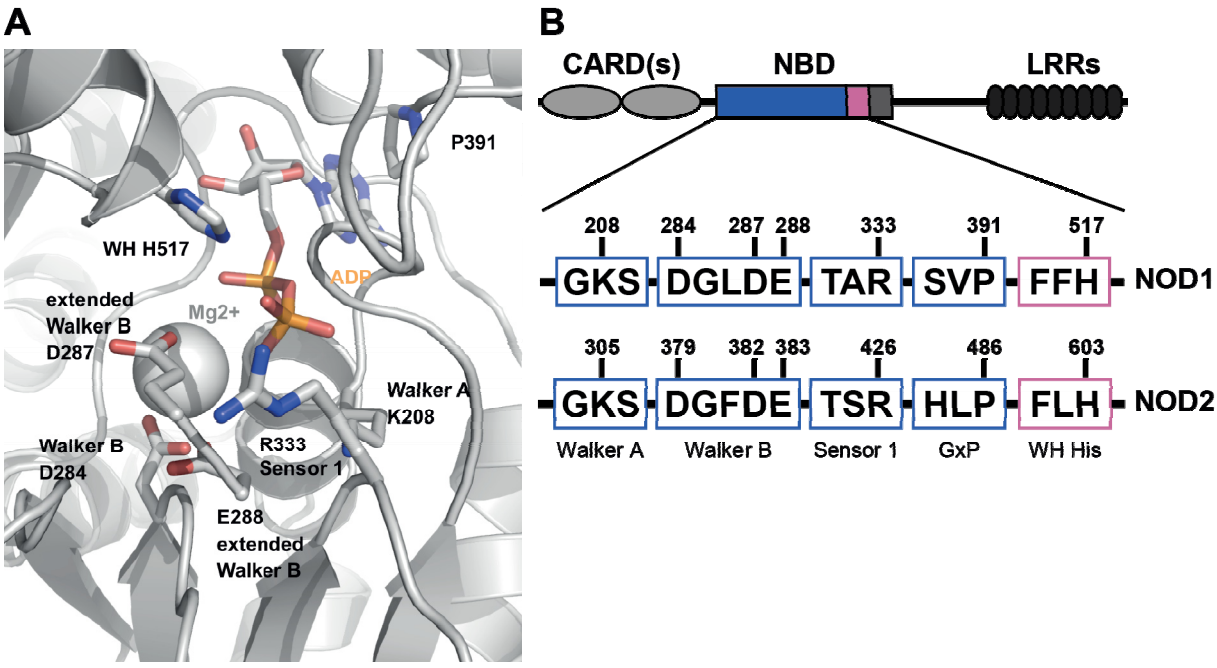

Figure 3.16: NOD1 and NOD2 ATPase domain
(A) Model of the NOD1 nucleotide-binding site with a bound ADP molecule and Mg^{2+} ion. Conserved sequence motifs Walker boxes A and B, extended Walker B box, Sensor 1, GxP and WH histidine are shown in sticks. Model generated by M. Proell and R. Schwarzenbacher. (B) Schematic representation of the domain architecture of NOD1 and NOD2. The NBD is composed of the NACHT (in blue), WH (in magenta) and SH domain. The magnification of the NACHT and WH domain indicates the position of the conserved amino acid residues analysed in this study.

Over-expression of NOD1 and NOD2 is known to induce auto-activation, therefore the amount of NOD1 and NOD2 was carefully titrated in preliminary assays (data not shown) and three established DNA concentrations were subsequently used for each construct. Importantly, comparable expression of all constructs was achieved as shown by Western blot analysis (Figure 3.17D).

Early publications already reported that the Walker A (P-loop) lysine (G**K**[S/T]), which is responsible for nucleotide binding (Hanson and Whiteheart 2005, Proell*, et al.* 2008), is essential for NOD1- and NOD2-mediated NF-κB signalling (Inohara*, et al.* 1999, Ogura*, et al.* 2001b). It was confirmed that mutation of the Walker A lysine to either alanine or arginine (NOD1: K208; NOD2: K305) resulted in unresponsiveness to elicitor stimulation and lack of auto-activation in both NOD1 and NOD2 (Figure 3.17A, B).

Similarly, mutation of the Mg^{2+}-co-ordinating aspartate residue in the Walker B box (**D**GhDE) of NOD1 (D284) and NOD2 (D379) resulted in complete loss of NF-κB activation (Figure 3.17A, B), demonstrating that both canonical ATPase features are essential for activation of NOD1 and NOD2. NLR proteins contain a modified Walker B box lacking the second acidic residue (D**G** instead of D[D/E]) that is usually responsible for priming of a water molecule required for ATP hydrolysis (Proell*, et al.* 2008). However, in most NLR proteins, including NOD1 and NOD2, the Walker B box is followed by a highly conserved patch of acidic residues, the extended Walker B box (DGh**DE**), suggesting that these acidic residues can functionally compensate for the missing second aspartate of the canonical Walker B box. To investigate the function of this modified Walker B box, the corresponding amino acids in NOD1 and NOD2 were replaced by alanine. Mutation of the aspartate residue of the extended Walker B box (NOD1: D287; NOD2: D382) reduced elicitor-induced NF-κB activation mediated by NOD1 by more than 50% compared to the wild type, whereas NOD2 showed only residual activity. Both NOD1 and NOD2 exhibit complete loss of auto-activation (Figure 3.17A, B). This indicates that the aspartate residue of the extended Walker B box is essential and might functionally complement the missing second acidic residue of the canonical Walker B box.

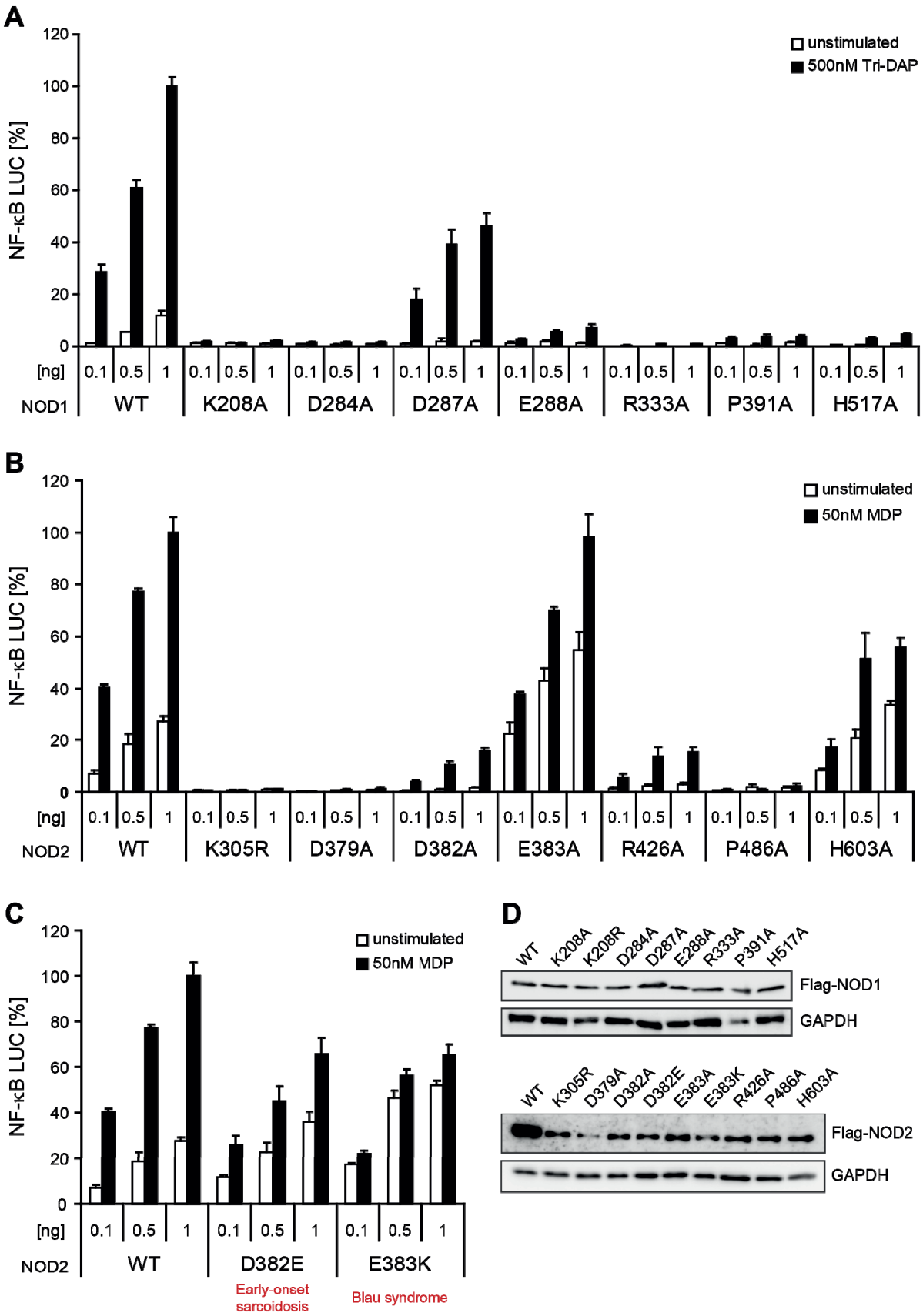

Figure 3.17: Functional analysis of conserved residues in NOD1- and NOD2-mediated NF-κB activation

(Legend continued on following page)

(Legend of Figure 3.17 / continued)
NF-κB activation of NOD1 (A) and NOD2 (B) WT and mutant proteins were assayed in HEK293T cells transfected with 0.1, 0.5 or 1 ng of the indicated plasmids together with a NF-κB luciferase reporter system. Cells were left unstimulated or stimulated for 16 h with 500 nM Tri-DAP (A) or 50 mM MDP (B). Percentage of normalized luciferase activity relative to 1 ng Flag-NOD1 WT (A) or Flag-NOD2 WT (B) is shown. Values are means +SD. (C) NF-κB activation of NOD2 WT, EOS- (D382E) and BS-associated (E383K) NOD2 mutants. NF-κB luciferase assay was conducted as described in (A) and (B). (D) Western blot analysis showing the expression levels of NOD1 and NOD2 constructs using anti-NOD1 7B10 and anti-Flag antibodies for NOD1 and NOD2, respectively (upper panels). GAPDH served as loading control (lower panels).

The glutamate residue of the extended Walker B box in NOD1 (E288) was also found to be essential for NF-κB activation and displayed an even stronger phenotype than the loss of the aspartate residue (Figure 3.17A). In sharp contrast, mutation of the corresponding amino acid in NOD2 (E383) led to significantly increased basal NF-κB activation (Figure 3.17B). This unexpected finding indicated a different function of the extended Walker B box residues in NOD1 and NOD2 signalling. Indeed, this result fits very well with the fact that naturally occurring mutations in the extended Walker B box lead to auto-activation of NOD2, whereas such mutations have not yet been reported for NOD1. Mutations in the NOD2 extended Walker B box are linked with early-onset sarcoidosis (EOS; D382E/A612T) (Kanazawa*, et al.* 2005) and Blau syndrome (BS; E383K) (van Duist*, et al.* 2005), two severe auto-inflammatory human diseases associated with hyperactive NOD2. In the assay system used here, this phenotype was recapitulated. Both NOD2 D382E and NOD2 E383K led to enhanced auto-activation compared to the wild type, whereas a somewhat lower response was observed with MDP (Figure 3.17C). Of note, the EOS mutation D382E displayed less basal activation than the E383K mutation. This observation was attributed to the fact that the single mutant NOD2 D382E instead of the double mutant D382E/A612T usually found in patients (Kanazawa*, et al.* 2005) was used in this study. Since both aspartate (D) and glutamate (E) are acidic residues, we suggest that glutamate might partially adopt the function of D382.

Next, the contribution of the conserved Sensor 1, GxP motif, and WH histidine to NOD1 and NOD2 activation was explored. The Sensor 1 motif is involved in co-ordinating the γ-phosphate of ATP, whereas the conserved proline residue in the GxP motif is thought to interact with the adenine moiety of ATP (for review see (Hanson and Whiteheart 2005)). Mutation of the Sensor 1 in NOD1 (R333) resulted in complete loss of NF-κB activation (Figure 3.17A), whereas the corresponding

mutation in NOD2 (R426) still showed residual NF-κB activation in response to MDP (Figure 3.17B). Mutation of the conserved proline in the GxP motif abolished elicitor-dependent NF-κB activation in both NOD1 (P391) and NOD2 (P486) (Figure 3.17A, B). Furthermore, mutation of the WH histidine completely blocked NF-κB activation by NOD1 (H517). In contrast, NOD2 H603A was still able to respond to MDP, albeit at reduced levels compared to the wild type and showed increased auto-activation (Figure 3.17B). The latter finding was similar to the results obtained when exchanging the glutamate in the extended Walker B box supporting our conclusion that NOD1 and NOD2 are differentially activated.

Table 1: Overview of conserved motifs in the ATPase domain, their proposed function and the analysed residues in NOD1 (top) and NOD2 (bottom, *italic*)

Motif	Proposed function	Mutation	Signalling[1]	Membrane localization
Walker A	Nucleotide binding	K208A	-	-
		K305R	-	-
Walker B first acidic residue	Coordination of Mg^{2+}	D284A	-	-
		D379A	-	-
Extended Walker B first acidic residue	Priming H_2O	D287A	++ no autoactivation	-
		D382A	+	-
Extended Walker B second acidic residue	Priming H_2O	E288A	-	-
		E383A	+++ high autoactivation	+
Sensor 1	Senses γ-phosphate of ATP	R333A	-	-
		R426A	+	-
GxP	Interacts with adenine of ATP	P391A	-	-
		P486A	-	-
Sensor 2 Conserved His	AAA+: nucleotide binding/hydrolysis[2] APAF-1: coordination of phosphate groups[2]	H517A	-	-
		H603A	++	+

[1] Ability to activate NF-κB as determined in Figure 3.17A and B (-, no activity [<10% of WT]; +, residual activity [>10% of WT]; ++, less active than WT; +++, activity comparable to WT).
[2] Supposed to be involved in nucleotide binding/hydrolysis bound by the neighbouring molecule.

Taken together, these results (summarized in Table 1) revealed that a functional Walker A and B box as well as Sensor 1 and GxP motif are crucial for NOD1 and NOD2 activation. Importantly, a function could be assigned to the extended Walker B box in NLRs. Furthermore, these data demonstrated that mutations of the extended Walker B box and the WH histidine have opposing effects on NOD1- and NOD2-mediated signalling, indicating different mechanisms of activation and regulation.

3.2.2 NOD1 and NOD2 activation status is reflected by their sub-cellular localization

Recently, it was reported that exogenously expressed active NOD1 and NOD2 localizes to the plasma membrane in various human cells, which relates to auto-activation of the over-expressed NLRs (Barnich*, et al.* 2005a, McDonald*, et al.* 2005, Lecine*, et al.* 2007, Kufer*, et al.* 2008). In order to complement the results of the NF-κB activation assays presented above, the sub-cellular localization of the NOD1 and NOD2 mutants was examined in HeLa cells by indirect immunofluorescence analysis. Figure 3.18A shows that only NOD1 WT localized to actin-rich regions at the plasma membrane, whereas all of the NOD1 mutants that did not show auto-activation in the NF-κB reporter assays (NOD1 K208A, D284A, E288A, R333A, P391A, and H517A) were restricted to the cytoplasm. Accordingly, NOD1 D287A, which showed only elicitor-mediated activation, also failed to localize to the plasma membrane upon over-expression (Figure 3.18A).

Indirect immunofluorescence analysis of NOD2 revealed increased membrane localization of the wild type, the highly auto-active NOD2 mutant E383A, and to a lesser extend NOD2 H603A (Figure 3.18B). The two disease-associated NOD2 mutants D382E (EOS) and E383K (BS), which exhibited the highest auto-activation level in the NF-κB assays were also recruited to the plasma membrane, whereas non-signalling active NOD2 mutants (NOD2 K305R, D379A, D382A, R426A, and P486A) exhibited an exclusively cytoplasmatic localization pattern (Figure 3.18B).

Figure 3.18: Sub-cellular localization of NOD1 and NOD2 mutants
Indirect immunofluorescence images of HeLa cells grown on cover slips were transfected with Flag-NOD1 (A) or Flag-NOD2 (B) constructs. Fixed cells were permeabilized and stained with DAPI, Phalloidin-FITC and anti-Flag antibody, detected by AlexaFluor 546 labelled secondary antibody. Images with signals for NOD1 and NOD2 alone (upper panels) and an overlay (lower panels; blue: DAPI, red: NOD1 or NOD2, green: actin) are shown. Bars: 10 µm.

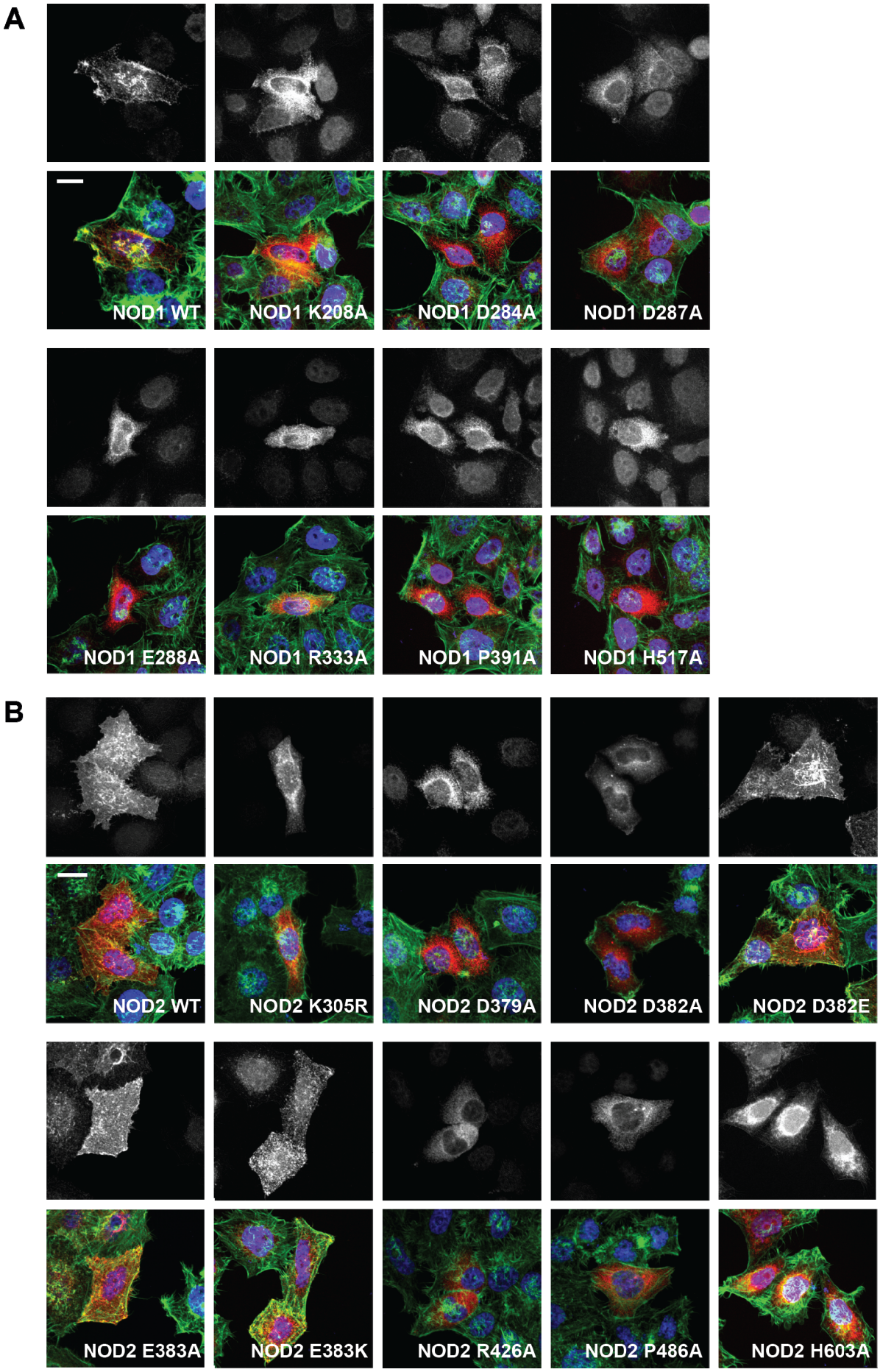

(Legend on previous page)

To confirm the differences in membrane association of the NOD1 and NOD2 mutants biochemically, membrane fractionations in HEK293T cells transfected with NOD1 and NOD2 mutants were performed. In agreement with the data presented above, NOD1 and NOD2 wild type as well as the auto-activating mutants NOD2 E383A and NOD2 H603A were present in the membrane fraction, whereas the non auto-activating mutants NOD1 K208A, NOD1 E288A and NOD1 H517A as well as NOD2 K305R and NOD2 D382A were only detectable in the cytosolic fractions (Figure 3.19).

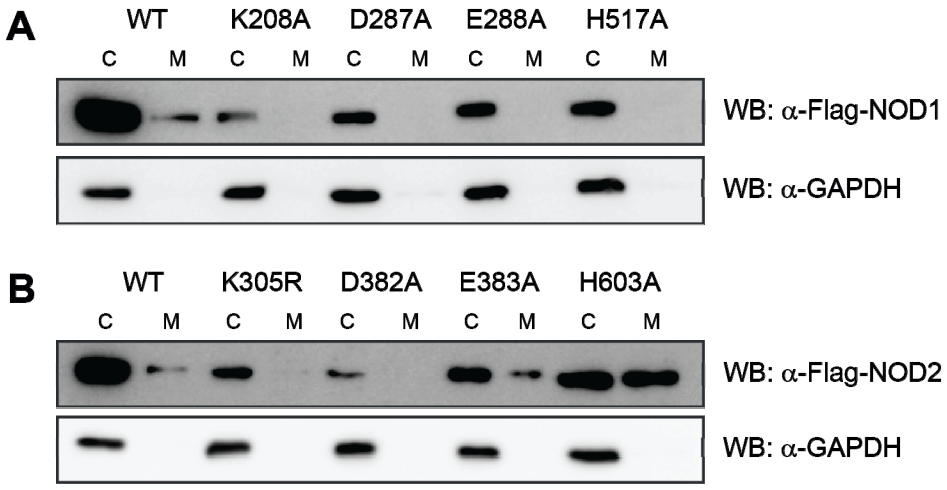

Figure 3.19: Cellular fractionation of NOD1 and NOD2 mutants
HEK293T cells were transfected with NOD1 or NOD2 plasmids as indicated. 24 h later, cells were lysed, cytosolic (C) and membrane (M) fractions were prepared and subjected to Western blot analysis using anti-Flag antibody. GAPDH served as loading control.

In summary, these data show that recruitment of NOD1 and NOD2 to the plasma membrane reflects their activation status in agreement with the results obtained in the NF-κB reporter assays.

4 Discussion

4.1 Analysis of the NOD1 and NOD2 ATPase domain

The molecular details underlying NOD1 and NOD2 activation are still not fully understood. In particular the role of ATP hydrolysis in NLR signalling is unclear, despite the general perception that NLRs function as nucleotide binding proteins. Since no high resolution structural data on NLRs are available to date, the current model of NLR activation is deducted from their apoptotic relative APAF1 and from *in vitro* studies on purified NLRP1, NLRP3, NLRP12, and NLRC4 (Lu*, et al.* 2005, Duncan*, et al.* 2007, Faustin*, et al.* 2007, Ye*, et al.* 2008). According to these studies the general assumption has been that nucleotide binding is required for NLR protein function, *i.e.* the induction of molecular platforms to promote downstream signalling events. However, the exact role of nucleotide hydrolysis in the activation process is unclear. Danot *et al.* proposed a model for STAND ATPases comprising the following steps: (I) elicitor recognition, (II) conformational changes leading to a semi-opened state, (III) nucleotide exchange (ATP for ADP) to drive oligomerization, and (IV) deactivation of the signalling platform by ATP hydrolysis (Danot*, et al.* 2009). According to this model, an ATP hydrolysis step is necessary only to stop signalling and, consequently, mutations of residues crucial for ATP hydrolysis should result in auto-activation. Our data do not entirely support this model for NOD1 and NOD2, as they clearly show that mutation of most of the ATPase features including the Walker A and B box, GxP motif and Sensor 1 led to complete loss of signalling. The requirement of a functional Walker A box in NOD1 and NOD2 activation was already reported (Inohara*, et al.* 1999, Ogura*, et al.* 2001b). This indicates that nucleotide binding and likely an initial nucleotide hydrolysis step is essential for both NOD1 and NOD2 activation. Differences between NOD1 and NOD2 activation in our analysis were discovered in the WH histidine. Whereas mutation of NOD1 H517A resulted in complete loss of NF-κB activation, NOD2 H603A showed reduced MDP-induced but higher basal NF-κB activation compared to the wild type.

Most NLR proteins contain a modified Walker B box lacking the second acidic residue and consecutively a highly conserved patch of acidic residues, the extended Walker B box (D[GAS]h**DE**). Although it was proposed that these acidic residues can functionally compensate for the missing one of the canonical Walker B box, this was

so far not experimentally tested. In a recent study Ye *et al.* used an NLRP12 Walker A/B box mutant in which the Walker A box and the first acidic residues of the canonical and extended Walker B box were mutated to alanine (GKS → AAA and DxxDE → AxxAE) (Ye*, et al.* 2008). This NLRP12 mutant displayed decreased ATP binding capacity and no ATPase activity compared to the wild type. However, this study did not identify the specific function of the individual residues involved. In the present work, a systematic mutational approach was chosen to also address this issue.

Dissection of the extended Walker B box revealed a function for the first acidic residue in both NOD1 and NOD2 activation, although NOD1 D287A still showed reduced elicitor-mediated NF-κB activation. While mutation of the second acidic residue in NOD1 (E288A) almost completely blocked NF-κB activation, the corresponding residue in NOD2 (E383A) had different effects: NOD2 E383A exhibited significantly higher auto-activation compared to the wild type. This suggests that E383 is necessary for NOD2 deactivation rather than activation, possibly by retaining the NOD2 signalling platform in an "on" state incapable of returning into the dormant form. We propose that in contrast to NOD1, NOD2 uses an additional hydrolysis step for deactivation mediated by the second acidic residue of the extended Walker B box (E383). Importantly, a recently identified BS-associated mutation (E383K) also maps to this position (van Duist*, et al.* 2005) and results in increased basal NF-κB activation compared to the wild type.

A theoretical explanation for different NOD1 and NOD2 deactivation mechanisms could lie in their differences in oligomerization. Based on the overall similarity of NLR proteins with APAF1 and cryo-EM analysis of recombinant NLRP1 (Faustin*, et al.* 2007), we hypothesize that NOD2 forms wheel-like oligomers where E383 is necessary for the second ATP hydrolysis step and NOD2 deactivation. Furthermore, NOD2 WH histidine H603 could be involved in this second ATP hydrolysis step of the neighbouring molecule as suggested for APAF1 (Hanson and Whiteheart 2005, Proell*, et al.* 2008). In contrast to NOD2, results obtained for NOD1, however, indicate that it might not form such multimeric signalling complexes, as the corresponding residues are not involved in its deactivation, but rather in the activation process. Therefore, NOD1 might use a mechanism other than ATP hydrolysis for deactivation. Indeed, the NOD1 CARD domain was recently reported to form dimers,

which could be involved in the formation of such a different signalling complex (Srimathi*, et al.* 2008).

Unfortunately, we have not yet been successful in producing soluble recombinant NOD1 and NOD2 protein in sufficient amounts and purity to conduct *in vitro* ATPase assays and obtain structural information. Thus, most of these interpretations await experimental verification *in vitro* once the problems of protein expression are overcome. Nonetheless, these data support the idea that NOD2 is more prone to auto-activation as the corresponding residues of all gain-of-function mutations affecting the NOD2 NBD domain are non-functional in NOD1. Moreover, none of the mutations in the NOD1 NBD domain analysed in this study resulted in enhanced signalling. The sensitivity of NOD2 for auto-activation is in line with the findings that (1) in contrast to NOD2, no naturally occurring NOD1 mutations exhibiting higher auto-activation has been reported in the literature, that (2) there are more disease-associated mutations found for NOD2 than NOD1 (Borzutzky*, et al.* 2009), that (3) NOD1 is expressed at basal levels in most tissues whereas NOD2 expression is more restricted to phagocytic and intestinal epithelial cells and can be induced by pathogenic stimuli (Ogura*, et al.* 2001b, Gutierrez*, et al.* 2002, Ogura*, et al.* 2003, Rosenstiel*, et al.* 2003, Oh*, et al.* 2005, Sabbah*, et al.* 2009), and that (4) more negative regulators are reported for NOD2 than for NOD1 (Kufer 2008, Lecat*, et al.* 2010). One of these NOD2-specific negative regulators is the E3 ubiquitin ligase TRIM27 identified in this study (discussed below). Additionally, to obtain comparable auto-activation in transient transfection assays less NOD2 than NOD1 is required.

In summary, we established a function for most ATPase signatures of NOD1 and NOD2 activation. We give evidence that mutations in the extended Walker B box and the WH histidine have opposing effects on NOD1- and NOD2-mediated signalling, suggesting different mechanisms for their activation and regulation. Finally, we showed that membrane localization correlated with signalling competence. Future research should shed light on the ATP binding and hydrolysis capacity of each mutant analysed in this study using recombinant NOD1 and NOD2 protein.

4.2 Characterization of TRIM27 as a new NOD2 interaction partner

In this study the E3 ubiquitin ligase TRIM27 was identified as a new interaction partner of NOD2. Mapping studies indicated that NOD2 binds via its NBD domain to the TRIM27 B30.2/PRY-SPRY domain. The PRY-SPRY domain is most commonly found at the C-terminus of TRIM proteins (Ozato*, et al.* 2008). Of note, the TRIM27 binding site of NOD2 correlates with the findings for other TRIM proteins: TRIM21 (also called Ro52) binds its interaction partners IRF3 and IRF8 via the B30.2/PRY-SPRY domain (Kong*, et al.* 2007, Higgs*, et al.* 2008, Yang*, et al.* 2009) and TRIM25 binds RIG-I via the C-terminal SPRY domain (Gack*, et al.* 2007). TRIM20, better known as pyrin, regulates caspase-1 activation and IL-1β production by interacting with caspase-1 and ASC via its PRY-SPRY and PYD domain, respectively (Richards*, et al.* 2001, Chae*, et al.* 2003, Chae*, et al.* 2006). Mutations in the human TRIM20 PRY-SPRY domain are associated with inherited familial Mediterranean fever (FMF) (French_FMF_Consortium 1997, International_FMF_Consortium 1997). Interestingly, mice are not able to phenocopy this effect as murine TRIM20 lacks the PRY-SPRY domain. Recently, it was shown that TRIM20 knock-in mice harbouring the mutant human PRY-SPRY domain reproduce the inflammatory phenotype found in patients. Additionally, they form ASC-dependent, NLRP3-independent inflammasomes, linking the TRIM20 PRY-SPRY domain to NLR protein functions (Chae*, et al.* 2011). Another intriguing example underscoring the involvement of PRY-SPRY domains in NLR regulation is found in zebrafish (*Danio rerio*). A certain class of NLR proteins in *D. rerio* comprises molecules harbouring a PRY-SPRY domain fused to the canonical NLR sequence (Laing*, et al.* 2008). Remarkably, PRY-SPRY domains from zebrafish NLRs are closely related to zebrafish TRIMs, suggesting domain shuffling during evolution (van der Aa*, et al.* 2009) and that TRIM and NLR proteins have been closely connected in evolution to function in innate immune responses.

TRIM proteins are involved in the regulation of PRR and IFN signalling pathways. Regulation occurs mainly by ubiquitination of the receptors, components of the signalling cascades or transcription factors. TRIM-mediated ubiquitination events can either enhance immune response as shown *e.g.* for TRIM8, TRIM21, TRIM23, TRIM25 and TRIM56 (Toniato*, et al.* 2002, Gack*, et al.* 2007, Kong*, et al.* 2007, Yang*, et al.* 2009, Arimoto*, et al.* 2010, Tsuchida*, et al.* 2010) or inhibit them as shown for TRIM21 and TRIM30α (Higgs*, et al.* 2008, Shi*, et al.* 2008, Hu*, et al.*

2010). In this study, TRIM27 was also shown to be involved in PRR signalling by negatively regulating NOD2. It was observed that dependent on functional TRIM27, NOD2 is ubiquitinated by K48-linked ubiquitin chains. Although no poly-ubiquitin chains were detected on NOD1, the ubiquitin-specific antibody displayed a strong signal for both, NOD1 and NOD2 proteins, suggesting mono-ubiquitination events (Figure 3.7). This signal was neither observed with K48- nor K63-specific antibodies. Recently, CIITA mono-ubiquitination was shown to enhance transcriptional potency (Greer*, et al.* 2003), while poly-ubiquitination leads to proteasomal degradation of CIITA. Future research should clarify whether NOD1 and NOD2 mono-ubiquitination has a biological function.

K48-linked ubiquitination usually targets proteins to degradation (Hershko and Ciechanover 1998), which is the function of some TRIM proteins in PRR and IFN signalling pathways: Mouse TRIM30α promotes ubiquitination and degradation – although not by proteasomal but rather by lysosomal degradation – of TAB2 and TAB3 thereby inhibiting TLR-induced NF-κB activation (Shi*, et al.* 2008), whereas TRIM8 decreases SOCS-1 protein levels leading to an inhibition of IFNγ signalling repression (Toniato*, et al.* 2002). Ubiquitinated NOD2 is also targeted for proteasomal degradation, as shown by inhibition of the 26S proteasome using bortezomib (Figure 3.9). Although we cannot formally exclude the possibility that the observed ubiquitination signal is caused by other proteins co-precipitating with the NOD2 complex, NOD2 protein stability is effectively dependent on TRIM27. This is demonstrated by the finding that knock-down of endogenous TRIM27 as well as over-expression of TRIM27 E3 inhibited NOD2 degradation (Figure 3.8). Regulation of PRRs by ubiquitination and proteasomal degradation seems to be a common theme: the E3 ubiquitin ligase Triad3A is known to control TLR4 and TLR9 signalling (Chuang and Ulevitch 2004) and recently the plant PRR flagellin-sensing 2 (FLS2) has been also shown to be ubiquitinated and degraded by PUB12/13 in a negative feedback loop (Lu*, et al.* 2011). We could now demonstrate that NOD2 is also regulated via such control mechanism. Recently, TRIM27 has also been shown to confer SUMO E3 ligase activity (Chu and Yang 2011). However, we did not detect SUMOylated NOD2, questioning the notion that NOD2 is a substrate for TRIM27-mediated SUMOylation (data not shown).

Luciferase assays in HEK293T cells showed that TRIM27 over-expression specifically reduces NOD2-mediated MDP-induced NF-κB activation in a dose-dependent manner, whereas TNF-induced NF-κB activation was not affected (Figure 3.13). The negative regulating effects of TRIM27 on NOD2 signalling are not necessarily explained by NOD2 degradation but might also be due to preventing adaptor protein recruitment to the NOD2 complex. However, TRIM27 did not inhibit the NOD2-RIP2 interaction. In contrast to our data, Zha *et al*. reported that TRIM27 interacts with IKKα, IKKβ, IKKε and TBK1 to negatively regulate NF-κB, IFNβ and ISRE activation induced by these kinases (Zha*, et al.* 2006). The discrepancies between the two studies remain unclear, although the observed effect by Zha *et al*. is independent of the RING domain.

In contrast to most TRIM proteins, TRIM27 expression is not altered in response to type I and II IFNs (Rajsbaum*, et al.* 2008, Carthagena*, et al.* 2009). Among the TRIM proteins induced by type I and II IFNs, many have been shown to confer antiviral activity, although IFN-inducibility is not a prerequisite for antiviral activity (Reymond*, et al.* 2001, Carthagena*, et al.* 2009). Constitutively expressed TRIM proteins have also been shown to trigger antiviral immune responses. However, an influence of TRIM27 over-expression on Sendai virus-induced IFNβ activation was not observed (data not shown), although this was recently reported (Zha*, et al.* 2006). We therefore assume that TRIM27 involvement in antiviral responses is unlikely, but future research should address this in more detail.

We showed that some mutations in the NBD domain of NOD2 can result in enhanced NF-κB activation whereas these do not increase the activity of NOD1 (see above and (Zurek*, et al.* 2011b)). Thus, NOD2 is likely more prone to auto-activation than NOD1 and needs to be more tightly controlled to prevent overwhelming inflammatory responses (see above). Here, another difference between NOD1 and NOD2 regulation is noted: NOD2, but not NOD1, is tightly controlled by ubiquitination and subsequent proteasomal degradation depending on TRIM27 E3 ligase activity. This identifies TRIM27 as an essential negative regulator of NOD2-mediated inflammatory responses.

The most frequent Crohn's disease-associated NOD2 mutation is NOD2fs. This mutation is thought to cause NOD2 loss-of-function, which is also supported by

several publications showing decreased cytokine production by different cell types harbouring this mutation in response to MDP (Inohara*, et al.* 2003, Netea*, et al.* 2004, Netea*, et al.* 2005, Kramer*, et al.* 2006). Impaired α-defensin production in the inflamed gastrointestinal tract of CD patients with the NOD2fs mutation (Wehkamp*, et al.* 2004) as well as accumulation of bacterial endotoxin in the intestinal tissue have been reported (Kosovac*, et al.* 2010). However, CD is characterized by high levels of NF-κB activation and TNFα production, and both anti-TNFα therapy as well as NF-κB inhibitors are efficient in treating CD (Hruz and Eckmann 2010). This would rather suggest that CD-associated NOD2 mutations are gain-of-function mutations and promote inflammatory responses. Accordingly, a study using NOD2fs knock-in mice reported increased NF-κB activation in response to MDP (Maeda*, et al.* 2005). However, these results are under debate and conflict with those found in patients and healthy individuals homozygous for the NOD2fs mutation (van Heel*, et al.* 2005). One hypothesis therefore suggests that the deficiencies in epithelial barrier function caused by NOD2 loss-of-function result in increased bacterial invasion and subsequent inflammation with impaired control mechanisms. Indeed, NOD2 signalling has also been reported to down-regulate TLR2-mediated NF-κB activation in mice. This regulatory mechanism was defective in mice with the NOD2fs mutation resulting in enhanced Th1 responses (Watanabe*, et al.* 2004). Moreover, the anti-inflammatory cytokine IL-10 is decreased in CD patients with Nod2 mutations (Netea*, et al.* 2004). In this study, enhanced TRIM27 expression in the colon of CD patients was detected. Although the NOD2 status of the patients analysed is unknown, enhanced TRIM27 expression will limit NOD2 function. Two scenarios for TRIM27 function in CD are conceivable: either TRIM27 negatively regulates inflammatory responses coming from hyperactive mutant NOD2 (in case of gain-of-function) or TRIM27 prevents additional inflammatory responses mediated by NOD2 WT. However, the role of TRIM27 in a NOD2 loss-of-function scenario remains puzzling. Of course, TRIM27 function in CD could also be independent of NOD2. Especially, since NOD2 is not the only CD susceptibility gene it would be interesting to correlate TRIM27 levels with the NOD2 status of CD patients. Clinically, the results identify TRIM27 as a new and promising target for treating NOD2-associated diseases. It is conceivable that targeting TRIM27 might be advantageous in Crohn's disease, when NOD2 activity is altered.

In conclusion, these data suggest that TRIM27 acts in a negative feedback loop on NOD2, as NOD2-TRIM27 binding is enhanced after NOD2 activation by MDP (Figure 3.6). The model drawn in Figure 1.2 summarizes TRIM27 function on NOD2.

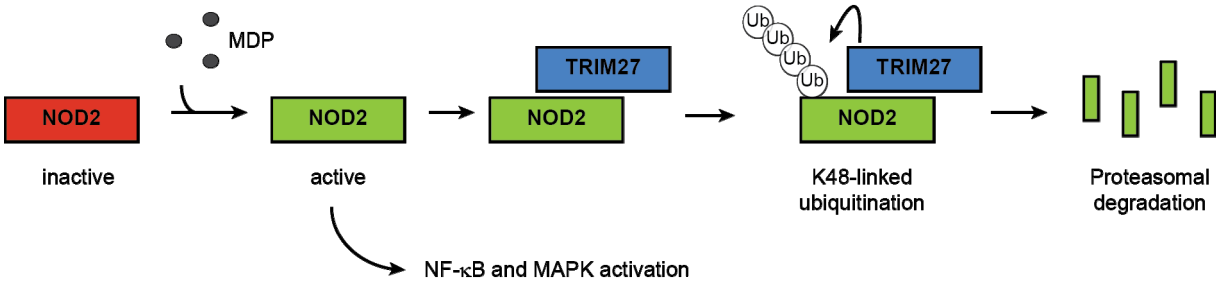

Figure 4.1: Model for TRIM27 function on NOD2
MDP activates NOD2, leading to NF-κB and MAPK signalling. Activation of NOD2 increases interaction with the E3 ubiquitin ligase TRIM27. This induces K48-linked ubiquitination and subsequent proteasomal degradation of NOD2.

In addition, evidence was provided that NOD2, unlike NOD1, can shuttle to the nucleus (Figure 3.11 and Figure 3.12). Since endogenous NOD1 and NOD2 proteins are difficult to detect, this could thus far only be demonstrated for ectopically expressed proteins. Until now, only two other members of the human NLR family are known to shuttle to the nucleus. CIITA, one of the founding members of the NLR family, has long been recognized as a regulator of MHC class II gene expression by acting as a scaffold for DNA-binding transcription factor assembly in the nucleus (Steimle*, et al.* 1993, Zika and Ting 2005). Recently, NLRC5 has also been shown to localize to the nucleus and to regulate MHC class I expression (Meissner*, et al.* 2010), although the exact function of NLRC5 in the nucleus remains controversial (Benko*, et al.* 2010). Nuclear import of macromolecules through the nuclear pore complex (NPC) is an active process and requires a nuclear localization signal (NLS) on the cargo protein. CIITA has been shown to possess three NLSs (Cressman*, et al.* 1999, Spilianakis*, et al.* 2000, Cressman*, et al.* 2001) and a bipartite NLS has also been identified in NLRC5 (Meissner*, et al.* 2010). However, preliminary sequence analysis failed to identify a bipartite NLS in NOD2. NOD2 recruitment to the nucleus could possibly be mediated by a so far unknown NLS sequence or carrier proteins. Nevertheless, we suppose that a small functional group of human NLR proteins with nuclear localization exists (Kufer and Sansonetti 2011). In common with CIITA and

NLRC5, NOD2 can be regarded as a member of this group possessing the ability to localize to the nucleus and/or having a function in gene expression.

Nuclear translocation and functionality have also been shown for several NLR-related plant R proteins. For tobacco N, barley MLA, arabidopsis RPS4 and potato RX R proteins nuclear localization is essential for defence activation (Burch-Smith*, et al.* 2007, Shen*, et al.* 2007, Tameling and Baulcombe 2007, Wirthmueller*, et al.* 2007). A revised model for R protein-mediated defence response suggests that pathogen recognition takes place in the cytoplasm, whereas transcriptional reprogramming to activate the immune response is carried out in the nucleus (Liu and Coaker 2008). For example, activated MLA has been shown to directly interact with repressive WRKY transcription factors in the nucleus and therefore enables defence gene transcription (Shen*, et al.* 2007). However, it is unlikely that plant R proteins elicit defence responses exclusively in the nucleus. For tobacco N, which confers resistance to Tobacco mosaic virus (TMV), MAP kinase activation in the cytosol is necessary for N-mediated resistance in addition to its nuclear functions (Jin*, et al.* 2003, Liu*, et al.* 2003). NOD2 might also not only recognize pathogens and activate MAP kinases and NF-κB in the cytosol, but possesses additional nuclear functions to mediate and control immune responses. TRIM27 is recruited to specific sub-nuclear compartments (Matsuura*, et al.* 2005) and was suggested as a transcriptional repressor (Shimono*, et al.* 2000, Bloor*, et al.* 2005). In analogy to the function of plant R proteins, one possibility is that TRIM27, in addition to its role in NOD2 regulation, is functionally involved in orchestrating NOD2 nuclear functions. It would be of great interest to further elucidate this issue.

Taken together, we revealed the importance of the ATPase domain in NOD1 and NOD2 and found evidence for differential activation mechanisms of these two closely related NLR proteins. We identified TRIM27 as a new interaction partner specific for NOD2 using yeast two-hybrid screening and co-immunoprecipitation analysis. This interaction is direct and enhanced upon NOD2 activation. TRIM27 induces K48-linked ubiquitination of NOD2, targeting it for proteasomal degradation. Thus, TRIM27 is critically involved in negatively regulating NOD2 activity. We also detected enhanced TRIM27 expression in Crohn's disease patients. These findings identify a new and promising target for therapeutic modulation of NOD2 activity in this disease.

5 References

Abbott DW, Wilkins A, Asara JM and Cantley LC (2004). "The Crohn's disease protein, NOD2, requires RIP2 in order to induce ubiquitinylation of a novel site on NEMO." Curr Biol **14**(24): 2217-27.

Abbott DW, Yang Y, Hutti JE, Madhavarapu S, Kelliher MA and Cantley LC (2007). "Coordinated regulation of Toll-like receptor and NOD2 signaling by K63-linked polyubiquitin chains." Mol Cell Biol **27**(17): 6012-25.

Arimoto K, Funami K, Saeki Y, Tanaka K, Okawa K, Takeuchi O, Akira S, Murakami Y and Shimotohno K (2010). "Polyubiquitin conjugation to NEMO by triparite motif protein 23 (TRIM23) is critical in antiviral defense." Proc Natl Acad Sci U S A **107**(36): 15856-61.

Bailly V, Lauder S, Prakash S and Prakash L (1997). "Yeast DNA repair proteins Rad6 and Rad18 form a heterodimer that has ubiquitin conjugating, DNA binding, and ATP hydrolytic activities." J Biol Chem **272**(37): 23360-5.

Barnich N, Aguirre JE, Reinecker HC, Xavier R and Podolsky DK (2005a). "Membrane recruitment of NOD2 in intestinal epithelial cells is essential for nuclear factor-{kappa}B activation in muramyl dipeptide recognition." J Cell Biol **170**(1): 21-6.

Barnich N, Hisamatsu T, Aguirre JE, Xavier R, Reinecker HC and Podolsky DK (2005b). "GRIM-19 interacts with nucleotide oligomerization domain 2 and serves as downstream effector of anti-bacterial function in intestinal epithelial cells." J Biol Chem **280**(19): 19021-6.

Benko S, Magalhaes JG, Philpott DJ and Girardin SE (2010). "NLRC5 limits the activation of inflammatory pathways." J Immunol **185**(3): 1681-91.

Bergsbaken T, Fink SL and Cookson BT (2009). "Pyroptosis: host cell death and inflammation." Nat Rev Microbiol **7**(2): 99-109.

Bertrand MJ, Doiron K, Labbe K, Korneluk RG, Barker PA and Saleh M (2009). "Cellular inhibitors of apoptosis cIAP1 and cIAP2 are required for innate immunity signaling by the pattern recognition receptors NOD1 and NOD2." Immunity **30**(6): 789-801.

Bielig H, Rompikuntal PK, Mitesh D, Zurek B, Lindmark B, Ramstedt M, Wai SN and Kufer TA (2011). "NOD-like receptor activation by outer-membrane vesicles (OMVs) from non-O1 non-O139 Vibrio cholerae is modulated by the quorum sensing regulator HapR." Infect Immun.

Bielig H, Zurek B, Kutsch A, Menning M, Philpott DJ, Sansonetti PJ and Kufer TA (2009). "A function for AAMP in Nod2-mediated NF-kappaB activation." Mol Immunol.

Bloor AJ, Kotsopoulou E, Hayward P, Champion BR and Green AR (2005). "RFP represses transcriptional activation by bHLH transcription factors." Oncogene **24**(45): 6729-36.

Boo KH and Yang JS (2010). "Intrinsic cellular defenses against virus infection by antiviral type I interferon." Yonsei Med J **51**(1): 9-17.

Borzutzky A, Fried A, Chou J, Bonilla FA, Kim S and Dedeoglu F (2009). "NOD2-associated diseases: Bridging innate immunity and autoinflammation." Clin Immunol.

Buchsbaum S, Morris C, Bochard V and Jalinot P (2007). "Human INT6 interacts with MCM7 and regulates its stability during S phase of the cell cycle." Oncogene **26**(35): 5132-44.

Burch-Smith TM, Schiff M, Caplan JL, Tsao J, Czymmek K and Dinesh-Kumar SP (2007). "A novel role for the TIR domain in association with pathogen-derived elicitors." PLoS Biol **5**(3): e68.

Burckstummer T, Baumann C, et al. (2009). "An orthogonal proteomic-genomic screen identifies AIM2 as a cytoplasmic DNA sensor for the inflammasome." Nat Immunol.

Cao T, Borden KL, Freemont PS and Etkin LD (1997). "Involvement of the rfp tripartite motif in protein-protein interactions and subcellular distribution." J Cell Sci **110 (Pt 14)**: 1563-71.

Cao T, Duprez E, Borden KL, Freemont PS and Etkin LD (1998). "Ret finger protein is a normal component of PML nuclear bodies and interacts directly with PML." J Cell Sci **111 (Pt 10)**: 1319-29.

Carthagena L, Bergamaschi A, et al. (2009). "Human TRIM gene expression in response to interferons." PLoS One **4**(3): e4894.

Chae JJ, Cho YH, Lee GS, Cheng J, Liu PP, Feigenbaum L, Katz SI and Kastner DL (2011). "Gain-of-Function Pyrin Mutations Induce NLRP3 Protein-Independent Interleukin-1beta Activation and Severe Autoinflammation in Mice." Immunity **34**(5): 755-68.

Chae JJ, Komarow HD, Cheng J, Wood G, Raben N, Liu PP and Kastner DL (2003). "Targeted disruption of pyrin, the FMF protein, causes heightened sensitivity to endotoxin and a defect in macrophage apoptosis." Mol Cell **11**(3): 591-604.

Chae JJ, Wood G, Masters SL, Richard K, Park G, Smith BJ and Kastner DL (2006). "The B30.2 domain of pyrin, the familial Mediterranean fever protein, interacts directly with caspase-1 to modulate IL-1beta production." Proc Natl Acad Sci U S A **103**(26): 9982-7.

Chamaillard M, Hashimoto M, et al. (2003). "An essential role for NOD1 in host recognition of bacterial peptidoglycan containing diaminopimelic acid." Nat Immunol **4**(7): 702-7.

Chen G and Goeddel DV (2002). "TNF-R1 signaling: a beautiful pathway." Science **296**(5573): 1634-5.

Chen L, Uchida K, Endler A and Shibasaki F (2007). "Mammalian tumor suppressor Int6 specifically targets hypoxia inducible factor 2 alpha for degradation by hypoxia- and pVHL-independent regulation." J Biol Chem **282**(17): 12707-16.

Chen ZJ and Sun LJ (2009). "Nonproteolytic functions of ubiquitin in cell signaling." Mol Cell **33**(3): 275-86.

Chu Y and Yang X (2011). "SUMO E3 ligase activity of TRIM proteins." Oncogene **30**(9): 1108-16.

Chuang TH and Ulevitch RJ (2004). "Triad3A, an E3 ubiquitin-protein ligase regulating Toll-like receptors." Nat Immunol **5**(5): 495-502.

Clark NM, Marinis JM, Cobb BA and Abbott DW (2008). "MEKK4 Sequesters RIP2 to Dictate NOD2 Signal Specificity." Curr Biol.

Cooney R, Baker J, et al. (2009). "NOD2 stimulation induces autophagy in dendritic cells influencing bacterial handling and antigen presentation." Nat Med.

Cressman DE, Chin KC, Taxman DJ and Ting JP (1999). "A defect in the nuclear translocation of CIITA causes a form of type II bare lymphocyte syndrome." Immunity **10**(2): 163-71.

Cressman DE, O'Connor WJ, Greer SF, Zhu XS and Ting JP (2001). "Mechanisms of nuclear import and export that control the subcellular localization of class II transactivator." J Immunol **167**(7): 3626-34.

da Silva Correia J, Miranda Y, Leonard N, Hsu J and Ulevitch RJ (2007a). "Regulation of Nod1-mediated signaling pathways." Cell Death Differ **14**(4): 830-9.

da Silva Correia J, Miranda Y, Leonard N and Ulevitch R (2007b). "SGT1 is essential for Nod1 activation." Proc Natl Acad Sci U S A **104**(16): 6764-9.

Danot O, Marquenet E, Vidal-Ingigliardi D and Richet E (2009). "Wheel of Life, Wheel of Death: A Mechanistic Insight into Signaling by STAND Proteins." Structure **17**(2): 172-82.

Davis S and Watson JC (1996). "In vitro activation of the interferon-induced, double-stranded RNA-dependent protein kinase PKR by RNA from the 3' untranslated regions of human alpha-tropomyosin." Proc Natl Acad Sci U S A **93**(1): 508-13.

Deshaies RJ and Joazeiro CA (2009). "RING domain E3 ubiquitin ligases." Annu Rev Biochem **78**: 399-434.

Dho SH and Kwon KS (2003). "The Ret finger protein induces apoptosis via its RING finger-B box-coiled-coil motif." J Biol Chem **278**(34): 31902-8.

Dugan JW, Albor A, et al. (2009). "Nucleotide oligomerization domain-2 interacts with 2'-5'-oligoadenylate synthetase type 2 and enhances RNase-L function in THP-1 cells." Mol Immunol **47**(2-3): 560-6.

Duncan JA, Bergstralh DT, Wang Y, Willingham SB, Ye Z, Zimmermann AG and Ting JP (2007). "Cryopyrin/NALP3 binds ATP/dATP, is an ATPase, and requires ATP binding to mediate inflammatory signaling." Proc Natl Acad Sci U S A **104**(19): 8041-6.

Eitel J, Krull M, et al. (2008). "Beta-PIX and Rac1 GTPase mediate trafficking and negative regulation of NOD2." J Immunol **181**(4): 2664-71.

Faustin B, Lartigue L, et al. (2007). "Reconstituted NALP1 inflammasome reveals two-step mechanism of caspase-1 activation." Mol Cell **25**(5): 713-24.

Fernandes-Alnemri T, Yu JW, Datta P, Wu J and Alnemri ES (2009). "AIM2 activates the inflammasome and cell death in response to cytoplasmic DNA." Nature.

Franchi L, Stoolman J, Kanneganti TD, Verma A, Ramphal R and Nunez G (2007). "Critical role for Ipaf in Pseudomonas aeruginosa-induced caspase-1 activation." Eur J Immunol **37**(11): 3030-9.

Franchi L, Warner N, Viani K and Nunez G (2009). "Function of Nod-like receptors in microbial recognition and host defense." Immunol Rev **227**(1): 106-28.

French_FMF_Consortium (1997). "A candidate gene for familial Mediterranean fever." Nat Genet **17**(1): 25-31.

Fritz JH, Girardin SE, Fitting C, Werts C, Mengin-Lecreulx D, Caroff M, Cavaillon JM, Philpott DJ and Adib-Conquy M (2005). "Synergistic stimulation of human monocytes and dendritic cells by Toll-like receptor 4 and NOD1- and NOD2-activating agonists." Eur J Immunol **35**(8): 2459-70.

Fritz JH, Le Bourhis L, et al. (2007). "Nod1-mediated innate immune recognition of peptidoglycan contributes to the onset of adaptive immunity." Immunity **26**(4): 445-59.

Frutuoso MS, Hori JI, Pereira MS, Junior DS, Sonego F, Kobayashi KS, Flavell RA, Cunha FQ and Zamboni DS (2010). "The pattern recognition receptors Nod1 and Nod2 account for neutrophil recruitment to the lungs of mice infected with Legionella pneumophila." Microbes Infect **12**(11): 819-27.

Gack MU, Shin YC, et al. (2007). "TRIM25 RING-finger E3 ubiquitin ligase is essential for RIG-I-mediated antiviral activity." Nature **446**(7138): 916-920.

Girardin SE, Boneca IG, et al. (2003a). "Nod1 detects a unique muropeptide from gram-negative bacterial peptidoglycan." Science **300**(5625): 1584-7.

Girardin SE, Boneca IG, Viala J, Chamaillard M, Labigne A, Thomas G, Philpott DJ and Sansonetti PJ (2003b). "Nod2 is a general sensor of peptidoglycan through muramyl dipeptide (MDP) detection." J Biol Chem **278**(11): 8869-72.

Girardin SE, Tournebize R, et al. (2001). "CARD4/Nod1 mediates NF-kappaB and JNK activation by invasive Shigella flexneri." EMBO Rep **2**(8): 736-42.

Greer SF, Zika E, Conti B, Zhu XS and Ting JP (2003). "Enhancement of CIITA transcriptional function by ubiquitin." Nat Immunol **4**(11): 1074-82.

Gutierrez O, Pipaon C, Inohara N, Fontalba A, Ogura Y, Prosper F, Nunez G and Fernandez-Luna JL (2002). "Induction of Nod2 in myelomonocytic and intestinal epithelial cells via nuclear factor-kappa B activation." J Biol Chem **277**(44): 41701-5.

Gyuris J, Golemis E, Chertkov H and Brent R (1993). "Cdi1, a human G1 and S phase protein phosphatase that associates with Cdk2." Cell **75**(4): 791-803.

Hanson PI and Whiteheart SW (2005). "AAA+ proteins: have engine, will work." Nat Rev Mol Cell Biol **6**(7): 519-29.

Harbers M, Nomura T, Ohno S and Ishii S (2001). "Intracellular localization of the Ret finger protein depends on a functional nuclear export signal and protein kinase C activation." J Biol Chem **276**(51): 48596-607.

Harton JA, Cressman DE, Chin KC, Der CJ and Ting JP (1999). "GTP binding by class II transactivator: role in nuclear import." Science **285**(5432): 1402-5.

Harton JA and Ting JP (2000). "Class II transactivator: mastering the art of major histocompatibility complex expression." Mol Cell Biol **20**(17): 6185-94.

Hasegawa M, Fujimoto Y, Lucas PC, Nakano H, Fukase K, Nunez G and Inohara N (2008). "A critical role of RICK/RIP2 polyubiquitination in Nod-induced NF-kappaB activation." Embo J **27**(2): 373-83.

Hasegawa M, Yamazaki T, Kamada N, Tawaratsumida K, Kim YG, Nunez G and Inohara N (2011). "Nucleotide-Binding Oligomerization Domain 1 Mediates Recognition of Clostridium difficile and Induces Neutrophil Recruitment and Protection against the Pathogen." J Immunol **186**(8): 4872-80.

Hasegawa N, Iwashita T, Asai N, Murakami H, Iwata Y, Isomura T, Goto H, Hayakawa T and Takahashi M (1996). "A RING finger motif regulates transforming activity of the rfp/ret fusion gene." Biochem Biophys Res Commun **225**(2): 627-31.

Henry J, Ribouchon M, Depetris D, Mattei M, Offer C, Tazi-Ahnini R and Pontarotti P (1997). "Cloning, structural analysis, and mapping of the B30 and B7 multigenic families to the major histocompatibility complex (MHC) and other chromosomal regions." Immunogenetics **46**(5): 383-95.

Hershko A and Ciechanover A (1998). "The ubiquitin system." Annu Rev Biochem **67**: 425-79.

Higgs R, Lazzari E, Wynne C, Ni Gabhann J, Espinosa A, Wahren-Herlenius M and Jefferies CA (2010). "Self protection from anti-viral responses--Ro52 promotes degradation of the transcription factor IRF7 downstream of the viral Toll-Like receptors." PLoS One **5**(7): e11776.

Higgs R, Ni Gabhann J, Ben Larbi N, Breen EP, Fitzgerald KA and Jefferies CA (2008). "The E3 ubiquitin ligase Ro52 negatively regulates IFN-beta production post-pathogen recognition by polyubiquitin-mediated degradation of IRF3." J Immunol **181**(3): 1780-6.

Hitotsumatsu O, Ahmad RC, et al. (2008). "The ubiquitin-editing enzyme A20 restricts nucleotide-binding oligomerization domain containing 2-triggered signals." Immunity **28**(3): 381-90.

Hornung V, Ablasser A, Charrel-Dennis M, Bauernfeind F, Horvath G, Caffrey DR, Latz E and Fitzgerald KA (2009). "AIM2 recognizes cytosolic dsDNA and forms a caspase-1-activating inflammasome with ASC." Nature.

Hruz P and Eckmann L (2010). "Innate immune defence: NOD2 and autophagy in the pathogenesis of Crohn's disease." Swiss Med Wkly **140**: w13135.

Hsu YM, Zhang Y, You Y, Wang D, Li H, Duramad O, Qin XF, Dong C and Lin X (2007). "The adaptor protein CARD9 is required for innate immune responses to intracellular pathogens." Nat Immunol **8**(2): 198-205.

Hu Y, Mao K, et al. (2010). "Tripartite-motif protein 30 negatively regulates NLRP3 inflammasome activation by modulating reactive oxygen species production." J Immunol **185**(12): 7699-705.

Hugot JP, Chamaillard M, et al. (2001). "Association of NOD2 leucine-rich repeat variants with susceptibility to Crohn's disease." Nature **411**(6837): 599-603.

Hysi P, Kabesch M, et al. (2005). "NOD1 variation, immunoglobulin E and asthma." Hum Mol Genet **14**(7): 935-41.

Inohara N, Koseki T, et al. (1999). "Nod1, an Apaf-1-like activator of caspase-9 and nuclear factor-kappaB." J Biol Chem **274**(21): 14560-7.

Inohara N, Koseki T, Lin J, del Peso L, Lucas PC, Chen FF, Ogura Y and Nunez G (2000). "An induced proximity model for NF-kappa B activation in the Nod1/RICK and RIP signaling pathways." J Biol Chem **275**(36): 27823-31.

Inohara N, Ogura Y, et al. (2003). "Host recognition of bacterial muramyl dipeptide mediated through NOD2. Implications for Crohn's disease." J Biol Chem **278**(8): 5509-12.

International_FMF_Consortium (1997). "Ancient missense mutations in a new member of the RoRet gene family are likely to cause familial Mediterranean fever. The International FMF Consortium." Cell **90**(4): 797-807.

Ismair MG, Vavricka SR, Kullak-Ublick GA, Fried M, Mengin-Lecreulx D and Girardin SE (2006). "hPepT1 selectively transports muramyl dipeptide but not Nod1-activating muramyl peptides." Can J Physiol Pharmacol **84**(12): 1313-9.

Isomura T, Tamiya-Koizumi K, Suzuki M, Yoshida S, Taniguchi M, Matsuyama M, Ishigaki T, Sakuma S and Takahashi M (1992). "RFP is a DNA binding protein associated with the nuclear matrix." Nucleic Acids Res **20**(20): 5305-10.

Iyer LM, Leipe DD, Koonin EV and Aravind L (2004). "Evolutionary history and higher order classification of AAA+ ATPases." J Struct Biol **146**(1-2): 11-31.

Jin H, Liu Y, Yang KY, Kim CY, Baker B and Zhang S (2003). "Function of a mitogen-activated protein kinase pathway in N gene-mediated resistance in tobacco." Plant J **33**(4): 719-31.

Jones JD and Dangl JL (2006). "The plant immune system." Nature **444**(7117): 323-9.

Kanazawa N, Okafuji I, et al. (2005). "Early-onset sarcoidosis and CARD15 mutations with constitutive nuclear factor-kappaB activation: common genetic etiology with Blau syndrome." Blood **105**(3): 1195-7.

Kaparakis M, Turnbull L, et al. (2009). "Bacterial membrane vesicles deliver peptidoglycan to NOD1 in epithelial cells." Cell Microbiol.

Kawai T and Akira S (2010). "The role of pattern-recognition receptors in innate immunity: update on Toll-like receptors." Nat Immunol **11**(5): 373-84.

Kerur N, Veettil MV, Sharma-Walia N, Bottero V, Sadagopan S, Otageri P and Chandran B (2011). "IFI16 Acts as a Nuclear Pathogen Sensor to Induce the Inflammasome in Response to Kaposi Sarcoma-Associated Herpesvirus Infection." Cell Host Microbe **9**(5): 363-75.

Kim YG, Park JH, Daignault S, Fukase K and Nunez G (2008a). "Cross-tolerization between Nod1 and Nod2 signaling results in reduced refractoriness to bacterial infection in Nod2-deficient macrophages." J Immunol **181**(6): 4340-6.

Kim YG, Park JH, Shaw MH, Franchi L, Inohara N and Nunez G (2008b). "The cytosolic sensors Nod1 and Nod2 are critical for bacterial recognition and host defense after exposure to Toll-like receptor ligands." Immunity **28**(2): 246-57.

Kobayashi KS, Chamaillard M, Ogura Y, Henegariu O, Inohara N, Nunez G and Flavell RA (2005). "Nod2-dependent regulation of innate and adaptive immunity in the intestinal tract." Science **307**(5710): 731-4.

Kong HJ, Anderson DE, et al. (2007). "Cutting edge: autoantigen Ro52 is an interferon inducible E3 ligase that ubiquitinates IRF-8 and enhances cytokine expression in macrophages." J Immunol **179**(1): 26-30.

Kosovac K, Brenmoehl J, Holler E, Falk W, Schoelmerich J, Hausmann M and Rogler G (2010). "Association of the NOD2 genotype with bacterial translocation via altered cell-cell contacts in Crohn's disease patients." Inflamm Bowel Dis **16**(8): 1311-21.

Kramer M, Boeck J, Reichenbach D, Kaether C, Schreiber S, Platzer M, Rosenstiel P and Huse K (2010). "NOD2-C2 - a novel NOD2 isoform activating NF-kappaB in a muramyl dipeptide-independent manner." BMC Res Notes **3**: 224.

Kramer M, Netea MG, de Jong DJ, Kullberg BJ and Adema GJ (2006). "Impaired dendritic cell function in Crohn's disease patients with NOD2 3020insC mutation." J Leukoc Biol **79**(4): 860-6.

Krieg A, Correa RG, Garrison JB, Le Negrate G, Welsh K, Huang Z, Knoefel WT and Reed JC (2009). "XIAP mediates NOD signaling via interaction with RIP2." Proc Natl Acad Sci U S A.

Kufer TA (2008). "Signal transduction pathways used by NLR-type innate immune receptors." Mol Biosyst **4**(5): 380-6.

Kufer TA, Banks DJ and Philpott DJ (2006a). "Innate immune sensing of microbes by Nod proteins." Ann N Y Acad Sci **1072**: 19-27.

Kufer TA, Kremmer E, Adam AC, Philpott DJ and Sansonetti PJ (2008). "The pattern-recognition molecule Nod1 is localized at the plasma membrane at sites of bacterial interaction." Cell Microbiol **10**(2): 477-86.

Kufer TA, Kremmer E, Banks DJ and Philpott DJ (2006b). "Role for erbin in bacterial activation of Nod2." Infect Immun **74**(6): 3115-24.

Kufer TA and Sansonetti PJ (2011). "NLR functions beyond pathogen recognition." Nat Immunol **12**(2): 121-8.

Laemmli UK (1970). "Cleavage of structural proteins during the assembly of the head of bacteriophage T4." Nature **227**(5259): 680-5.

Laing KJ, Purcell MK, Winton JR and Hansen JD (2008). "A genomic view of the NOD-like receptor family in teleost fish: identification of a novel NLR subfamily in zebrafish." BMC Evol Biol **8**: 42.

LeBlanc PM, Yeretssian G, Rutherford N, Doiron K, Nadiri A, Zhu L, Green DR, Gruenheid S and Saleh M (2008). "Caspase-12 modulates NOD signaling and regulates antimicrobial peptide production and mucosal immunity." Cell Host Microbe **3**(3): 146-57.

Lecat A, Piette J and Legrand-Poels S (2010). "The protein Nod2: an innate receptor more complex than previously assumed." Biochem Pharmacol **80**(12): 2021-31.

Lecine P, Esmiol S, et al. (2007). "The NOD2-RICK complex signals from the plasma membrane." J Biol Chem **282**(20): 15197-207.

Legrand-Poels S, Kustermans G, Bex F, Kremmer E, Kufer TA and Piette J (2007). "Modulation of Nod2-dependent NF-kappaB signaling by the actin cytoskeleton." J Cell Sci **120**(Pt 7): 1299-310.

Li P, Nijhawan D, Budihardjo I, Srinivasula SM, Ahmad M, Alnemri ES and Wang X (1997). "Cytochrome c and dATP-dependent formation of Apaf-1/caspase-9 complex initiates an apoptotic protease cascade." Cell **91**(4): 479-89.

Lipinski S, Till A, Sina C, Arlt A, Grasberger H, Schreiber S and Rosenstiel P (2009). "DUOX2-derived reactive oxygen species are effectors of NOD2-mediated antibacterial responses." J Cell Sci **122**(Pt 19): 3522-30.

Liu J and Coaker G (2008). "Nuclear trafficking during plant innate immunity." Mol Plant **1**(3): 411-22.

Liu S and Chen ZJ (2011). "Expanding role of ubiquitination in NF-kappaB signaling." Cell Res **21**(1): 6-21.

Liu Y, Jin H, Yang KY, Kim CY, Baker B and Zhang S (2003). "Interaction between two mitogen-activated protein kinases during tobacco defense signaling." Plant J **34**(2): 149-60.

Lu C, Wang A, Wang L, Dorsch M, Ocain TD and Xu Y (2005). "Nucleotide binding to CARD12 and its role in CARD12-mediated caspase-1 activation." Biochem Biophys Res Commun **331**(4): 1114-9.

Lu D, Lin W, et al. (2011). "Direct ubiquitination of pattern recognition receptor FLS2 attenuates plant innate immunity." Science **332**(6036): 1439-42.

Lukasik E and Takken FL (2009). "STANDing strong, resistance proteins instigators of plant defence." Curr Opin Plant Biol.

Maeda S, Hsu LC, Liu H, Bankston LA, Iimura M, Kagnoff MF, Eckmann L and Karin M (2005). "Nod2 mutation in Crohn's disease potentiates NF-kappaB activity and IL-1beta processing." Science **307**(5710): 734-8.

Magalhaes JG, Sorbara MT, Girardin SE and Philpott DJ (2011). "What is new with Nods?" Curr Opin Immunol **23**(1): 29-34.

Mariathasan S, Newton K, Monack DM, Vucic D, French DM, Lee WP, Roose-Girma M, Erickson S and Dixit VM (2004). "Differential activation of the inflammasome by caspase-1 adaptors ASC and Ipaf." Nature **430**(6996): 213-8.

Marina-Garcia N, Franchi L, Kim YG, Hu Y, Smith DE, Boons GJ and Nunez G (2009). "Clathrin- and dynamin-dependent endocytic pathway regulates muramyl dipeptide internalization and NOD2 activation." J Immunol **182**(7): 4321-7.

Martinon F and Tschopp J (2007). "Inflammatory caspases and inflammasomes: master switches of inflammation." Cell Death Differ **14**(1): 10-22.

Matsuura T, Shimono Y, Kawai K, Murakami H, Urano T, Niwa Y, Goto H and Takahashi M (2005). "PIAS proteins are involved in the SUMO-1 modification, intracellular translocation and transcriptional repressive activity of RET finger protein." Exp Cell Res **308**(1): 65-77.

Mayor A, Martinon F, De Smedt T, Petrilli V and Tschopp J (2007). "A crucial function of SGT1 and HSP90 in inflammasome activity links mammalian and plant innate immune responses." Nat Immunol **8**(5): 497-503.

McDonald C, Chen FF, Ollendorff V, Ogura Y, Marchetto S, Lecine P, Borg JP and Nunez G (2005). "A role for Erbin in the regulation of Nod2-dependent NF-kappaB signaling." J Biol Chem **280**(48): 40301-9.

McNab FW, Rajsbaum R, Stoye JP and O'Garra A (2010). "Tripartite-motif proteins and innate immune regulation." Curr Opin Immunol.

Medzhitov R (2007). "Recognition of microorganisms and activation of the immune response." Nature **449**(7164): 819-26.

Meissner TB, Li A, Biswas A, Lee KH, Liu YJ, Bayir E, Iliopoulos D, van den Elsen PJ and Kobayashi KS (2010). "NLR family member NLRC5 is a transcriptional regulator of MHC class I genes." Proc Natl Acad Sci U S A **107**(31): 13794-9.

Morris-Desbois C, Bochard V, Reynaud C and Jalinot P (1999). "Interaction between the Ret finger protein and the Int-6 gene product and co-localisation into nuclear bodies." J Cell Sci **112 (Pt 19)**: 3331-42.

Munoz E, Courtois G, Veschambre P, Jalinot P and Israel A (1994). "Tax induces nuclear translocation of NF-kappa B through dissociation of cytoplasmic complexes containing p105 or p100 but does not induce degradation of I kappa B alpha/MAD3." J Virol **68**(12): 8035-44.

Nakayama EE and Shioda T (2010). "Anti-retroviral activity of TRIM5 alpha." Rev Med Virol **20**(2): 77-92.

Napolitano LM, Jaffray EG, Hay RT and Meroni G (2011). "Functional interactions between ubiquitin E2 enzymes and TRIM proteins." Biochem J **434**(2): 309-19.

Nembrini C, Kisielow J, Shamshiev AT, Tortola L, Coyle AJ, Kopf M and Marsland BJ (2009). "The kinase activity of Rip2 determines its stability and consequently Nod1- and Nod2-mediated immune responses." J Biol Chem.

Netea MG, Ferwerda G, et al. (2005). "Nucleotide-binding oligomerization domain-2 modulates specific TLR pathways for the induction of cytokine release." J Immunol **174**(10): 6518-23.

Netea MG, Kullberg BJ, de Jong DJ, Franke B, Sprong T, Naber TH, Drenth JP and Van der Meer JW (2004). "NOD2 mediates anti-inflammatory signals induced by TLR2 ligands: implications for Crohn's disease." Eur J Immunol **34**(7): 2052-9.

O'Neill LA and Bowie AG (2010). "Sensing and signaling in antiviral innate immunity." Curr Biol **20**(7): R328-33.

Ogura Y, Bonen DK, et al. (2001a). "A frameshift mutation in NOD2 associated with susceptibility to Crohn's disease." Nature **411**(6837): 603-6.

Ogura Y, Inohara N, Benito A, Chen FF, Yamaoka S and Nunez G (2001b). "Nod2, a Nod1/Apaf-1 family member that is restricted to monocytes and activates NF-kappaB." J Biol Chem **276**(7): 4812-8.

Ogura Y, Lala S, et al. (2003). "Expression of NOD2 in Paneth cells: a possible link to Crohn's ileitis." Gut **52**(11): 1591-7.

Oh HM, Lee HJ, et al. (2005). "Induction and localization of NOD2 protein in human endothelial cells." Cell Immunol **237**(1): 37-44.

Ozato K, Shin DM, Chang TH and Morse HC, 3rd (2008). "TRIM family proteins and their emerging roles in innate immunity." Nat Rev Immunol **8**(11): 849-60.

Pan Q, Kravchenko V, et al. (2006). "NF-kappa B-inducing kinase regulates selected gene expression in the Nod2 signaling pathway." Infect Immun **74**(4): 2121-7.

Park JH, Kim YG, McDonald C, Kanneganti TD, Hasegawa M, Body-Malapel M, Inohara N and Nunez G (2007a). "RICK/RIP2 mediates innate immune responses induced through Nod1 and Nod2 but not TLRs." J Immunol **178**(4): 2380-6.

Park JH, Kim YG, Shaw M, Kanneganti TD, Fujimoto Y, Fukase K, Inohara N and Nunez G (2007b). "Nod1/RICK and TLR signaling regulate chemokine and antimicrobial innate immune responses in mesothelial cells." J Immunol **179**(1): 514-21.

Patel CA and Ghiselli G (2005). "The RET finger protein interacts with the hinge region of SMC3." Biochem Biophys Res Commun **330**(1): 333-40.

Poeck H, Bscheider M, et al. (2010). "Recognition of RNA virus by RIG-I results in activation of CARD9 and inflammasome signaling for interleukin 1 beta production." Nat Immunol **11**(1): 63-9.

Poyet JL, Srinivasula SM, Tnani M, Razmara M, Fernandes-Alnemri T and Alnemri ES (2001). "Identification of Ipaf, a human caspase-1-activating protein related to Apaf-1." J Biol Chem **276**(30): 28309-13.

Proell M, Riedl SJ, Fritz JH, Rojas AM and Schwarzenbacher R (2008). "The Nod-like receptor (NLR) family: a tale of similarities and differences." PLoS ONE **3**(4): e2119.

Rajsbaum R, Stoye JP and O'Garra A (2008). "Type I interferon-dependent and -independent expression of tripartite motif proteins in immune cells." Eur J Immunol **38**(3): 619-30.

Rasband WS (2007). ImageJ. Bethesda, Maryland, USA, U.S. National Institutes of Health.

Ratner AJ, Aguilar JL, Shchepetov M, Lysenko ES and Weiser JN (2007). "Nod1 mediates cytoplasmic sensing of combinations of extracellular bacteria." Cell Microbiol **9**(5): 1343-51.

Reubold TF, Wohlgemuth S and Eschenburg S (2011). "Crystal structure of full-length apaf-1: how the death signal is relayed in the mitochondrial pathway of apoptosis." Structure **19**(8): 1074-83.

Reymond A, Meroni G, et al. (2001). "The tripartite motif family identifies cell compartments." Embo J **20**(9): 2140-51.

Rhodes DA, de Bono B and Trowsdale J (2005). "Relationship between SPRY and B30.2 protein domains. Evolution of a component of immune defence?" Immunology **116**(4): 411-7.

Richards N, Schaner P, Diaz A, Stuckey J, Shelden E, Wadhwa A and Gumucio DL (2001). "Interaction between pyrin and the apoptotic speck protein (ASC) modulates ASC-induced apoptosis." J Biol Chem **276**(42): 39320-9.

Riedl SJ, Li W, Chao Y, Schwarzenbacher R and Shi Y (2005). "Structure of the apoptotic protease-activating factor 1 bound to ADP." Nature **434**(7035): 926-33.

Roberts TL, Idris A, et al. (2009). "HIN-200 Proteins Regulate Caspase Activation in Response to Foreign Cytoplasmic DNA." Science.

Rosenstiel P, Fantini M, Brautigam K, Kuhbacher T, Waetzig GH, Seegert D and Schreiber S (2003). "TNF-alpha and IFN-gamma regulate the expression of the NOD2 (CARD15) gene in human intestinal epithelial cells." Gastroenterology **124**(4): 1001-9.

Rosenstiel P, Huse K, et al. (2006). "A short isoform of NOD2/CARD15, NOD2-S, is an endogenous inhibitor of NOD2/receptor-interacting protein kinase 2-induced signaling pathways." Proc Natl Acad Sci U S A **103**(9): 3280-5.

Sabbah A, Chang TH, Harnack R, Frohlich V, Tominaga K, Dube PH, Xiang Y and Bose S (2009). "Activation of innate immune antiviral responses by Nod2." Nat Immunol **10**(10): 1073-80.

Sardiello M, Cairo S, Fontanella B, Ballabio A and Meroni G (2008). "Genomic analysis of the TRIM family reveals two groups of genes with distinct evolutionary properties." BMC Evol Biol **8**: 225.

Schroder K and Tschopp J (2010). "The inflammasomes." Cell **140**(6): 821-32.

Shen QH, Saijo Y, et al. (2007). "Nuclear activity of MLA immune receptors links isolate-specific and basal disease-resistance responses." Science **315**(5815): 1098-103.

Shi M, Deng W, et al. (2008). "TRIM30 alpha negatively regulates TLR-mediated NF-kappa B activation by targeting TAB2 and TAB3 for degradation." Nat Immunol **9**(4): 369-77.

Shim JH, Xiao C, et al. (2005). "TAK1, but not TAB1 or TAB2, plays an essential role in multiple signaling pathways in vivo." Genes Dev **19**(22): 2668-81.

Shimono Y, Murakami H, Hasegawa Y and Takahashi M (2000). "RET finger protein is a transcriptional repressor and interacts with enhancer of polycomb that has dual transcriptional functions." J Biol Chem **275**(50): 39411-9.

Spilianakis C, Papamatheakis J and Kretsovali A (2000). "Acetylation by PCAF enhances CIITA nuclear accumulation and transactivation of major histocompatibility complex class II genes." Mol Cell Biol **20**(22): 8489-98.

Srimathi T, Robbins SL, Dubas RL, Hasegawa M, Inohara N and Park YC (2008). "Monomer/dimer transition of the caspase-recruitment domain of human Nod1." Biochemistry **47**(5): 1319-25.

Steimle V, Otten LA, Zufferey M and Mach B (1993). "Complementation cloning of an MHC class II transactivator mutated in hereditary MHC class II deficiency (or bare lymphocyte syndrome)." Cell **75**(1): 135-46.

Suzuki T, Franchi L, et al. (2007). "Differential regulation of caspase-1 activation, pyroptosis, and autophagy via Ipaf and ASC in Shigella-infected macrophages." PLoS Pathog **3**(8): e111.

Swaan PW, Bensman T, Bahadduri PM, Hall MW, Sarkar A, Bao S, Khantwal CM, Ekins S and Knoell DL (2008). "Bacterial Peptide Recognition and Immune Activation Facilitated by Human Peptide Transporter PEPT2." Am J Respir Cell Mol Biol.

Tada H, Aiba S, Shibata K, Ohteki T and Takada H (2005). "Synergistic effect of Nod1 and Nod2 agonists with toll-like receptor agonists on human dendritic cells to generate interleukin-12 and T helper type 1 cells." Infect Immun **73**(12): 7967-76.

Takaoka A, Wang Z, et al. (2007). "DAI (DLM-1/ZBP1) is a cytosolic DNA sensor and an activator of innate immune response." Nature **448**(7152): 501-5.

Takeuchi O and Akira S (2010). "Pattern recognition receptors and inflammation." Cell **140**(6): 805-20.

Tameling WI and Baulcombe DC (2007). "Physical association of the NB-LRR resistance protein Rx with a Ran GTPase-activating protein is required for extreme resistance to Potato virus X." Plant Cell **19**(5): 1682-94.

Tao M, Scacheri PC, Marinis JM, Harhaj EW, Matesic LE and Abbott DW (2009). "ITCH K63-ubiquitinates the NOD2 binding protein, RIP2, to influence inflammatory signaling pathways." Curr Biol **19**(15): 1255-63.

Tezel G, Nagasaka T, Iwahashi N, Asai N, Iwashita T, Sakata K and Takahashi M (1999). "Different nuclear/cytoplasmic distributions of RET finger protein in different cell types." Pathol Int **49**(10): 881-6.

Ting JP, Lovering RC, et al. (2008a). "The NLR gene family: a standard nomenclature." Immunity **28**(3): 285-7.

Ting JP, Willingham SB and Bergstralh DT (2008b). "NLRs at the intersection of cell death and immunity." Nat Rev Immunol **8**(5): 372-9.

Toniato E, Chen XP, Losman J, Flati V, Donahue L and Rothman P (2002). "TRIM8/GERP RING finger protein interacts with SOCS-1." J Biol Chem **277**(40): 37315-22.

Travassos LH, Carneiro LA, et al. (2009). "Nod1 and Nod2 direct autophagy by recruiting ATG16L1 to the plasma membrane at the site of bacterial entry." Nat Immunol **11**(1): 55-62.

Tsuchida T, Zou J, Saitoh T, Kumar H, Abe T, Matsuura Y, Kawai T and Akira S (2010). "The ubiquitin ligase TRIM56 regulates innate immune responses to intracellular double-stranded DNA." Immunity **33**(5): 765-76.

Uehara A, Yang S, Fujimoto Y, Fukase K, Kusumoto S, Shibata K, Sugawara S and Takada H (2005). "Muramyldipeptide and diaminopimelic acid-containing desmuramylpeptides in combination with chemically synthesized Toll-like receptor agonists synergistically induced production of interleukin-8 in a NOD2- and NOD1-dependent manner, respectively, in human monocytic cells in culture." Cell Microbiol **7**(1): 53-61.

Unterholzner L, Keating SE, et al. (2010). "IFI16 is an innate immune sensor for intracellular DNA." Nat Immunol **11**(11): 997-1004.

van der Aa LM, Levraud JP, Yahmi M, Lauret E, Briolat V, Herbomel P, Benmansour A and Boudinot P (2009). "A large new subset of TRIM genes highly diversified by duplication and positive selection in teleost fish." BMC Biol **7**: 7.

van Duist MM, Albrecht M, Podswiadek M, Giachino D, Lengauer T, Punzi L and De Marchi M (2005). "A new CARD15 mutation in Blau syndrome." Eur J Hum Genet **13**(6): 742-7.

van Heel DA, Ghosh S, et al. (2005). "Muramyl dipeptide and toll-like receptor sensitivity in NOD2-associated Crohn's disease." Lancet **365**(9473): 1794-6.

Viala J, Chaput C, et al. (2004). "Nod1 responds to peptidoglycan delivered by the Helicobacter pylori cag pathogenicity island." Nat Immunol **5**(11): 1166-74.

Watanabe T, Kitani A, Murray PJ and Strober W (2004). "NOD2 is a negative regulator of Toll-like receptor 2-mediated T helper type 1 responses." Nat Immunol **5**(8): 800-8.

Wehkamp J, Harder J, et al. (2004). "NOD2 (CARD15) mutations in Crohn's disease are associated with diminished mucosal alpha-defensin expression." Gut **53**(11): 1658-64.

Weidinger S, Klopp N, et al. (2005). "Association of NOD1 polymorphisms with atopic eczema and related phenotypes." J Allergy Clin Immunol **116**(1): 177-84.

Windheim M, Lang C, Peggie M, Plater LA and Cohen P (2007). "Molecular mechanisms involved in the regulation of cytokine production by muramyl dipeptide." Biochem J **404**(2): 179-90.

Wirthmueller L, Zhang Y, Jones JD and Parker JE (2007). "Nuclear accumulation of the Arabidopsis immune receptor RPS4 is necessary for triggering EDS1-dependent defense." Curr Biol **17**(23): 2023-9.

Yamamoto-Furusho JK, Barnich N, Xavier R, Hisamatsu T and Podolsky DK (2006). "Centaurin beta1 down-regulates nucleotide-binding oligomerization domains 1- and 2-dependent NF-kappaB activation." J Biol Chem **281**(47): 36060-70.

Yang K, Shi HX, Liu XY, Shan YF, Wei B, Chen S and Wang C (2009). "TRIM21 is essential to sustain IFN regulatory factor 3 activation during antiviral response." J Immunol **182**(6): 3782-92.

Ye Z, Lich JD, Moore CB, Duncan JA, Williams KL and Ting JP (2008). "ATP binding by monarch-1/NLRP12 is critical for its inhibitory function." Mol Cell Biol **28**(5): 1841-50.

Yen HC, Gordon C and Chang EC (2003). "Schizosaccharomyces pombe Int6 and Ras homologs regulate cell division and mitotic fidelity via the proteasome." Cell **112**(2): 207-17.

Zha J, Han KJ, Xu LG, He W, Zhou Q, Chen D, Zhai Z and Shu HB (2006). "The Ret finger protein inhibits signaling mediated by the noncanonical and canonical IkappaB kinase family members." J Immunol **176**(2): 1072-80.

Zika E and Ting JP (2005). "Epigenetic control of MHC-II: interplay between CIITA and histone-modifying enzymes." Curr Opin Immunol **17**(1): 58-64.

Zurek B, Bielig H and Kufer TA (2011a). "Cell-Based Reporter Assay to Analyze Activation of Nod1 and Nod2." Methods Mol Biol **748**: 107-119.

Zurek B, Proell M, Wagner RN, Schwarzenbacher R and Kufer TA (2011b). "Mutational analysis of human NOD1 and NOD2 NACHT domains reveals different modes of activation." Innate Immun.

6 Abstract

The nucleotide-binding domain and leucine-rich repeat containing gene (NLR) family member NOD2 is involved in mediating antimicrobial innate immune responses. Uncontrolled NOD2 activity can lead to severe inflammatory disorders, but the regulation of NOD2 is still poorly understood.

The NOD2 ATPase domain seems to exhibit a crucial regulatory function. Mutations affecting conserved residues of this domain are linked to the auto-inflammatory diseases Blau syndrome and early-onset sarcoidosis, whereas mutation of the Walker A box lead to signalling repression. Conserved amino acids within the ATPase domain of NOD2 and the related NLR protein NOD1 were analysed in a systematic mutational approach. The results revealed that a functional Walker A and B box, GxP motif and Sensor 1 are important for both NOD1 and NOD2 activation, as mutation of these residues strongly impaired NF-κB activation. This indicates that nucleotide binding and an initial nucleotide hydrolysis step are essential for both NOD1 and NOD2 activation. Furthermore, the data gave evidence that mutations in the extended Walker B box and the WH histidine have opposing effects on NOD1- and NOD2-mediated signalling. Whereas they were non-functional in NOD1, NOD2 auto-activation was enhanced compared to the wild type. This led us to propose that NOD2 is more prone for auto-activation and need to be more tightly controlled than NOD1.

In line with this assumption, NOD2, but not NOD1, was found to be subjected to rapid protein turnover involving ubiquitin-mediated proteasomal degradation. A yeast two-hybrid screen identified TRIM27 as a new binding partner for NOD2. The specificity of this interaction was confirmed by reciprocal co-immunoprecipitation experiments in a human cell line. The interaction was mediated by the NOD2 nucleotide-binding domain (NBD) and the TRIM27 PRY-SPRY motif. TRIM27 is a RING domain E3 ubiquitin ligase. NOD2, but not NOD1, was identified to be ubiquitinated with K48-linked ubiquitin chains and subjected to proteasomal degradation dependent on functional TRIM27. Accordingly, TRIM27 negatively affected NOD2-mediated pro-inflammatory responses. The NOD2-TRIM27 interaction was enhanced upon stimulation with the NOD2 agonist MDP. This suggests that TRIM27 is involved in a negative feed-back loop to control NOD2-mediated signalling. Of note, TRIM27 is a

nuclear protein in most human cells. This study demonstrated that also NOD2 can shuttle to the nucleus and co-localizes with TRIM27.

NOD2 loss-of-function mutations are associated with Crohn's disease. Analysis of colonic biopsies from Crohn's disease patients revealed significantly enhanced TRIM27 mRNA expression, underscoring a physiological role of TRIM27 in regulating NOD2 signalling. We conclude that TRIM27 negatively regulates NOD2-mediated signalling by destabilization of NOD2 and suggest that TRIM27 could be a new and promising target for therapeutically intervention in NOD2-associated diseases.

7 Zusammenfassung

NOD2 ist ein Mitglied der NLR-Proteinfamilie und an der Entwicklung angeborener Immunantworten beteiligt. Unkontrollierte NOD2-Aktivität kann zu schweren entzündlichen Krankheiten führen, allerdings ist bislang noch nicht ausreichend bekannt, wie NOD2 reguliert wird.

Die ATPase Domäne in NOD2 besitzt eine wichtige regulatorische Funktion. Mutationen von konservierten Aminosäuren in dieser Domäne sind mit Autoimmunerkrankungen wie dem Blau-Syndrom und der *early onset* Sarkoidose verbunden, aber auch mit der Inhibierung des NOD2-Signalweges wie z.B. bei einer Mutation der Walker A Box. In einer systematischen Mutationsanalyse wurden konservierte Aminosäuren der ATPase Domäne von NOD2 und des verwandten Proteins NOD1 untersucht. Die Ergebnisse zeigten, dass für die Aktivierung von NOD1 und NOD2 sowohl eine funktionelle Walker A und B Box als auch das GxP-Motiv und der Sensor 1 wichtig sind, da Mutationen von diesen die NF-κB-Aktivierung stark beeinträchtigten. Dies weist darauf hin, dass eine Nukleotid-Bindung und ein initialer Nukleotid-Hydrolyseschritt für die Aktivierung von NOD1 und NOD2 notwendig sind. Weiterhin konnte gezeigt werden, dass Mutationen der erweiterten Walker B Box sowie des konservierten Histidin in der WH-Domäne (*winged helix*) unterschiedliche Auswirkungen auf die NOD1- und NOD2-Aktivierung haben. Während sie in NOD1 nicht mehr funktionell sind, führen sie bei NOD2 zu einer erhöhten Autoaktivierung im Vergleich zum Wildtyp. Wir nehmen daher an, dass NOD2 leichter autoaktiviert werden kann und besser als NOD1 kontrolliert werden muss.

In Übereinstimmung mit dieser Annahme wurde gezeigt, dass NOD2 aber nicht NOD1 einem schnelleren Proteinumsatz unterliegt, welcher durch Ubiquitin-vermittelten proteasomalen Abbau erfolgt. In einem Hefe-Zwei-Hybrid-Screen wurde TRIM27 als neuer Interaktionspartner von NOD2 identifiziert. Die Spezifität dieser Interaktion wurde durch reziproke Co-Immunoprezipitationsexperimente bestätigt. Die Interaktion erfolgt über die Nukleotid-bindende Domäne (NBD) von NOD2 und das TRIM27 PRY-SPRY-Motiv. TRIM27 ist eine RING-Domänen E3 Ubiquitin Ligase. Es wurde gezeigt, dass NOD2 – nicht jedoch NOD1 – abhängig von funktionellem TRIM27 mit K48-verlinkten Ubiquitinketten modifiziert wird, was wiederum zur

proteasomalen Degradation von NOD2 führt. Dementsprechend negativ beeinflusste TRIM27 die NOD2-vermittelten pro-inflammatorischen Immunantworten. Die NOD2-TRIM27-Interaktion wurde durch die Stimulation mit dem NOD2-Agonisten MDP verstärkt. Dies deutet darauf hin, dass TRIM27 in einen negativen *Feedback-Loop* der den NOD2-Signalweg kontrolliert, involviert ist. In humanen Zellen ist TRIM27 hauptsächlich im Zellkern lokalisiert. Es wurde gezeigt, dass auch NOD2 in den Zellkern transportiert werden kann und dort mit TRIM27 co-lokalisiert.

NOD2-Mutationen, die zu einem Funktionsverlust von NOD2 führen, sind mit Morbus Crohn assoziiert. Kolonbiopsien von Morbus Crohn-Patienten zeigten eine signifikant erhöhte Expression von TRIM27 mRNA, was die physiologische Rolle von TRIM27 bei der NOD2-Regulation verdeutlicht. Aus diesen Daten kann geschlossen werden, dass TRIM27 NOD2-vermittelte Immunreaktionen durch eine Destabilisierung von NOD2 negativ reguliert. TRIM27 könnte daher ein neuer, vielversprechender Angriffspunkt für therapeutische Maßnahmen bei NOD2-assoziierten Krankheiten sein.

Danksagung

Dr. Thomas Kufer danke ich für die Möglichkeit, in seiner Arbeitsgruppe meine Doktorarbeit anzufertigen. Danke, für die sehr gute Betreuung, deine stete Diskussionsbereitschaft, deinen Einsatz für deine Doktoranden, dein Bemühen uns zu exponieren und uns die vielfältigen und interessanten Seiten der Wissenschaft zu zeigen!

Prof. Dr. Jonathan Howard, meinem offiziellem Doktorvater, danke ich für die Übernahme der Erstkorrektur und Begutachtung meiner Arbeit.

Prof. Dr. Mats Paulsson danke ich für Übernahme der Zweitkorrektur und Begutachtung meiner Arbeit.

Prof. Dr. Robert Schwarzenbacher und seiner Gruppe, besonders Dr. Martina Pröll und Ana Gimeno, danke ich für die gute Zusammenarbeit. Danke für die tollen NLR Meetings und die Zeit während meines Forschungsaufenthaltes in Salzburg!

Dr. Ida Schoultz, Luisa Napolitano und Dr. Germana Meroni danke ich für die Zusammenarbeit beim TRIM-Projekt, Dr. Kirstin Keusekotten und Dr. Gerrit Praefcke für die Hilfe bei der TRIM Expression und Eveline Bennek und Dr. Gernot Sellge für die TRIM27 Patientendaten.

Der AG Kufer danke ich für die gemeinsame Zeit in und außerhalb des Labors! Danke Maureen, für deine Hilfe und Organisation! Danke Harald, für die Diskussionen und deine Hilfe bei diversen Fragen! Danke Andi, für die NOD1 Immunofluoreszenzbilder und deine Hilfe bei Wochenendversuchen! Danke Katja, für dein Wissen und deine Erfahrung! Danke Katharina, für die Vorarbeit im TRIM-Projekt! Danke Anna D., Helen und Anna K. für eure Hilfsbereitschaft und die gemeinsame Zeit!

Den Mitarbeiterinnen und Mitarbeitern der AGs Kashkar, Krönke und Brodesser, den Gastro G’s und Frau Kwade danke ich für die gemeinsame Zeit im Haus 37!

Danke Thomas, Olli, Katja, Harald und Frauke für das Korrekturlesen!

Erklärung

Ich versichere, dass ich die von mir vorgelegte Dissertation selbstständig angefertigt, die benutzen Quellen und Hilfsmittel vollständig angegeben und die Stellen der Arbeit – einschließlich Tabellen, Karten und Abbildungen –, die anderen Werken im Wortlaut oder dem Sinn nach entnommen sind, in jedem Einzelfall als Entlehnung kenntlich gemacht habe; dass diese Dissertation noch keiner anderen Fakultät oder Universität zur Prüfung vorgelegen hat; dass sie – abgesehen von unten angegebenen Teilpublikationen – noch nicht veröffentlicht worden ist sowie, dass ich eine solche Veröffentlichung vor Abschluss des Promotionsverfahrens nicht vornehmen werde.

Die Bestimmungen der Promotionsordnung sind mir bekannt. Die von mir vorgelegte Dissertation ist von Prof. Dr. Jonathan Howard und Prof. Dr. Mats Paulsson betreut worden.

Teilpublikationen:

Zurek B, Proell M, Wagner RN, Schwarzenbacher R, Kufer TA. **Mutational analysis of human NOD1 and NOD2 NACHT domains reveals different modes of activation,** *Innate Immun* (2011); [Epub ahead of print]

Köln, im August 2011

Birte Helene Zurek